

Braid Forcing, Hyperbolic Geometry, and Pseudo-Anosov Sequences of Low Entropy

Thesis by
Rupert William Venzke

In Partial Fulfillment of the Requirements
for the Degree of
Doctor of Philosophy



California Institute of Technology
Pasadena, California

2008
(Defended May 14, 2008)

© 2008

Rupert William Venzke

All Rights Reserved

To D. Ray Morton, without whose assistance this thesis would not have been possible

Acknowledgements

I would like to thank adviser Danny Calegari, who supervised this project and who provided countless leads for the research contained herein.

Thank you to the Caltech Mathematics Department, who paid my bills for the past five years and who provided an excellent educational opportunity.

Thanks to Danny Calegari, Nikolai Makarov, Michael Aschbacher, and Paolo Ghiggini for judging this very thesis defense.

Thanks to the Department of Mathematical and Computing Sciences of the Tokyo Institute of Technology for assisting in research. To Sadayoshi Kojima, for hosting my stay in Japan. To Eiko Kin and Mitsuhiko Takasawa for many interesting mathematical discussions, and for teaching me SnapPea.

Thanks also to Eriko Hironaka, Ji-Young Ham, Won Taek Song, and Jin-Hwan Cho who were involved as well in the collaborative work with TiTech on low-growth pseudo-Anosov mappings.

Thank you to Andre de Carvalho and Toby Hall for collaboration on dynamics of the horseshoe map. Moreover, it should be pointed out that Toby Hall's train-track program is the basis for much of the work in this paper.

Thank you to Michael Handel for some info regarding the case of four-strand braids.

A thank you as well to Nathan Dunfield and Colin Adams for help with hyperbolic geometry.

Thanks to Martin Scharlemann (UC Santa Barbara), David Bachman and Jim Hoste (Pitzer College), and Benson Farb (U. Chicago) and their respective institutions for hosting me briefly this Fall. Thank you additionally to Jim Hoste for helping with KnotScape.

Thanks very much to Pam Fong for helping to get many of the programs working on my office computer.

A giant thank you to the Northwestern University Mathematics Department for providing post-Caltech support to continue this research.

A huge thank you to my family in Pennsylvania for their help not only the past five years, but as long as I can remember.

Thank you to Dan Prigel and the Lucky Baldwin's/JPL/Caltech group for productive Wednesday evening discussions.

Last, but certainly not least, thanks to D. Ray Morton, whose help goes without saying.

Abstract

We view braids as automorphisms of punctured disks and define a partial order on pseudo-Anosov braids called the forcing order. The order measures whether one automorphism induces another given automorphism on the surface. Pseudo-Anosov growth rate decreases relative to the order and appears to give a good measure of braid complexity. Unfortunately it appears difficult computationally to determine explicitly the partial order structure by hand. We use several computer algorithms to study the bottom part of the partial order when the number of braid strands is fixed. From the algorithms, we build sequences of low entropy pseudo-Anosov n -strand braids that are minimal in the sense that they do not force any other pseudo-Anosov braids on the same number of strands. The sequences are an extension of work done by Hironaka and Kin, and we conjecture the sequences to achieve minimal entropy among certain non-trivial classes of braids. In general, the lowest entropy pseudo-Anosov braids appear to have mapping tori that come from Dehn surgery on very low volume hyperbolic 3-manifolds, and we begin to analyze the relation between entropy and hyperbolic volume. Moreover, the low-growth families contain non-trivial low-growth families of horseshoe braids and we proceed to study dynamics of the horseshoe map as well.

Contents

Acknowledgements	iv
Abstract	vi
1 Summary of Results	1
1.1 Initial Definitions	1
1.2 Main Results	3
1.2.1 Low-Dilatation Pseudo-Anosov Braids	3
1.2.2 Dilatation and Hyperbolic Volume	6
1.2.3 Sharkovskii's Theorem and Horseshoe Dynamics	7
2 Background for the Research	9
2.1 Braids	9
2.1.1 Definitions	9
2.1.2 Pseudo-Anosov Braids	10
2.1.3 Forcing	12
2.2 Entropy	15
2.2.1 Markov Partitions	15
2.2.2 Entropy	16
2.2.3 Entropy and Forcing	17
2.3 Example of Braids on 3 Strands	17
2.3.1 Description of the Group	17
2.3.2 Description of the Order	17
3 Computer Experiments	19
3.1 Programs Utilized	19
3.1.1 Hall's Implementation of the Bestvina-Handel Algorithm	19
3.1.2 Mathematica	20
3.1.3 Java/C++	20

3.1.4	SnapPea	21
3.1.5	KnotTwister	21
3.2	The Fundamental $\tilde{\psi}_3$ Braid	21
3.3	Finding “Simple” Braids	22
3.4	2–Cusp Mapping Tori	24
3.5	3–Cusp Mapping Tori	25
3.6	More Cusps	26
3.7	Powers of $\tilde{\psi}_3$	26
4	Construction of the Psi and Psi-Tilde Sequences	27
4.1	The ψ_n Sequence	27
4.1.1	The Case of n Odd, $n \geq 7$	27
4.1.2	The Case $n = 4k, k \geq 2$	30
4.1.3	The Case $n = 8k + 2, k \geq 2$	32
4.1.4	The Case $n = 8k + 6, k \geq 1$	34
4.2	The $\tilde{\psi}_n$ Sequence	37
4.2.1	The Case of n Odd, $n \geq 5$	37
4.2.2	The Case $n = 4k, k \geq 2$	38
4.2.3	The Case $n = 8k + 2, k \geq 1$	40
4.2.4	The Case $n = 8k + 6, k \geq 1$	41
4.3	Exceptional Cases	43
4.3.1	The ψ_5 Braid	43
4.3.2	The ψ_6 Braid	45
4.3.3	The ψ_{10} Braid	46
4.3.4	The $\tilde{\psi}_3$ Braid	48
4.3.5	The $\tilde{\psi}_4$ Braid	48
4.3.6	The $\tilde{\psi}_6$ Braid	49
4.3.7	The ζ_6 Braid	49
4.3.8	The $\tilde{\zeta}_6$ Braid	51
5	Entropy Considerations for the Psi and Psi-Tilde Sequences	53
5.1	Asymptotic Behavior	53
5.2	Astounding Sequences and the Sequential Value	55
5.3	Sparsity	55
6	Minimality of the Psi and Psi-Tilde Sequences	57
6.1	The $\tilde{\psi}_n$ Sequence	57

6.1.1	The Case of n Odd, $n \geq 5$	57
6.1.2	The Case $n = 4k, k \geq 2$	61
6.1.3	The Case $n = 8k + 2, k \geq 1$	64
6.1.4	The Case $n = 8k + 6, k \geq 1$	67
6.2	The ψ_n Sequence	69
6.2.1	The Case of n Odd, $n \geq 7$	69
6.2.2	The Case $n = 4k, k \geq 2$	72
6.2.3	The Case $n = 8k + 2, k \geq 2$	75
6.2.4	The Case $n = 8k + 6, k \geq 1$	78
6.3	Exceptional Cases	81
7	Initial Analysis of Mapping Tori	82
7.1	Kirby Calculus	82
7.2	Dehn Surgery Realization of Mapping Tori	83
7.2.1	The Case of ψ_n, n Odd	83
7.2.2	Other Cases	88
7.3	Volume Concept	88
8	Horseshoe Braids	91
8.1	The Horseshoe Map	91
8.2	“The Forcing Relation for Horseshoe Braid Types”	93
8.3	Star-Shaped Train-Tracks	95
8.4	The $\Omega_{p,q}$ and $\tilde{\Omega}_{p,q}$ Braids	97
8.5	Forcing for M_{magic}	99
9	Mapping Tori with More Cusps	101
9.1	Construction of the θ_n Sequence	101
9.2	Surgeries on M_{hip} and M_{cool}	103
9.3	Minimally Twisted Chain Links and the Finite Cyclic Whitehead Link Covers	107
	Bibliography	113

Chapter 1

Summary of Results

1.1 Initial Definitions

This paper concerns a certain partial order on braids called the “forcing order”, which will be defined carefully in Chapter 2. Relevant to this order is the notion of minimality.

Definition 1.1. *A pseudo-Anosov n -strand braid is defined to be **minimal** if there is no other pseudo-Anosov n -braid (same number of strands) below it in the braid forcing order.*

Our thesis hopes to identify several sequences of pseudo-Anosov braids critical in understanding of the braid forcing order. Before stating our results and conjectures, we proceed to give definitions for some of the most relevant sequences.

Definition 1.2. *Define the n -strand braid L_n to be $L_n = \sigma_{n-1}\sigma_{n-2}\dots\sigma_2\sigma_1$ ($n \in \mathbb{N}, n \geq 2$), where σ_i is the usual braid group generator.*

Definition 1.3. *We define the (ψ_n) sequence of n -strand braids ($n \in \mathbb{N}, n \geq 5$) via*

1. $\psi_n = L_n^2\sigma_1^{-1}\sigma_2^{-1}$ when $n = 2k + 1$ is odd and $n \geq 5$
2. $\psi_n = L_n^{2k+1}\sigma_1^{-1}\sigma_2^{-1}$ when $n = 4k, k > 1$
3. $\psi_n = L_n^{2k+1}\sigma_1^{-1}\sigma_2^{-1}$ when $n = 8k + 2, k > 0$
4. $\psi_n = L_n^{6k+5}\sigma_1^{-1}\sigma_2^{-1}$ when $n = 8k + 6, k > 0$
5. $\psi_6 = \sigma_5\sigma_4\sigma_3\sigma_2\sigma_1\sigma_5\sigma_4\sigma_3\sigma_5\sigma_4$.

Definition 1.4. *We define the $(\tilde{\psi}_n)$ sequence of n -strand braids ($n \in \mathbb{N}, n \geq 3$) via*

1. $\tilde{\psi}_n = \psi_n\sigma_2\sigma_1^2\sigma_2$, when $n \geq 7$
2. $\tilde{\psi}_3 = \sigma_2\sigma_1^{-1}$

3. $\tilde{\psi}_4 = \sigma_3\sigma_2\sigma_1^{-1}$
4. $\tilde{\psi}_5 = \psi_5\sigma_2\sigma_1^2\sigma_2$
5. $\tilde{\psi}_6 = \psi_6 = \sigma_5\sigma_4\sigma_3\sigma_2\sigma_1\sigma_5\sigma_4\sigma_3\sigma_5\sigma_4$.

Definition 1.5. We define the $(\mathcal{U}(\psi_n))$ sequence of $(n+1)$ -strand braids $(n \in \mathbb{N}, n \geq 7)$ via

1. $\mathcal{U}(\psi_n) = L_{n+1}^2\sigma_1^{-1}\sigma_2^{-1}\sigma_n\sigma_{n-1}$ when $n = 2k+1$ is odd and $n \geq 7$
2. $\mathcal{U}(\psi_n) = L_n^{2k+1}\sigma_1^{-1}\sigma_2^{-1}\sigma_n\sigma_{n-1}\dots\sigma_{2k}$ when $n = 4k, k > 1$
3. $\mathcal{U}(\psi_n) = L_n^{2k+1}\sigma_1^{-1}\sigma_2^{-1}\sigma_n\sigma_{n-1}\dots\sigma_{6k+2}$ when $n = 8k+2, k > 0$
4. $\mathcal{U}(\psi_n) = L_n^{6k+5}\sigma_1^{-1}\sigma_2^{-1}\sigma_n\sigma_{n-1}\dots\sigma_{2k+2}$ when $n = 8k+6, k > 0$.

Definition 1.6. We define the $(\mathcal{U}(\tilde{\psi}_n))$ sequence of $(n+1)$ -strand braids $(n \in \mathbb{N}, n \geq 4$ and $n \neq 6)$ via

1. $\mathcal{U}(\tilde{\psi}_n) = \mathcal{U}(\psi_n)\sigma_2\sigma_1^2\sigma_2$, when $n \geq 5$ and $n \neq 6$
2. $\mathcal{U}(\tilde{\psi}_4) = \sigma_4\sigma_3\sigma_2\sigma_1^{-1}\sigma_4$.

Definition 1.7. We define the $(\Pi_{n,3})$ sequence of n -strand braids for $n \equiv 1, 5 \pmod{6}, n \geq 11$ via

1. $\Pi_{n,3} = L_n^{2k+1}\sigma_1^{-1}\sigma_2^{-1}$, when $n = 6k+1$ and $k \geq 2$
2. $\Pi_{n,3} = L_n^{2k+1}\sigma_{n-1}\sigma_{n-2}$, when $n = 6k+5$ and $k \geq 1$.

Definition 1.8. We define the n -strand $\Omega_{p,q}$ braids, where $n = pq+1$ and q is a fixed natural number, via

1. $\Omega_{p,q} = L_n^p\sigma_1^{-1}\sigma_2^{-1}$, when $p > 1$ and $p \in \mathbb{N}$
2. $\Omega_{p,q} = L_n^{n-1}\sigma_1\sigma_2$, when $p = 1$.

Definition 1.9. We define the n -strand $\tilde{\Omega}_{p,q}$ braids, where $n = pq+2$ and q is a fixed natural number, via

1. $\tilde{\Omega}_{p,q} = L_n^p(\sigma_1^{-1}\sigma_2^{-1})(\sigma_{n-1}\sigma_{n-2}\dots\sigma_{n-p})$, when $p > 1$ and $p \in \mathbb{N}$
2. $\tilde{\Omega}_{p,q} = L_n^{n-1}(\sigma_1\sigma_2)L_n\sigma_1^{-1}$, when $p = 1$.

Definition 1.10. We define the (H_n) sequence, $n \in \mathbb{N}, n \geq 7$, via

1. if $n-1 = p$, with $p = 2k+1$ a prime, then $H_n = \tilde{\Omega}_{2,k} = L_n^2(\sigma_1^{-1}\sigma_2^{-1})(\sigma_{n-1}\sigma_{n-2})$

2. if $n - 1$ is composite, with smallest prime factor α and corresponding quotient $\beta = \frac{n-1}{\alpha}$, then

$$H_n = \Omega_{\alpha,\beta} = L_n^\alpha \sigma_1^{-1} \sigma_2^{-1}.$$

Definition 1.11. Define the n -strand braid sequence $\tilde{\theta}_n$ via $\tilde{\theta}_n = L_n^3 \sigma_1^{-1} \sigma_2^{-1} \sigma_{n-4}^{-1} \sigma_{n-5}^{-1}$ for $n = 4 + 3k, k \in \mathbb{N}$.

Definition 1.12. We define the braid θ_n , for $n = 4 + 3k$ and $k \in \mathbb{N}$, to be the horseshoe braid with horseshoe code $10^{k+1}10^k10^k$.

Definition 1.13. Define the braid \dagger_n , for $n = 4k + 6$ and $k \in \mathbb{N}$, to be the horseshoe braid with horseshoe code $10^{k+1}10^{k+1}10^k10^k$.

Definition 1.14. Define the horseshoe braid \diamond_k^j on $n = (2k + 3)h$ strands to be the braid with horseshoe code $(10^{k+1})^h(10^k)^h$ when $j = 2h$ is even. In the event that $j = 2h + 1$ is odd, we define the horseshoe braid \diamond_k^j on $n = (2k + 3)h + (k + 1)$ strands to be the braid with horseshoe code $(10^{k+1})^h(10^k)^{h+1}$.

1.2 Main Results

1.2.1 Low-Dilatation Pseudo-Anosov Braids

The (ψ_n) and $(\tilde{\psi}_n)$ sequences appear to have reasonably low growth rate.

Theorem 1.15. For $n \geq 7$, the growth rate λ_n of ψ_n is equal to the largest real root of the polynomial

1. $x^{2k+1} - 2x^{k+1} - 2x^k + 1$, when $n = 2k + 1$
2. $x^{4k} - 2x^{2k+1} - 2x^{2k-1} + 1$, when $n = 4k$
3. $x^{8k+2} - 2x^{4k+3} - 2x^{4k-1} + 1$, when $n = 8k + 2$
4. $x^{8k+6} - 2x^{4k+5} - 2x^{4k+1} + 1$, when $n = 8k + 6$.

Moreover the growth rate $\tilde{\lambda}_n$ of $\tilde{\psi}_n$ satisfies $\tilde{\lambda}_n = \lambda_n$.

Corollary 1.16. We have $\lim_{n \rightarrow \infty} \lambda_n^n = \lim_{n \rightarrow \infty} \tilde{\lambda}_n^n = (2 + \sqrt{3})^2$.

The constant $(2 + \sqrt{3})^2$ has come up several different places in our investigation, and seems like a useful constant in the braid forcing theory for some reason. We would like to know whether we can improve on this constant somehow among pseudo-Anosov sequences.

Theorem 1.17. The (ψ_n) and $(\tilde{\psi}_n)$ sequences are sequences of minimal braids.

Definition 1.18. Define the magic 3–manifold, denoted M_{magic} , to be the complement (in S^3) of the alternating 3–component chain link.

Theorem 1.19. The mapping tori of the (ψ_n) and $(\tilde{\psi}_n)$ sequence braids are all isometric to manifolds obtained by Dehn surgery on a single cusp of M_{magic} , with the exception of $n = 6$. The mapping tori for the exceptional $\psi_6, \tilde{\psi}_6$ are actually isometric to M_{magic} . Otherwise, the surgery coefficients for the ψ_n sequence are

1. $\frac{k+1}{k}, n = 2k + 1$ odd
2. $\frac{2k+1}{2k-1}, n = 4k$
3. $\frac{4k+3}{4k-1}, n = 8k + 2$
4. $\frac{4k+5}{4k+1}, n = 8k + 6$.

The numerators/denominators of these surgery coefficients correspond to the exponents of nonzero terms in the characteristic polynomials of Theorem 2.1. Further, the surgery coefficients corresponding to $\tilde{\psi}_n$ and ψ_n are reciprocals when $n \geq 5$ and $n \neq 6$.

The surgery coefficients on a cusp of M_{magic} yielding hyperbolic/non-hyperbolic manifolds were computed earlier in a paper by Martelli and Petronio [27]. Fortunately, the coefficients in our list do yield hyperbolic manifolds.

Theorem 1.20 (Thurston). *The mapping torus for a braid is hyperbolic iff the braid is pseudo-Anosov.*

Applying these theorems yields the following

Corollary 1.21. *The sequences (ψ_n) and $(\tilde{\psi}_n)$ consist entirely of pseudo-Anosov braids.*

If it were true in general that minimal braids were unique up to certain symmetries, then we would know the ψ_n and $\tilde{\psi}_n$ braids to attain minimal growth among pseudo-Anosov n –strand braids. However, we have the following

Theorem 1.22. *The sequence $(\Pi_{n,3})$ is a sequence of minimal pseudo-Anosov braids. Moreover, the mapping tori for this sequence are isometric to surgeries on a cusp of M_{magic} with surgery coefficients $\frac{3k+2}{3k-1}$, when $n = 6k + 1$, and surgery coefficients $\frac{3k+4}{3k+1}$, when $n = 6k + 5$.*

Corollary 1.23. *Minimal braids are not unique in general.*

In spite of non-uniqueness of minimal braids, we do have a number of conjectures regarding growth of the (ψ_n) and $(\tilde{\psi}_n)$ sequences. Note that the ψ_n sequence consists of horseshoe braids when n is odd [22].

Conjecture 1.24. *The (ψ_n) sequence, n odd, attains minimal growth among pseudo-Anosov n -strand horseshoe braids whose mapping torus consists of two cusps.*

Conjecture 1.25. *The (ψ_n) sequence, n odd, attains minimal growth among pseudo-Anosov n -strand horseshoe braids.*

Conjecture 1.26. *The (ψ_n) and $(\tilde{\psi}_n)$ sequences attain minimal growth among pseudo-Anosov n -strand braids having mapping tori with 2 cusps.*

Conjecture 1.27. *The (ψ_n) and $(\tilde{\psi}_n)$ sequences attain minimal growth among pseudo-Anosov n -strand braids.*

What we do know is that the lowest growth pseudo-Anosov braids tend to have sparse Markov matrices as the number of strands gets large. Our above (ψ_n) and $(\tilde{\psi}_n)$ sequences are good examples of this.

Lemma 1.28. *There exist Markov matrices M_n, \tilde{M}_n for $\psi_n, \tilde{\psi}_n$ respectively, $n \geq 11$, such that the sum of the entries of each matrix is $n + 4$.*

There are certain upper bounds on the sum of the entries of a Markov matrix for a pseudo-Anosov braid in terms of its growth. For instance,

Theorem 1.29 (Ham, Song [20]). *For a pseudo-Anosov braid having growth λ and $g \times g$ Markov matrix M , the sum $|M|$ of the entries of M satisfies $|M| - g + 1 \leq \lambda^g$.*

Using our low-growth sequences (ψ_n) and $(\tilde{\psi}_n)$, we obtain

Corollary 1.30. *Any Markov matrix M for a pseudo-Anosov braid of minimal growth must satisfy $|M| \leq K + 50$, where K is the dimension of M .*

We have many ideas on how to potentially improve this bound and suspect the bound to be quite a bit lower. Indeed, we have

Conjecture 1.31. *With possibly the exception of some trivial cases, pseudo-Anosov growth can essentially be minimized by minimizing the sum of the entries for associated Markov matrices.*

From experimental considerations, we observe many of the lowest growth (beyond absolute minimal growth) braids to have a form similar to the ψ_n and $\tilde{\psi}_n$.

Conjecture 1.32. *Define $K(n)$ to be the largest integer so that the lowest $K(n)$ growth pseudo-Anosov n -strand braids with 2-cusp mapping tori are all achieved by braids with expressions of the form $L_n^z \sigma_1 \sigma_2$ or $L_n^z \sigma_1^{-1} \sigma_2^{-1}$. Then, $K(n) \rightarrow \infty$ as $n \rightarrow \infty$.*

Consider next the following fact regarding the $\mathcal{U}(\psi_n)$ and $\mathcal{U}(\tilde{\psi}_n)$

Lemma 1.33. *The $\mathcal{U}(\psi_n)$ and $\mathcal{U}(\tilde{\psi}_n)$ can be formed by adding a single puncture to the non-punctured singularity of an appropriate train-track for the ψ_n and $\tilde{\psi}_n$, respectively.*

More generally we expect all of the lowest growth behavior of pseudo-Anosov with mapping tori of any number of cusps to be produced in such a manner. This leads to the more sophisticated conjecture

Conjecture 1.34. *Define $\tilde{K}(n)$ to be the largest integer so that the lowest $\tilde{K}(n)$ growth pseudo-Anosov n -strand braids are all achieved by adding punctures (possibly zero punctures) to invariant train-tracks of braids with expressions of the form $L_n^z \sigma_1 \sigma_2$ or $L_n^z \sigma_1^{-1} \sigma_2^{-1}$. Then, $\tilde{K}(n) \rightarrow \infty$ as $n \rightarrow \infty$.*

One could of course study sequences with slightly higher growth than that of the above mentioned ones. All of the train-tracks we have come across thus far in our investigations for pseudo-Anosov n -braids of the form $L_n^z \sigma_1 \sigma_2$ or $L_n^z \sigma_1^{-1} \sigma_2^{-1}$ have either had zero singularities or precisely one central non-punctured singularity, in which cases the train-track map is virtually a rotation. Based on this, we note the sequences described in the conjecture above all appear to consist of powers of L_n with a few extra generators tacked on at the end. Relative to some appropriate notion of “very small dilatation sequence”, this analysis leads to the conjecture of Benson Farb

Conjecture 1.35 (Farb). *All very small dilatation pseudo-Anosov braids should be the product of an element of finite order with something having support contained in a subsurface of universally bounded complexity.*

We conclude here by remarking for now that the \diamond_k^j braids seem to be useful in studying low-growth behavior among pseudo-Anosov braids whose mapping tori have more cusps. The $\theta_{3k+4} = \diamond_k^3$ sequence is the next lowest growth pseudo-Anosov sequence we have come across besides braids whose mapping tori are isometric to surgeries on M_{magic} . Adding punctures to all the non-punctured singularities of an appropriate train-track for the θ_{3k+4} yields some very low growth pseudo-Anosov braids with 4-cusp mapping tori, for instance.

1.2.2 Dilatation and Hyperbolic Volume

Going back to M_{magic} once again, we observe now that M_{magic} has relatively low volume ≈ 5.33 .

Conjecture 1.36. *M_{magic} attains minimal volume among 3-cusp hyperbolic 3-manifolds.*

It is possible for low growth pseudo-Anosov braids to have large volume mapping tori as the number of strands grows.

Theorem 1.37 (Kin, Takasawa [24]). *There exist sequences (α_n) of n -strand pseudo-Anosov braids with growth tending to 1 whose mapping tori have precisely 2 cusps and have volume tending to ∞ .*

In spite of this, we make the following conjecture

Conjecture 1.38 (Kin, Takasawa). *All of the lowest possible growth pseudo-Anosov sequences have extremely low volume mapping tori.*

More generally, this suggests a method for producing low-dilatation automorphisms of orientable genus g surfaces.

Conjecture 1.39 (Kin, Takasawa). *In order to find very low dilatation automorphisms of orientable genus g surfaces Σ_g , one can simply study low volume hyperbolic 3-manifolds fibered over Σ_g and use the monodromy automorphism. Conversely, one should be able to produce lots of low-volume fibered hyperbolic 3-manifolds by taking the mapping tori of very low dilatation automorphisms of Σ_g .*

1.2.3 Sharkovskii’s Theorem and Horseshoe Dynamics

So far, we have been examining the case of general pseudo-Anosov braids. What happens if we restrict now to the case of braids forced by the Smale horseshoe map? This leads us to an analysis of the $\Omega_{p,q}$ braids defined earlier.

Theorem 1.40. *The $\Omega_{p,q}$ braids have mapping tori resulting from $\frac{(p-1)q+1}{q}$ Dehn surgery on a cusp of M_{magic} .*

This is how we originally developed the set of $\Omega_{p,q}$ braids. Independent research by Carvalho and Hall led them recently to define the same set of braids via different techniques.

Theorem 1.41 (Carvalho, Hall). *The $\Omega_{p,q}$ and $\tilde{\Omega}_{p,q}$ are braids of horseshoe type. More specifically, in terms of height and decoration, $\Omega_{p,q} = P^{\frac{0^{q-3}}{(p-1)q+1}}$ when $q \geq 3$, where 0^{q-3} denotes simply a string of $q-3$ zeros. (There are similar expressions in the cases $q = 1, 2$.)*

We note now that the $\Omega_{p,q}$ braids have train-tracks with precisely one asymmetrical “spoke” consisting of a different number of edges than the other “spokes”. In the $n = 4k$ case, the ψ_n sequence has precisely two asymmetrical spokes and does not consist of horseshoe braids. More generally, among braids corresponding to positive surgeries on M_{magic} , we suspect that having more than one asymmetrical spoke may be the obstruction to horseshoe-ness. This leads to the following conjecture

Conjecture 1.42. *With possibly some trivial exceptions, and up to natural symmetries, the set $\{\Omega_{p,q} : p, q \in \mathbb{N}\}$ is precisely the set of horseshoe braids corresponding to positive surgeries on M_{magic} .*

Based on our conjecture earlier that lowest growth braids came from surgery on M_{magic} , we have

Conjecture 1.43. *When $n \neq r + 1$, r prime, pseudo-Anosov growth is often minimized by braids in the set $\{\Omega_{p,q} : p, q \in \mathbb{N}\}$.*

Moreover, we expect the following

Conjecture 1.44. *Define $J(n)$ to be the largest integer so that the lowest $J(n)$ growths among pseudo-Anosov horseshoe n -braids may be attained by braids of the form $\Omega_{p,q}$ and $\tilde{\Omega}_{p,q}$. Then, $J(n) \rightarrow \infty$ and $n \rightarrow \infty$.*

Some further analysis in this direction leads to the horseshoe growth minimization conjecture.

Conjecture 1.45 (Horseshoe Growth Minimization). *For most naturals n where H_n is defined, growth among horseshoe braids is minimized by the H_n .*

Recall that the definition of braid forcing order is intended to generalize the idea of the period forcing order of interval maps in the classical Sharkovskii theorem. Consequently, we would like to find analogues of the Sharkovskii theorem in the pseudo-Anosov braid forcing setting.

Theorem 1.46 (Carvalho, Hall). $\Omega_{p,q} \succeq \Omega_{p',q'}$ iff $\frac{(p-1)q+1}{p-1} \geq \frac{(p'-1)q'+1}{p'-1}$ and $q \leq q'$.

Note that our expression $\frac{(p-1)q+1}{q}$ for the surgery coefficient corresponding to $\Omega_{p,q}$ is quite similar to the expression $\frac{(p-1)q+1}{p-1}$ of the theorem. This suggests an approach for computing the more general order with respect to M_{magic} .

Conjecture 1.47. *After some simple coordinate change on M_{magic} , the braid forcing order on the set of braids corresponding to positive surgeries on M_{magic} is essentially given by the usual order on surgery coefficients (along with perhaps some auxiliary condition, i.e., $q \leq q'$).*

We observed earlier that the ψ_n and $\tilde{\psi}_n$ braids were all minimal. These were braids where the surgery coefficients were very close to 1. Considering now surgeries of fixed denominator, the horseshoe theory applies in fact to show that the $\Omega_{p,2}$ are all minimal. More generally,

Conjecture 1.48. *Pseudo-Anosov braids with mapping tori resulting from non-trivial surgery on M_{magic} are all minimal.*

We suspect however that not all minimal pseudo-Anosov braids arise from surgeries on M_{magic} . For instance, we suspect the θ_n braids defined earlier are potentially minimal as well, although we have not computed this yet.

Last, observe that if we fix q , the sequences $\Omega_{p,q}$ will be linearly ordered (i.e., $\Omega_{p,q} \succeq \Omega_{p',q}$ iff $p \leq p'$). The above concepts thus imply the existence of many linearly ordered sequences of minimal braids in the forcing partial order.

Chapter 2

Background for the Research

2.1 Braids

2.1.1 Definitions

Definition 2.1. Let $\Sigma_{g,k,r}$ denote the genus g surface with k punctures and r boundary S^1 components. We define the **mapping class group** $MCG(\Sigma_{g,k,r})$ to be the group of diffeotopy classes of diffeomorphisms $f : \Sigma_{g,k,r} \rightarrow \Sigma_{g,k,r}$, under the operation of composition (which will be well defined).

Definition 2.2. Consider the surface $\Sigma_{g,k,r}$ with subsets $A, B \subseteq \Sigma_{g,k,r}$. We define the **relative mapping class group** $MCG(\Sigma_{g,k,r} \text{ rel } A, B)$ to be the group of diffeotopy classes of diffeomorphisms $f : \Sigma_{g,k,r} \rightarrow \Sigma_{g,k,r}$ simultaneously leaving A invariant and fixing B pointwise, again under the operation of composition.

Definition 2.3. Let D be the closed unit disk in \mathbb{R}^2 and let $A_n \subseteq D$ be some set of n elements. Then, we define the **geometric n -braid group** B_n via $B_n = MCG(D \text{ rel } A_n, \partial D)$, where ∂D is the boundary of D .

Definition 2.4. We define the **algebraic n -braid group** $\tilde{B}_n, n \geq 2$, to be the group having generators $\sigma_1, \sigma_2, \dots, \sigma_{n-1}$ and relations

1. $\sigma_i \sigma_j = \sigma_j \sigma_i$, whenever $|i - j| \geq 2$
2. $\sigma_i \sigma_{i+1} \sigma_i = \sigma_{i+1} \sigma_i \sigma_{i+1}$, for $i \in \{1, 2, \dots, n - 2\}$.

Theorem 2.5 (Artin). We have a group isomorphism $B_n \cong \tilde{B}_n$, i.e., the geometric n -braid group defined above is the same as the algebraic n -braid group.

Further information on introductory braid theory may be found in Birman [5].

2.1.2 Pseudo-Anosov Braids

Example 2.6. *Let's consider first an example of a torus map. We will view here a torus T^2 as the usual quotient space of the standard unit square $[0, 1] \times [0, 1]$ formed by identifying opposite boundary edges in the same direction. Then, define the **Arnold Cat Map** $f : T^2 \rightarrow T^2$ via $f(x, y) = ((2x+y) \bmod 1, (x+y) \bmod 1)$ for $(x, y) \in [0, 1] \times [0, 1]$. This yields indeed an automorphism of the torus. (More generally, linear toral automorphisms correspond to the elements of $SL(2, Z)$.)*

Observe that the matrix $A = \begin{pmatrix} 2 & 1 \\ 1 & 1 \end{pmatrix}$ has characteristic polynomial $x^2 - 3x + 1$, with corresponding

eigenvalues $\lambda_1 = \frac{1}{2}(3 + \sqrt{5})$ and $\lambda_2 = \frac{1}{2}(3 - \sqrt{5})$. We have eigenvectors $\xi_1 = \begin{pmatrix} \frac{1}{2}(1 + \sqrt{5}) \\ 1 \end{pmatrix}$ and

$\xi_2 = \begin{pmatrix} \frac{1}{2}(1 - \sqrt{5}) \\ 1 \end{pmatrix}$. Observe that the eigenvalues λ_1 and λ_2 are inverse to one another since

*the determinant of A is 1. Thus, our map f expands by the factor λ_1 along the direction ξ_1 , while contracting by the same factor (expanding by an inverse factor) along the direction ξ_2 . We get an unstable foliation \mathfrak{F}^u of T^2 by considering "lines" parallel to ξ_1 , and a corresponding stable foliation \mathfrak{F}^s of T^2 by considering "lines" parallel to ξ_2 . Note that these are necessarily transverse foliations since the vectors ξ_1 and ξ_2 are orthogonal. Our map f is thus an example of what is called an **Anosov** automorphism (diffeomorphism in this case).*

Definition 2.7. *A diffeomorphism $f : \Sigma_{g,k,r} \rightarrow \Sigma_{g,k,r}$ is called **pseudo-Anosov** if, aside from possibly finitely many singularities, this map preserves some pair of transverse measured foliations \mathfrak{F}^s (the stable foliation) and \mathfrak{F}^u (the unstable foliation) so that f expands by a factor $\lambda > 1$ (referred to as the **growth rate** or **dilatation**) along \mathfrak{F}^u and contracts by the same factor (expands by an inverse factor) along \mathfrak{F}^s . This is a generalization of the notion of an **Anosov** diffeomorphism, in which no singularities are present.*

Definition 2.8. *A mapping class group element is called **pseudo-Anosov** if it contains some pseudo-Anosov representative. Likewise, we call a mapping class group element **Anosov** if it contains some Anosov representative.*

It is possible to construct pseudo-Anosov maps from Anosov maps, and to conversely generate Anosov maps from pseudo-Anosov maps

Theorem 2.9 (Brown [7]). *Let $\sigma \in MCG(\Sigma_{1,0,0}) = SL(z^2)$ be hyperbolic. Then for each $g > 1$, $\exists n$ with $0 < n \leq 4g^2$, such that σ^n lifts to an orientable pseudo-Anosov element of $MCG(\Sigma_{g,0,0})$ with a quadratic expansion factor equal to that of σ^n .*

This result is a sort of converse to the following result.

Theorem 2.10 (Franks-Rykken [16]). *A pseudo-Anosov map with orientable foliations and a quadratic dilatation factors via a branched covering to an Anosov automorphism on $\Sigma_{1,0,0}$.*

Definition 2.11. *We define a **train-track** for $\Sigma_{g,k,r}$ to be some family of embedded curves in $\Sigma_{g,k,r}$ such that*

1. *the curves meet at a finite set of vertices called switches*
2. *away from the switches, the curves are smooth and do not touch each other*
3. *at each switch, three curves meet with the same tangent line, with two curves entering from direction and one from the other.*

Definition 2.12. *Let T_1 and T_2 be train-tracks on $\Sigma_{g,k,r}$. We say that T_1 **carries** T_2 if there exists a smooth map $h : (\Sigma_{g,k,r}, T_2) \rightarrow (\Sigma_{g,k,r}, T_1)$ such that*

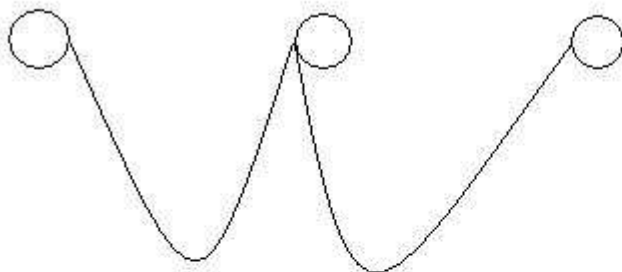
1. *the restriction to each tangent line of T_2 is an isomorphism onto a tangent line of T_1*
2. *there is a smooth homotopy $H : \Sigma_{g,k,r} \times [0, 1] \rightarrow \Sigma_{g,k,r}$ with $H(x, 0) = id$, $H(x, 1) = h$, and $H|_{\Sigma_{g,k,r} \times t}$ a diffeomorphism for all $t < 1$.*

Definition 2.13. *Consider the diffeomorphism $f : \Sigma_{g,k,r} \rightarrow \Sigma_{g,k,r}$ and let T be a train-track for $\Sigma_{g,k,r}$. We call T an **invariant train-track** for f if T carries $f(T)$.*

Further background on train-tracks may be found in [31].

Algorithm 2.14 (Bestvina-Handel [3]). *There is an algorithm for producing an invariant train-track for any given diffeomorphism $f : \Sigma_{g,k,r} \rightarrow \Sigma_{g,k,r}$. This algorithm has been implemented in a number of computer programs for varying choices of g, k, r .*

Example 2.15. *Consider the braid $\beta = \sigma_2^2 \sigma_1^{-1}$. Applying the Bestvina-Handel algorithm, one sees that this mapping class group element possesses a representative with the train-track drawn below*



The singularities (punctures) lie within the “circular” peripheral loops — one per peripheral loop. Indeed, it may be shown that every pseudo-Anosov 3–braid possesses a train-track like this.

Theorem 2.16 (Thurston). *Every mapping class group element contains some representative that is either*

1. *periodic, i.e., some power is the identity*
2. *reducible*
3. *pseudo-Anosov .*

These cases however are not necessarily mutually exclusive.

Additional ideas may be found in [8].

2.1.3 Forcing

Definition 2.17. *Let φ be a braid on j strands and let ψ be a braid on k strands. We say $\varphi \succeq \psi$ if for any j –element set $B \subseteq D$ (D the closed unit disk) and any $f : D \rightarrow D$ representing φ relative to B , there exists an f –invariant k –element set $C \subseteq D$ such that f relative to C instead is a representative of ψ . This relation \succeq turns out to give a well-defined partial order on the set of all*

finite strand braids. We refer to the above partial order as the **braid forcing order**. Further, the relation $\varphi \succeq \psi$ is often stated alternatively as φ “forces” ψ .

Definition 2.18. We define now an order on \mathbb{N} called the **Sharkovskii order**. Let $x, y \in \mathbb{N}$. We say that $x \succ y$ in the Sharkovskii order iff every continuous map $f : \mathbb{R} \rightarrow \mathbb{R}$ having a point of period x must also have some point of period y .

Theorem 2.19 (Sharkovskii’s Theorem). *The above order indeed yields a well-defined total order that may be described explicitly as*

$$3 \succ 5 \succ 7 \succ \dots \succ$$

$$2 \cdot 3 \succ 2 \cdot 5 \succ 2 \cdot 7 \succ \dots \succ$$

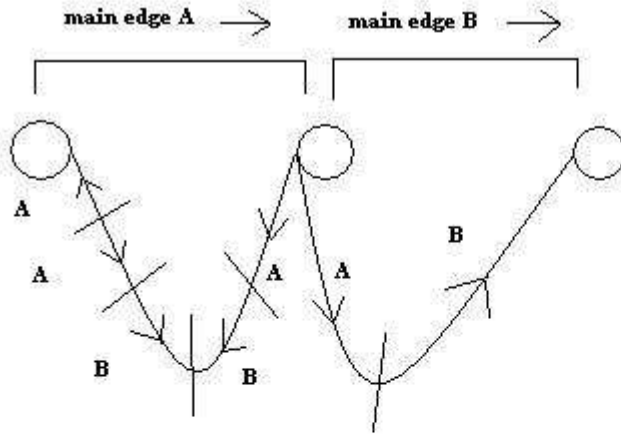
$$2^2 \cdot 3 \succ 2^2 \cdot 5 \succ 2^2 \cdot 7 \succ \dots \succ$$

...

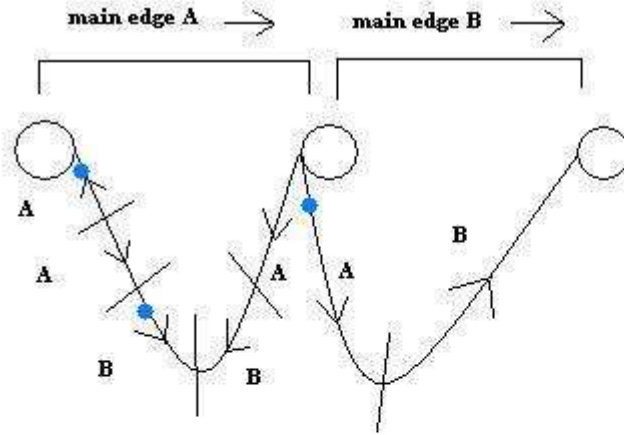
$$\dots \succ 2^4 \succ 2^3 \succ 2^2 \succ 2 \succ 1.$$

Remark 2.20. The braid forcing order defined above is intended to be a 2–dimensional generalization of the Sharkovskii order for 1–dimensional dynamics. This is in part our motivation for analyzing the braid forcing order as defined.

Example 2.21. Consider the 3–strand braids $\alpha = \sigma_2 \sigma_1^{-1}$ and $\beta = \sigma_2^2 \sigma_1^{-1}$. We know from before that both braids admit the invariant train-track described in Example 2.15. Consider now the following diagram below



This is the train-track from earlier. However, we have now included information about how the train-track maps over itself under the action of β . Call the first main edge A and the second main edge B, both directed from left to right. The braid β maps edge A initially over edge A in the reverse direction, then over edges A and B in the forward direction, and finally over edges B and A in the reverse direction. Further, the braid β maps edge B over edges A and B successively in the forward direction. We observe that there must necessarily be some β invariant 3–element set consisting of one point from the first edge A subinterval of edge A, one point from the first edge B subinterval of edge A, and one point from the edge A subinterval of edge B. We have labelled such an invariant set with blue dots in the diagram from earlier.



If one now fills in the original singularities and instead deletes these three blue points, then the original map β relative the blue points instead will actually be the map α . One can see this by folding the subintervals together in the natural way and looking at how the blue points swirl around one another. Thus we have shown $\beta \succ \alpha$ in the braid forcing order.

2.2 Entropy

2.2.1 Markov Partitions

Definition 2.22. Consider a pseudo-Anosov diffeomorphism $f : \Sigma_{g,k,r} \rightarrow \Sigma_{g,k,r}$ with associated unstable and stable foliations \mathfrak{F}^u and \mathfrak{F}^s , respectively. For $p \in \Sigma_{g,k,r}$ and any rectangle $R \subseteq \Sigma_{g,k,r}$, denote by $\mathfrak{F}^u(p)$ the leaf of the \mathfrak{F}^u containing p and denote by $\mathfrak{F}^u(p, R)$ the component of \mathfrak{F}^u containing p (with analogous definitions for $\mathfrak{F}^s(p)$ and $\mathfrak{F}^s(p, R)$). Define a **Markov partition** $P = \{R_1, \dots, R_m\}$ of f to be a collection of rectangles R_i , each contained in $\Sigma_{g,0,r} \supseteq \Sigma_{g,k,r}$, satisfying

1. $\Sigma_{g,0,r} = \cup_i R_i$
2. no singularity/puncture is contained within the interior of some R_i
3. the R_i have pairwise disjoint interiors

4. if $p \in R_i$ and $f(p) \in R_j$, then $\mathfrak{F}^u(f(p), R_j) \subseteq f(\mathfrak{F}^u(p, R_i))$ and $\mathfrak{F}^s(f(p), R_j) \subseteq f(\mathfrak{F}^s(p, R_i))$.

Theorem 2.23 (Adler, Weiss). *Every pseudo-Anosov diffeomorphism $f : \Sigma_{g,k,r} \rightarrow \Sigma_{g,k,r}$ has a Markov partition.*

Definition 2.24. *Let S be an alphabet (set) $S = \{x_1, x_2, \dots, x_n\}$ of cardinality n . Denote by Z_S the set of all bi-infinite sequences of elements of S . Define the **shift operator** T on Z_S via $T(y)_j = y_{j+1}$ for $y \in Z_S$. Define the full **Bernoulli Shift** on S to be the pair (Z_S, T) of sequences, with associated shift operator. One may then define a **subshift of finite type** on S to be a pair $(W_F, T|_{W_F})$, where F is some finite set of finite sequences (blocks) of elements from S , W_F is the subset of Z_S consisting of bi-infinite sequences not containing any blocks of F , and $T|_{W_F}$ is the restriction of T to W_F .*

Example 2.25. *Subshifts of finite type arise in a natural way from Markov partitions. For instance, consider a diffeomorphism $f : \Sigma_{g,k,r} \rightarrow \Sigma_{g,k,r}$ with associated Markov partition $P = \{R_1, \dots, R_n\}$. Consider the set $S = \{1, 2, \dots, n\}$ and let F be the finite set of two element sequences (i, j) such that $\mathfrak{F}^u(f(p), R_j) \subsetneq f(\mathfrak{F}^u(p, R_i))$ and/or $\mathfrak{F}^s(f(p), R_j) \subsetneq f(\mathfrak{F}^s(p, R_i))$ for some $p \in R_i$ with corresponding $f(p) \in R_j$. Then, we have the subshift of finite type $(W_F, T|_{W_F})$ corresponding to the original diffeomorphism f .*

Definition 2.26. *For a pseudo-Anosov diffeomorphism $f : \Sigma_{g,k,r} \rightarrow \Sigma_{g,k,r}$ with corresponding Markov partition $P = \{R_1, \dots, R_n\}$, we define the associated $n \times n$ **Markov Matrix** (also referred to as adjacency matrix) M for f, P via $M_{i,j} = \#$ of components of $\text{int } \mathfrak{F}^s(p_1, R_i) \cap \text{int } f(\mathfrak{F}^u(p_2, R_j))$ for $p_1 \in \text{int } R_i$ and $p_2 \in \text{int } R_j$ (which will be well defined, independent of the choice of p_1, p_2).*

Definition 2.27. *Let $f : \Sigma_{g,k,r} \rightarrow \Sigma_{g,k,r}$ be a pseudo-Anosov diffeomorphism with invariant train-track τ and some associated ordering of the main edges. Since τ carries $f(\tau)$, the main edges of τ get mapped over the main edges of τ by f . In analogy with the previous definition, we define the **Markov matrix** M of the (labelled) train-track τ relative to f via $M_{i,j} =$ the number of times edge j gets mapped over edge i by f . In general, when referring to the Markov matrix from now on, we will be thinking in the context of Markov matrices for invariant train-tracks.*

2.2.2 Entropy

Definition 2.28. *Consider a diffeomorphism $f : \Sigma_{g,k,r} \rightarrow \Sigma_{g,k,r}$. Let $n \in \mathbb{N}$ and $x, y \in \Sigma_{g,k}$. Denote by $O(x, n)$ and $O(y, n)$ the n -orbit sequences $x, f(x), \dots, f^{n-1}(x)$ and $y, f(y), \dots, f^{n-1}(y)$, respectively. For $\epsilon > 0$, the n -orbits $O(x, n)$ and $O(y, n)$ are called ϵ -**different** if there is a $j \in [0, n-1)$ such that the distance from $f^j(x)$ to $f^j(y)$ is larger than ϵ . Let $r(n, \epsilon, f) =$ the maximum number of ϵ -different n -orbits. Set $h(\epsilon, f) = \limsup_{n \rightarrow \infty} \frac{1}{n} \log r(n, \epsilon, f)$. We define the (**topological**) **entropy $h(f)$** of f to be $h(f) = \sup_{\epsilon > 0} h(\epsilon, f)$.*

Theorem 2.29. *For a pseudo-Anosov mapping class group element, entropy is minimal on the pseudo-Anosov diffeomorphism, and is log of the dilatation.*

Definition 2.30. *We define the **growth rate** (or **dilatation**) of a pseudo-Anosov mapping class group element to be the dilatation of the pseudo-Anosov representative diffeomorphism.*

Theorem 2.31. *Dilatation of a pseudo-Anosov mapping class element is equal to the largest real eigenvalue of a Markov matrix associated to an invariant train-track for the representative pseudo-Anosov diffeomorphism.*

2.2.3 Entropy and Forcing

The relation between entropy and forcing is studied in Boyland [6]. We will often make use of the following useful idea

Theorem 2.32. *Entropy is monotone under braid forcing, i.e., if $\varphi \succeq \psi$, then the entropy function E satisfies $E(\varphi) \geq E(\psi)$. Moreover this inequality is strict in the sense that $\varphi \succ \psi$ implies $E(\varphi) > E(\psi)$ strictly.*

2.3 Example of Braids on 3 Strands

2.3.1 Description of the Group

The forcing order on 3–braids has been analyzed by Handel [21].

Lemma 2.33. *Consider the "half-twist" n –braid $\partial_n = \prod_{i=1}^{n-1} (\prod_{j=1}^{n-1} \sigma_{n-i-j+1})$. The center of B_n is generated by the full twist ∂_n^2 .*

Lemma 2.34. *The 3–braid group B_3 has the classical quotient group description $B_3/(\partial_n^2) \cong SL(2, \mathbb{Z})$.*

Lemma 2.35. *Consider the 3–braids $L = \sigma_1^{-1}$ and $R = \sigma_2$. Then, every element of B_3 may be written in the form $\partial_n^{2k} w$, where $k \in \mathbb{Z}$ and w is some word in L and R .*

2.3.2 Description of the Order

Lemma 2.36. *The braid forcing order on B_3 descends to a partial order on the quotient of B_3 by its cyclic center.*

Theorem 2.37 (Handel [21]). *Let φ and ψ be two braids in the quotient of B_3 by its cyclic center and let m_φ and m_ψ be corresponding words in L and R . Then, $\varphi \succeq \psi$ iff m_ψ is obtained from m_φ via deletion of letters and cyclic permutations.*

Remark 2.38. There is a similar theorem of Handel for the full braid group that includes an additional rule for dealing with powers of ∂_n^2 .

Chapter 3

Computer Experiments

3.1 Programs Utilized

3.1.1 Hall's Implementation of the Bestvina-Handel Algorithm

Numerous computer algorithms were utilized in this research and it seems likely that a large percentage of the conjectures in this paper would not have been arrived at without the aid of such algorithms. The braid forcing question is one that surfaced in the 1970s, but was computationally intractable. For instance, the set of orbits and their corresponding braids forced by a general braid is simply too difficult to compute directly by hand without the assistance of the modern computer. Moreover, one needs relevant info about a braid after finding the correct expression. As mentioned earlier, probably the most critical program is Toby Hall's **Trains** algorithm. This application computes an invariant train-track, corresponding train-track map, and growth (i.e., implements the Bestvina-Handel algorithm) for a given braid described as an expression in the usual generators. There are a number of other implementations of the algorithm, but this one seems by far the most effective for our purposes. The program may be downloaded at

http://www.liv.ac.uk/math/PURE/MIN_SET/CONTENT/members/T_Hall.html .

There are two versions, a Windows-based version and a Unix-based version. The Windows version is much more convenient to use, but breaks down for some of the harder computations. Moreover, the Windows version lacks the batch processing utility of the Unix version used to sift through long lists of braids. Fortunately, the Unix version can handle many critical examples where the Windows version crashes. Braids crashing the Windows version tend to be ones with many edges (possibly thousands) in the Markov partition for a train-track edge. An important class of examples crashing the Windows version is the set of pure n -braids, when n reaches perhaps 10 or sooner. A key example of a braid crashing the Windows version, yet surviving the Unix version is the 6-braid

$$\sigma_1^{-1}\sigma_2\sigma_5\sigma_4^{-1}\sigma_3^{-1}\sigma_4\sigma_5^{-1}\sigma_2^{-1}\sigma_1\sigma_1^2\sigma_2^{-1}\sigma_5^{-2}\sigma_4\sigma_3^{-1}\sigma_4^{-1}\sigma_5^2\sigma_2\sigma_1^{-2}$$

$$\sigma_1^{-1}\sigma_2\sigma_5\sigma_4^{-1}\sigma_3\sigma_4\sigma_5^{-1}\sigma_2^{-1}\sigma_1\sigma_1^2\sigma_2^{-1}\sigma_5^{-2}\sigma_4\sigma_3\sigma_4^{-1}\sigma_5^2\sigma_2\sigma_1^{-2}$$

lying in the kernel of the Burau representation [4].

3.1.2 Mathematica

Mathematica was used to do many of the computations involving Markov matrices. For instance, we know from earlier that the growth of a pseudo-Anosov braid may be computed as the largest real eigenvalue of the Markov matrix. Thus, Mathematica is great for computing entropies of braids having Markov matrices of large dimension (the Trains program is not valid for braids having too many strands, perhaps $n > 50$). Another important computation here is the computation of the number of orbits of specified size for a pseudo-Anosov n -braid. Corresponding to a given Markov matrix, one can introduce the associated directed adjacency graph.

Definition 3.1. *For an $r \times r$ Markov matrix M , we define the **directed adjacency graph associated to M** to be the directed graph with r vertices x_1, \dots, x_r and having exactly $M_{i,j}$ directed edges from x_j to x_i .*

Lemma 3.2. *The number of directed paths of length q from x_i to x_j in the directed adjacency graph associated to M is equal to $(M^q)_{i,j}$.*

Using this lemma, we see that

Lemma 3.3. *Consider an $r \times r$ Markov matrix M associated to a pseudo-Anosov braid and some corresponding train-track map, where r is a prime. If the number of fixed points of the train-track map is a finite number s , then the number of orbits of size r for the train-track map is equal to $(\text{trace}(M^r) - s)/r$.*

When r is not a prime, we may compute the number of orbits similarly, using inclusion-exclusion to subtract off repeating paths. Again, Mathematica is especially useful here in the case of Markov matrices with large dimension.

3.1.3 Java/C++

There were two key programs developed by us over the course of this research to investigate the forcing order:

1. program to compute braids forced by powers of $\tilde{\psi}_3$
2. program to compute the order among trigoned pseudo-Anosov 4-braids .

Originally $C++$ was being used, but ultimately programs were done in Java to

1. avoid certain precision issues
2. be more compatible with the local Unix server .

Source code for the programs may be found at

<http://www.its.caltech.edu/~rupert> .

3.1.4 SnapPea

SnapPea is the main program used to do computations in hyperbolic geometry. Of particular interest here are the SnapPea functions that compute hyperbolic volume and perform Dehn surgeries. Later on, we will want to describe certain manifolds of interest in terms of Dehn surgery on other manifolds. The hyperbolic volume function was critical initially in searching for and figuring out the correct manifolds/surgery coefficients. Normally, manifolds are input in terms of link diagrams. We utilized however a specific algorithm of Nathan Dunfield as well for inputting mapping tori of braids. These programs, as well as many others, may be downloaded from the CompuTop site:

<http://www.math.uiuc.edu/~nmd/computop/index.html> .

3.1.5 KnotTwister

This program computes fiberings for hyperbolic manifolds over different surfaces. In light of the entropy minimization/volume minimization conjecture of Kin and Takasawa, this program should aid substantially in the construction of low-growth maps on more complex surfaces. Although we have not utilized this program much to date, we suspect this application will likely form the basis for the next stage of our research — quite analogous to the role of Hall’s program in this thesis. The input for the program is a hyperbolic 3–manifold’s fundamental group, which may in turn be computed from SnapPea. The program and documentation may be found at Stefan Friedl’s homepage:

<http://www.labmath.uqam.ca/~friedl/index.html> .

3.2 The Fundamental $\tilde{\psi}_3$ Braid

Consider the braid $\tilde{\psi}_3 = \sigma_2\sigma_1^{-1}$ examined briefly as an example in Chapter 2. From Handel’s Theorem about the braid forcing structure on 3–strand braids [21], we know that $\tilde{\psi}_3$ is the only pseudo-Anosov braid in B_3/Center that does not force any other pseudo-Anosov braids. From this standpoint, $\tilde{\psi}_3$ may easily be considered to be the simplest pseudo-Anosov 3–strand braid. Also, we know that

there are no pseudo-Anosov 2–strand braids. Since the train-track and train-track map for $\tilde{\psi}_3$ are simpler than for higher-strand braids, $\tilde{\psi}_3$ could easily be considered the easiest pseudo-Anosov braid to work with in general.

However, one should not be deceived into believing the dynamics of the $\tilde{\psi}_3$ map are trivial. In Chapter 8, we’ll define and explore a well-known map called the Smale horseshoe.

Theorem 3.4. *The Smale horseshoe map exhibits chaotic behavior.*

The Smale horseshoe contains chaotic behavior, and our $\tilde{\psi}_3$ is indeed even more complex. More directly, one can also appeal to the theorem of Li-Yorke [23]

Theorem 3.5 (Li-Yorke). *Period Three implies Chaos.*

Either way, our $\tilde{\psi}_3$ braid is seen to produce a reasonable amount of dynamics.

One has the following Corollary of Handel’s Forcing Theorem

Corollary 3.6. *Every pseudo-Anosov 3–braid is forced by some power of $\tilde{\psi}_3$.*

Experimentally, one observes that many higher-strand pseudo-Anosov braids are forced by some 3–strand pseudo-Anosov braids. It seems very plausible to conjecture

Conjecture 3.7. *Every pseudo-Anosov braid (on any number of strands) is forced by some pseudo-Anosov 3–braid.*

Consequently, an application of the above corollary leads us to

Conjecture 3.8. *Every pseudo-Anosov braid (on any number of strands) is forced by some power of $\tilde{\psi}_3$.*

This suggests that $\tilde{\psi}_3$ is universal in the sense that it encodes information about all pseudo-Anosov braids. This principle, coupled with the relative computational simplicity of $\tilde{\psi}_3$, is a key motivating idea of what follows in our thesis.

The above method is an attempt to realize pseudo-Anosov braids in some especially nice concrete way. An alternative potential method we are studying at present utilizes the concept of templates outlined in [17].

3.3 Finding “Simple” Braids

Having observed the simplest 3–strand braid, we would now like to ask

Question 3.9. *For $n \in \mathbb{N}$, what is the “simplest” pseudo-Anosov n –braid?*

This question is perhaps not exactly well posed. First, we have put “simplest” in quotation marks. Second, it’s not clear that there is some essentially unique “simplest” pseudo-Anosov n -braid. From a dynamical viewpoint, there are perhaps two reasonable ways to precisely rephrase this question.

Question 3.10. *For $n \in \mathbb{N}$, what are the minimal pseudo-Anosov n -braids?*

Question 3.11. *For $n \in \mathbb{N}$, what is the minimal entropy achieved by pseudo-Anosov n -braids?*

From earlier, we know that entropy is a strictly monotone decreasing function relative to the forcing order. Thus, any pseudo-Anosov n -braid achieving minimal entropy must necessarily be minimal. The second question is easier to pursue initially, so we shall begin with this question and return later to the matter of minimality.

It is maybe not entirely obvious at first why our entropy minimization question above should even be well posed. Consider the following inequality of Ham and Song

Theorem 3.12 (Ham, Song [20]). *For a pseudo-Anosov braid having growth λ and $g \times g$ Markov matrix M , the sum $|M|$ of the entries of M satisfies $|M| - g + 1 \leq \lambda^g$.*

Observe moreover that

Theorem 3.13. *For $n \in \mathbb{N}$, there exist a finite number of train-tracks such that any pseudo-Anosov n -braid exhibits one such invariant train-track.*

Together, these results imply

Corollary 3.14. *For $n \in \mathbb{N}$, entropy is indeed minimized among the set of pseudo-Anosov n -braids.*

Aside from theoretical interest in computing the entropy minimizers, there is additionally practical interest with regards to the braid forcing question. Direct computation of the braids forced by a particular braid can often become infeasible (even with use of computers), when the initial braid is too complex. The problem is that there may be too many orbits of a required size for a given map of the disk. However, low entropy pseudo-Anosov representatives of n -braids tend to have relatively few orbits of size n and the computations become feasible (this is a consequence of the Ham, Song inequality). Thus, there is a practical motivation for knowing exactly what constitutes low pseudo-Anosov growth for a given n . When one knows what the low-growth braids are, one can compute the forcing relation among low-growth braids and then attempt to generalize.

With this in mind, one may now ask

Question 3.15. *How does one find the entropy minimizers?*

Based on our conjecture above that all pseudo-Anosov n -braids are forced by some power of $\tilde{\psi}_3$, we propose the following strategy.

Strategy 3.16 (Finding entropy minimizers). *For $k, n \in \mathbb{N}$, the braid $\tilde{\psi}_3^k$ forces finitely many pseudo-Anosov n -braids. Fixing n whilst allowing k to increase, attempt to compute the limit as k increases of the minimal entropy among pseudo-Anosov n -braids forced by $\tilde{\psi}_3^k$. Such a limit would necessarily give the minimal entropy. Moreover, we know the limit would in fact be achieved at some $k = k_0$ for a fixed n . Some entropy minimizer would necessarily then be in the list of n -braids forced by $\tilde{\psi}_3^{k_0}$.*

This strategy seems quite straightforward, but is actually a much more ambitious task than one might at first imagine. Nonetheless, as we shall see, the strategy does eventually lead to some extremely reasonable conjectures. In pursuing this strategy, we must first answer

Question 3.17. *For $n \in \mathbb{N}$, what is the minimal entropy among pseudo-Anosov n -braids forced by $\tilde{\psi}_3$?*

Even this is not necessarily an easy question. One problem is that we need to compute braids whose associated permutations on the n punctures could potentially have lots of cycles. This can become a quite-difficult-to-handle computation. We thus reduce further finally to the simpler question

Question 3.18. *For $n \in \mathbb{N}$, what is the minimal entropy among pseudo-Anosov n -braids forced by $\tilde{\psi}_3$ that have exactly 2 cusps in the associated mapping torus?*

This is the question we shall now proceed to address.

3.4 2-Cusp Mapping Tori

We recall now the definition of the ψ_n and $\tilde{\psi}_n$ sequences

Definition 3.19. *Define the n -strand braid L_n to be $L_n = \sigma_{n-1}\sigma_{n-2}\dots\sigma_2\sigma_1$ ($n \in \mathbb{N}, n \geq 2$), where σ_i is the usual braid group generator.*

Definition 3.20. *We define the (ψ_n) sequence of n -strand braids ($n \in \mathbb{N}, n \geq 5$) via*

1. $\psi_n = L_n^2\sigma_1^{-1}\sigma_2^{-1}$ when $n = 2k + 1$ is odd and $n \geq 5$
2. $\psi_n = L_n^{2k+1}\sigma_1^{-1}\sigma_2^{-1}$ when $n = 4k, k > 1$
3. $\psi_n = L_n^{2k+1}\sigma_1^{-1}\sigma_2^{-1}$ when $n = 8k + 2, k > 0$
4. $\psi_n = L_n^{6k+5}\sigma_1^{-1}\sigma_2^{-1}$ when $n = 8k + 6, k > 0$
5. $\psi_6 = \sigma_5\sigma_4\sigma_3\sigma_2\sigma_1\sigma_5\sigma_4\sigma_3\sigma_5\sigma_4$.

Definition 3.21. *We define the $(\tilde{\psi}_n)$ sequence of n -strand braids ($n \in \mathbb{N}, n \geq 3$) via*

1. $\tilde{\psi}_n = \psi_n \sigma_2 \sigma_1^2 \sigma_2$, when $n \geq 7$
2. $\tilde{\psi}_3 = \sigma_2 \sigma_1^{-1}$
3. $\tilde{\psi}_4 = \sigma_3 \sigma_2 \sigma_1^{-1}$
4. $\tilde{\psi}_5 = \psi_5 \sigma_2 \sigma_1^2 \sigma_2$
5. $\tilde{\psi}_6 = \sigma_5 \sigma_4 \sigma_3 \sigma_2 \sigma_1 \sigma_5 \sigma_4 \sigma_3 \sigma_5 \sigma_4$.

Using Java, we developed a computer program explicitly designed to answer the final question of the preceding section. Here are the results:

Theorem 3.22 (computer-assisted proof). *For $n \leq 16, n \neq 6$, the minimal entropy among pseudo-Anosov n -braids forced by $\tilde{\psi}_3$ that have exactly 2 cusps in the associated mapping torus is attained by $\tilde{\psi}_n$. In the case $n = 6$, the minimal growth among such braids is attained instead by the pseudo-Anosov braid $\zeta_6 = \sigma_5 \sigma_4 \sigma_3 \sigma_2 \sigma_1 \sigma_5 \sigma_4$.*

3.5 3-Cusp Mapping Tori

Having completed an initial examination of the 2-cusp case, we would now like to answer

Question 3.23. *For $n \in \mathbb{N}$, what is the minimal entropy among pseudo-Anosov n -braids forced by $\tilde{\psi}_3$ that have exactly 3 cusps in the associated mapping torus?*

Definition 3.24. *We define the $(\mathcal{U}(\psi_n))$ sequence of $(n+1)$ -strand braids ($n \in \mathbb{N}, n \geq 7$) via*

1. $\mathcal{U}(\psi_n) = L_{n+1}^2 \sigma_1^{-1} \sigma_2^{-1} \sigma_n \sigma_{n-1}$ when $n = 2k + 1$ is odd and $n \geq 7$
2. $\mathcal{U}(\psi_n) = L_n^{2k+1} \sigma_1^{-1} \sigma_2^{-1} \sigma_n \sigma_{n-1} \dots \sigma_{2k}$ when $n = 4k, k > 1$
3. $\mathcal{U}(\psi_n) = L_n^{2k+1} \sigma_1^{-1} \sigma_2^{-1} \sigma_n \sigma_{n-1} \dots \sigma_{6k+2}$ when $n = 8k + 2, k > 0$
4. $\mathcal{U}(\psi_n) = L_n^{6k+5} \sigma_1^{-1} \sigma_2^{-1} \sigma_n \sigma_{n-1} \dots \sigma_{2k+2}$ when $n = 8k + 6, k > 0$.

Definition 3.25. *We define the $(\mathcal{U}(\tilde{\psi}_n))$ sequence of $(n+1)$ -strand braids ($n \in \mathbb{N}, n \geq 4$ and $n \neq 6$) via*

1. $\mathcal{U}(\tilde{\psi}_n) = \mathcal{U}(\psi_n) \sigma_2 \sigma_1^2 \sigma_2$, when $n \geq 5$ and $n \neq 6$
2. $\mathcal{U}(\tilde{\psi}_4) = \sigma_4 \sigma_3 \sigma_2 \sigma_1^{-1} \sigma_4$.

Adjusting our Java program to handle this scenario, we have

Theorem 3.26 (computer-assisted proof). *For $n = 5, 6, 8, 9, 10, 11$, the minimal entropy among pseudo-Anosov n -braids forced by $\tilde{\psi}_3$ that have exactly 3 cusps in the associated mapping torus is attained by $\mathcal{U}(\tilde{\psi}_{n-1})$.*

We examine this pattern further in Chapter 5 and beyond.

3.6 More Cusps

We note briefly here that in the case of braids whose mapping tori have more cusps, the lowest growth pseudo-Anosov braids generally appear experimentally to be formed by adding punctures to some appropriate subset of non-punctured singularities of low-growth pseudo-Anosov braids with 2-cusp mapping tori, although this is not necessarily easy to see at first by looking at braid words.

3.7 Powers of $\tilde{\psi}_3$

Following the strategy outlined earlier, we would now like to understand what low-growth braids are forced by higher powers of $\tilde{\psi}_3$. Experimenting with the second power, $\tilde{\psi}_3^2$, programs have thus failed thus far to produce lower-growth braids than the ψ_n and $\tilde{\psi}_n$. This suggests that the first power $\tilde{\psi}_3$ alone is already perhaps strong enough to provide some non-trivial understanding of low-growth behavior.

Chapter 4

Construction of the Psi and Psi-Tilde Sequences

4.1 The ψ_n Sequence

4.1.1 The Case of n Odd, $n \geq 7$

This chapter presents an explicit construction of the ψ_n and $\tilde{\psi}_n$ braids in terms of train-tracks and train-track maps. Once the train-track maps have been given, it is not hard to see the braids have the expressions given previously in terms of the usual braid group generators.

The construction proceeds in several stages, depending on the value of n . The case of the ψ_n , n odd and $n \geq 7$ is perhaps the easiest to follow (although other cases are very similar), and indeed was the first case discovered.

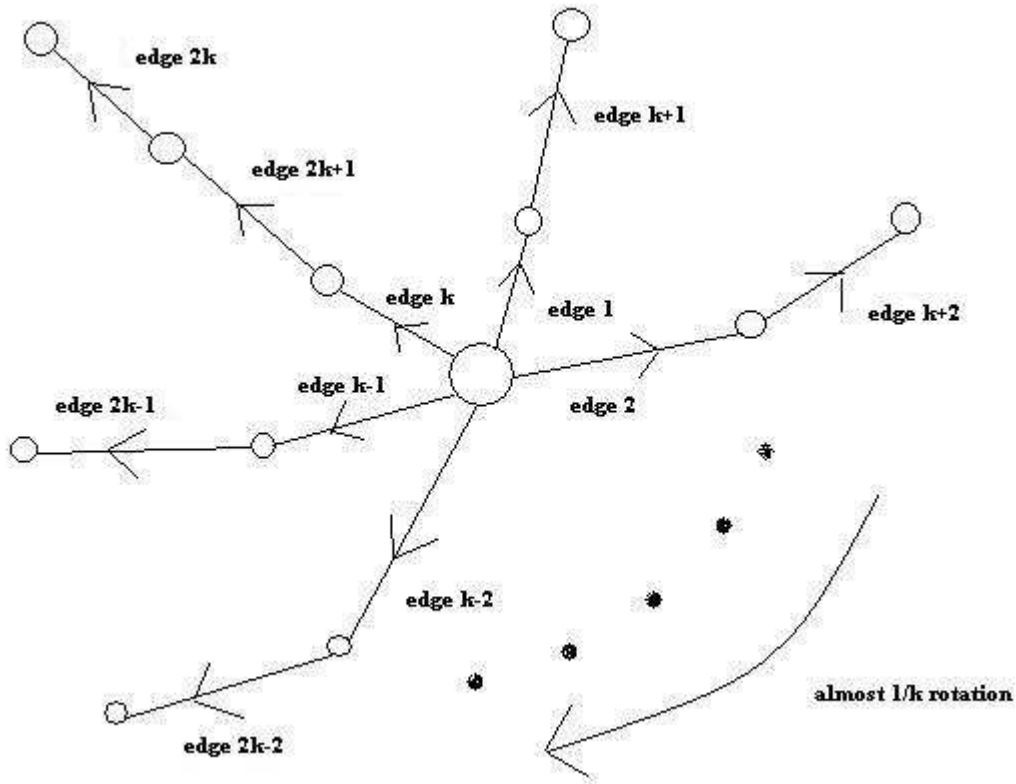
Definition 4.1 (Hironaka, Kin [22]). *For $n = 2g + 1, g \geq 3$, define the n -braids $\sigma_{g-1, g+1}$ via*

$$\sigma_{g-1, g+1} = (\sigma_1^{-1} \sigma_2^{-1} \dots \sigma_{g-1}^{-1})(\sigma_{g-1}^{-1} \sigma_{g-2}^{-1} \dots \sigma_1^{-1})(\sigma_1^{-1} \sigma_2^{-1} \dots \sigma_{2g}^{-1}) .$$

This sequence was originally produced by Hironaka and Kin as a low-growth sequence exhibiting certain asymptotic behavior predicted by Penner [30]. This sequence is quite similar to the ψ_n in this case.

Lemma 4.2. *The braid $\sigma_{g-1, g+1}$ is conjugate to ψ_n^{-1} .*

Let's consider now the following train-track diagram below



Assume throughout this chapter (and indeed throughout the paper), unless otherwise stated, that each train-track singularity of valence ≤ 2 in a train-track graph diagram is a once-punctured singularity having exactly one peripheral edge. In the case of singularities having valence ≥ 3 , assume the singularity is non-punctured with main adjoining edges joined cyclically via peripheral edges. In this case if we write $n = 2k + 1$, then there are exactly k peripheral edges at that singularity and k is the number of “spokes” of main edges meeting there.

Having constructed these train-tracks, next consider the following train-track maps (omitting peripheral edges) where the (directed) edges are as specified in the train-track diagram:

$$\begin{aligned}
 e_1 &\rightarrow e_2 \\
 e_2 &\rightarrow e_3 \\
 &\dots \\
 &\dots \\
 e_{k-2} &\rightarrow e_{k-1} \\
 e_{k-1} &\rightarrow e_k \\
 e_k &\rightarrow e_1 \quad e_{k+1} \\
 e_{k+1} &\rightarrow e_{k+2} \\
 e_{k+2} &\rightarrow e_{k+3}
 \end{aligned}$$

$$\begin{aligned}
& \dots \\
& \dots \\
& e_{2k-2} \rightarrow e_{2k-1} \\
& e_{2k-1} \rightarrow e_{2k+1} e_{2k} \\
& e_{2k} \rightarrow e_1^{-1} e_k e_{2k+1} \\
& e_{2k+1} \rightarrow e_{k+1}^{-1} .
\end{aligned}$$

Specifying some additional information regarding peripheral edges in a natural way gives rise to an essentially unique braid in $B_n/(\partial_n^2)$. Using this particular train-track map, we may compute expressions for the corresponding braid.

Theorem 4.3. *For $n \in \mathbb{N}$, n odd and $n \geq 7$, an expression (in terms of the usual braid generators) for the automorphism ψ_n of D_n described in terms of the chosen train-track map above is $\psi_n = L_n^2 \sigma_1^{-1} \sigma_2^{-1}$.*

The associated train track map is virtually a $\frac{1}{k}$ -rotation of the train track, with each set of edges e_i, e_{k+i} getting rotated to edges e_{i+1}, e_{k+i+1} , with the exception of spokes with edges e_{k-1}, e_{2k-1} and e_k, e_{2k}, e_{2k+1} .

We will find it useful to work with the following matrix

Definition 4.4. *For $n \in \mathbb{N}$, $n \geq 2$, define the $n \times n$ matrix*

$$Z_n = \begin{pmatrix} 0 & 0 & 0 & \dots & 0 & 0 & 1 \\ 1 & 0 & 0 & \dots & 0 & 0 & 0 \\ 0 & 1 & 0 & \dots & 0 & 0 & 0 \\ 0 & 0 & 1 & \dots & 0 & 0 & 0 \\ \dots & \dots & \dots & \dots & \dots & \dots & \dots \\ \dots & \dots & \dots & \dots & \dots & \dots & \dots \\ 0 & 0 & 0 & \dots & 1 & 0 & 0 \\ 0 & 0 & 0 & \dots & 0 & 1 & 0 \end{pmatrix} .$$

The Markov matrices for our Markov partition above are similar to the Z_n . Consider the following matrices

Definition 4.5. For $n \in \mathbb{N}, n$ odd and $n \geq 7$, define the $n \times n$ matrix

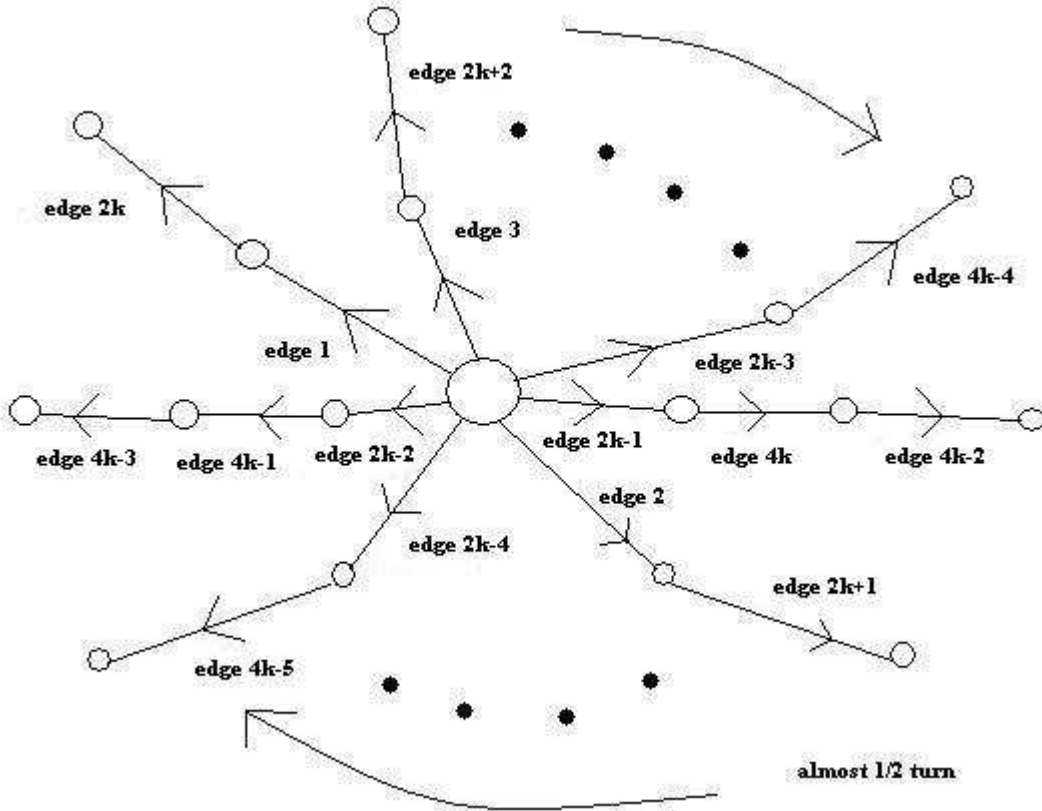
$$W_{i,j}^n = \begin{cases} 1, & (i,j) = (1,k); \\ 1, & (i,j) = (2k+1,2k-1); \\ 1, & (i,j) = (1,2k); \\ 1, & (i,j) = (k,2k); \\ -1, & (i,j) = (1,2k+1); \\ 1, & (i,j) = (k+1,2k+1); \\ 0, & \text{else .} \end{cases}$$

Fact 4.6. The Markov matrices for our train-track maps above are $M_n = Z_n + W^n$.

These matrices will be useful later on in analyzing the braids.

4.1.2 The Case $n = 4k, k \geq 2$

Having disposed of the case of odd n for the ψ_n , we move on to the case $n = 4k, k \geq 2$, which is the next simplest. Let's consider now the following train-track diagram below



Having constructed these train-tracks, next consider the following train-track maps (omitting peripheral edges) where the (directed) edges are as specified in the train-track diagram:

The corresponding train-track map is

$$\begin{aligned}
e_1 &\rightarrow e_2 \\
e_2 &\rightarrow e_3 \\
&\dots \\
&\dots \\
e_{2k-4} &\rightarrow e_{2k-3} \\
e_{2k-3} &\rightarrow e_{2k-2} \\
e_{2k-2} &\rightarrow e_{2k-1} \\
e_{2k-1} &\rightarrow e_1 e_{2k} \\
e_{2k} &\rightarrow e_{2k+1} \\
e_{2k+1} &\rightarrow e_{2k+2} \\
&\dots \\
&\dots \\
e_{4k-5} &\rightarrow e_{4k-4} \\
e_{4k-4} &\rightarrow e_{4k-1} e_{4k-3} \\
e_{4k-3} &\rightarrow e_{4k-2} \\
e_{4k-2} &\rightarrow e_1^{-1} e_{2k-2} e_{4k-1} \\
e_{4k-1} &\rightarrow e_{4k} \\
e_{4k} &\rightarrow e_{2k}^{-1} .
\end{aligned}$$

Specifying some additional information regarding peripheral edges in a natural way gives rise to an essentially unique braid in $B_n/(\partial_n^2)$. Using this particular train-track map, we may compute expressions for the corresponding braid.

Theorem 4.7. *For $n \in \mathbb{N}, n = 4k$ and $k \geq 2$, an expression (in terms of the usual braid generators) for the automorphism ψ_n of D_n described in terms of the chosen train-track map above is $\psi_n = L_n^{2k+1} \sigma_1^{-1} \sigma_2^{-1}$.*

Recall that in the case of odd n , our train-track map was essentially a $\frac{1}{k}$ -rotation clockwise. In this case, our train-track map is virtually a $\frac{1}{2}$ -rotation, with a small bit of additional twist.

The Markov matrices for our Markov partition above are again similar to the Z_n defined earlier. Consider the following matrices

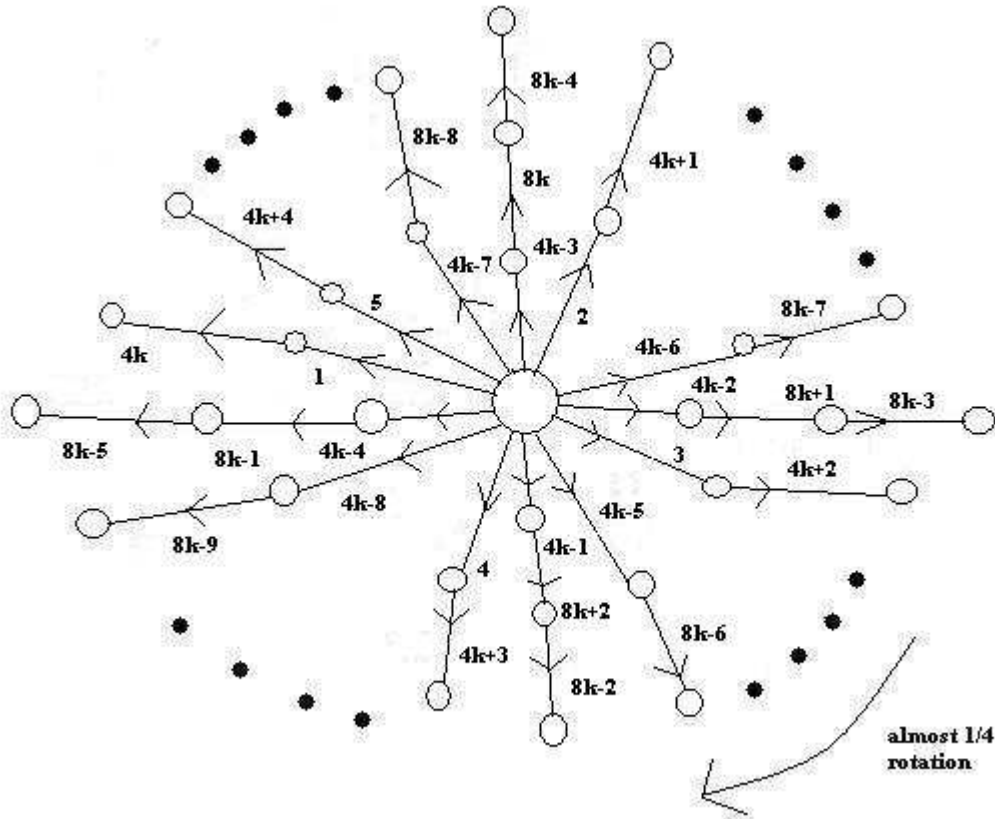
Definition 4.8. For $n \in \mathbb{N}, n = 4k$ and $k \geq 2$, define the $n \times n$ matrix

$$W_{i,j}^n = \begin{cases} 1, & (i,j) = (1,2k-1); \\ 1, & (i,j) = (4k-1,4k-4); \\ 1, & (i,j) = (1,4k-2); \\ 1, & (i,j) = (2k-2,4k-2); \\ -1, & (i,j) = (1,4k); \\ 1, & (i,j) = (2k,4k); \\ 0, & \text{else .} \end{cases}$$

Fact 4.9. The Markov matrices for our train-track maps above are $M_n = Z_n + W^n$.

4.1.3 The Case $n = 8k + 2, k \geq 2$

The case in which $n = 4k + 2$ is quite a bit trickier initially than the previous cases. It turns out that in this scenario we must actually consider two subcases: $n = 8k + 2$ and $n = 8k + 6$. Although both subcases are similar, the braids in the $n = 8k + 2$ are easier to find. Let's consider now the following train-track diagram below



Having constructed these train-tracks, next consider the following train-track maps (omitting

peripheral edges) where the (directed) edges are as specified in the train-track diagram:

The corresponding train-track map is

$$e_1 \rightarrow e_2$$

$$e_2 \rightarrow e_3$$

....

....

$$e_{4k-6} \rightarrow e_{4k-5}$$

$$e_{4k-5} \rightarrow e_{4k-4}$$

$$e_{4k-4} \rightarrow e_{4k-3}$$

$$e_{4k-3} \rightarrow e_{4k-2}$$

$$e_{4k-2} \rightarrow e_{4k-1}$$

$$e_{4k-1} \rightarrow e_1 \ e_{4k}$$

$$e_{4k} \rightarrow e_{4k+1}$$

$$e_{4k+1} \rightarrow e_{4k+2}$$

....

....

$$e_{8k-7} \rightarrow e_{8k-6}$$

$$e_{8k-6} \rightarrow e_{8k-1} \ e_{8k-5}$$

$$e_{8k-5} \rightarrow e_{8k-4}$$

$$e_{8k-4} \rightarrow e_{8k-3}$$

$$e_{8k-3} \rightarrow e_{8k-2}$$

$$e_{8k-2} \rightarrow e_1^{-1} \ e_{4k-4} \ e_{8k-1}$$

$$e_{8k-1} \rightarrow e_{8k}$$

$$e_{8k} \rightarrow e_{8k+1}$$

$$e_{8k+1} \rightarrow e_{8k+2}$$

$$e_{8k+2} \rightarrow e_{4k}^{-1} .$$

Specifying some additional information regarding peripheral edges in a natural way gives rise to an essentially unique braid in $B_n/(\partial_n^2)$. Using this particular train-track map, we may compute expressions for the corresponding braid.

Theorem 4.10. *For $n \in \mathbb{N}, n = 8k + 2$ and $k \geq 2$, an expression (in terms of the usual braid generators) for the automorphism ψ_n of D_n described by the chosen train-track map above is $\psi_n = L_n^{2k+1} \sigma_1^{-1} \sigma_2^{-1}$.*

Analogous to previous cases, our train-track map is now essentially a $\frac{1}{4}$ -rotation clockwise.

Consider the following matrices

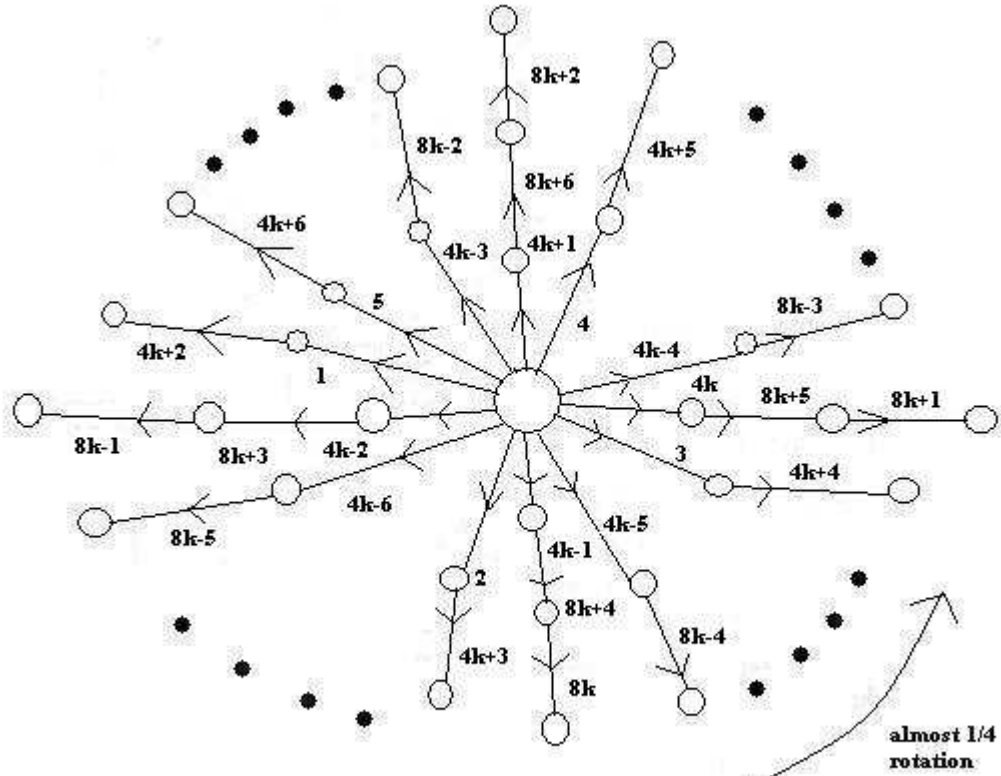
Definition 4.11. For $n \in \mathbb{N}, n = 8k + 2$ and $k \geq 2$, define the $n \times n$ matrix

$$W_{i,j}^n = \begin{cases} 1, & (i,j) = (1,4k-1); \\ 1, & (i,j) = (8k-1,8k-6); \\ 1, & (i,j) = (1,8k-2); \\ 1, & (i,j) = (4k-4,8k-2); \\ -1, & (i,j) = (1,8k+2); \\ 1, & (i,j) = (4k,8k+2); \\ 0, & \text{else .} \end{cases}$$

Fact 4.12. The Markov matrices for our train-track maps above are $M_n = Z_n + W^n$.

4.1.4 The Case $n = 8k + 6, k \geq 1$

Finally, we come to the case of ψ_n where $n = 8k + 6, k \geq 1$. This is in fact the trickiest case of all to construct experimentally, although we see ultimately it is basically the same as the $n = 8k + 2$ case. The first one is defined for $n = 14$, and indeed the computations for 14–strand braids can get complex. While our first braid in the $n = 8k + 2$ case was defined for the larger number $n = 18$, there are similarities with the exceptional ψ_{10} braid that allow for easier generalization. Let's consider now the following train-track diagram below



Having constructed these train-tracks, next consider the following train-track maps (omitting peripheral edges) where the (directed) edges are as specified in the train-track diagram:

$$e_1 \rightarrow e_2$$

$$e_2 \rightarrow e_3$$

....

....

$$e_{4k-4} \rightarrow e_{4k-3}$$

$$e_{4k-3} \rightarrow e_{4k-2}$$

$$e_{4k-2} \rightarrow e_{4k-1}$$

$$e_{4k-1} \rightarrow e_{4k}$$

$$e_{4k} \rightarrow e_{4k+1}$$

$$e_{4k+1} \rightarrow e_1 \quad e_{4k+2}$$

$$e_{4k+2} \rightarrow e_{4k+3}$$

$$e_{4k+3} \rightarrow e_{4k+4}$$

....

....

$$e_{8k-3} \rightarrow e_{8k-2}$$

$$\begin{aligned}
e_{8k-2} &\rightarrow e_{8k+3} e_{8k-1} \\
e_{8k-1} &\rightarrow e_{8k} \\
e_{8k} &\rightarrow e_{8k+1} \\
e_{8k+1} &\rightarrow e_{8k+2} \\
e_{8k+2} &\rightarrow e_1^{-1} e_{4k-2} e_{8k+3} \\
e_{8k+3} &\rightarrow e_{8k+4} \\
e_{8k+4} &\rightarrow e_{8k+5} \\
e_{8k+5} &\rightarrow e_{8k+6} \\
e_{8k+6} &\rightarrow e_{4k+2}^{-1} .
\end{aligned}$$

Specifying some additional information regarding peripheral edges in a natural way gives rise to an essentially unique braid in $B_n/(\partial_n^2)$. Using this particular train-track map, we may compute expressions for the corresponding braid.

Theorem 4.13. *For $n \in \mathbb{N}, n = 8k + 6$ and $k \geq 1$, an expression (in terms of the usual braid generators) for the automorphism ψ_n of D_n described in terms of the chosen train-track map above is $\psi_n = L_n^{6k+5} \sigma_1^{-1} \sigma_2^{-1}$.*

In the $n = 8k + 2$ case, our train-track map was virtually a $\frac{1}{4}$ -rotation clockwise. For the $n = 8k + 6$ case, we are dealing similarly with a $\frac{3}{4}$ -rotation clockwise.

Definition 4.14. *For $n \in \mathbb{N}, n = 8k + 6$ and $k \geq 1$, define the $n \times n$ matrix*

$$W_{i,j}^n = \begin{cases} 1, & (i,j) = (1,4k+1); \\ 1, & (i,j) = (8k+3,8k-2); \\ 1, & (i,j) = (1,8k+2); \\ 1, & (i,j) = (4k-2,8k+2); \\ -1, & (i,j) = (1,8k+6); \\ 1, & (i,j) = (4k+2,8k+6); \\ 0, & \text{else} . \end{cases}$$

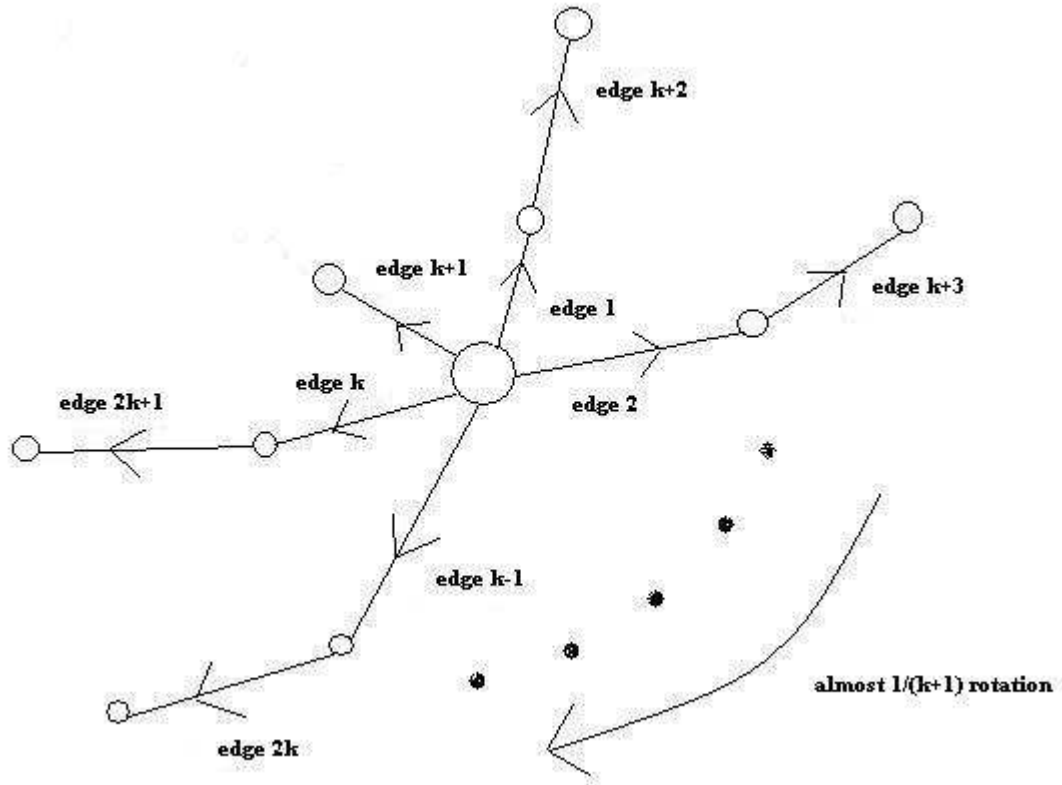
Fact 4.15. *The Markov matrices for our train-track maps above are $M_n = Z_n + W^n$.*

This completes our construction of the ψ_n sequence in the non-exceptional cases. The remaining cases $n = 5, 6, 10$ will be considered separately. But first, we turn to the $\tilde{\psi}_n$ sequence.

4.2 The $\tilde{\psi}_n$ Sequence

4.2.1 The Case of n Odd, $n \geq 5$

The $\tilde{\psi}_n$ sequence is a sort of “dual” sequence to the ψ_n sequence. That this is the case will become especially clear later on when we study mapping tori. For the moment, however, it suffices to observe the strong relationship between the train-tracks and train-track maps for the two sequences. Earlier we observed the train-tracks for the ψ_n sequence to consist of many 2–edge “spokes”, and a number of exceptional 3–edge “spokes” arranged symmetrically about the central non-punctured singularity. Analogously, our train-tracks for the $\tilde{\psi}_n$ sequence will have many 2–edge spokes like before, but this time instead a small number of exceptional 1–edge spokes. Moreover, our train-track maps for the $\tilde{\psi}_n$ will be again essentially rotations of the train-track, in precise analogy with the different cases for the ψ_n . Let’s consider now the following train-track diagram below



Having constructed these train-tracks, next consider the following train-track maps (omitting peripheral edges) where the (directed) edges are as specified in the train-track diagram:

$$e_1 \rightarrow e_2$$

$$e_2 \rightarrow e_3$$

....

$$\begin{aligned}
& \dots \\
& e_{k-1} \rightarrow e_k \\
& e_k \rightarrow e_{k+1} \\
& e_{k+1} \rightarrow e_1 e_{k+2} \\
& e_{k+2} \rightarrow e_{k+3} \\
& e_{k+3} \rightarrow e_{k+4} \\
& \dots \\
& \dots \\
& e_{2k} \rightarrow e_{2k+1} \\
& e_{2k+1} \rightarrow e_{k+1}^{-1} e_1 e_{k+2} e_{k+2}^{-1} .
\end{aligned}$$

Specifying some additional information regarding peripheral edges in a natural way gives rise to an essentially unique braid in $B_n/(\partial_n^2)$. Using this particular train-track map, we may compute expressions for the corresponding braid.

Theorem 4.16. *For $n \in \mathbb{N}$, n odd and $n \geq 5$, an expression (in terms of the usual braid generators) for the automorphism $\tilde{\psi}_n$ of D_n described by the chosen train-track map above is $\tilde{\psi}_n = L_n^2 \sigma_1 \sigma_2$.*

Note that for the $\tilde{\psi}_n$, $n = 2k + 1$ odd, we have a $\frac{1}{k+1}$ -rotation clockwise instead of a $\frac{1}{k}$ -rotation clockwise, although this is of course the same after a shift in index.

For the $\tilde{\psi}_n$ sequence, we work with matrices \tilde{W}_n and \tilde{M}_n in analogy to the W_n and M_n from previously.

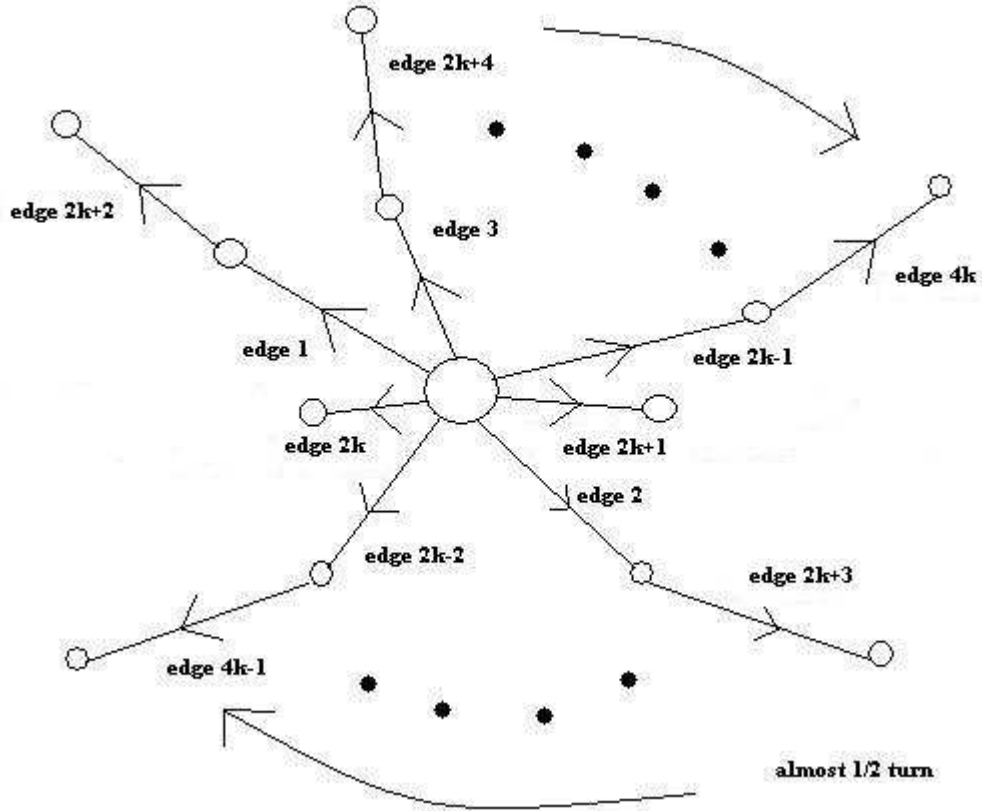
Definition 4.17. *For $n \in \mathbb{N}$, n odd and $n \geq 5$, define the $n \times n$ matrix*

$$\tilde{W}_{i,j}^n = \begin{cases} 1, & (i,j) = (1,k+1) \\ 1, & (i,j) = (k+1, 2k+1); \\ 2, & (i,j) = (k+2, 2k+1); \\ 0, & \text{else} . \end{cases}$$

Fact 4.18. *The Markov matrices for our train-track maps above are $\tilde{M}_n = Z_n + \tilde{W}^n$.*

4.2.2 The Case $n = 4k, k \geq 2$

Moving along, we analyze next the $\tilde{\psi}_n$ for $n = 4k, k \geq 2$. Let's consider now the following train-track diagram below



Having constructed these train-tracks, next consider the following train-track maps (omitting peripheral edges) where the (directed) edges are as specified in the train-track diagram:

$$e_1 \rightarrow e_2$$

$$e_2 \rightarrow e_3$$

....

....

$$e_{2k-2} \rightarrow e_{2k-1}$$

$$e_{2k-1} \rightarrow e_{2k}$$

$$e_{2k} \rightarrow e_{2k+1}$$

$$e_{2k+1} \rightarrow e_1 \ e_{2k+2}$$

$$e_{2k+2} \rightarrow e_{2k+3}$$

$$e_{2k+3} \rightarrow e_{2k+4}$$

....

....

$$e_{4k-1} \rightarrow e_{4k}$$

$$e_{4k} \rightarrow e_{2k}^{-1} \ e_1 \ e_{2k+2} \ e_{2k+2}^{-1} .$$

Specifying some additional information regarding peripheral edges in a natural way gives rise

to an essentially unique braid in $B_n/(\partial_n^2)$. Using this particular train-track map, we may compute expressions for the corresponding braid.

Theorem 4.19. *For $n \in \mathbb{N}, n = 4k$ and $k \geq 2$, an expression (in terms of the usual braid generators) for the automorphism $\tilde{\psi}_n$ of D_n corresponding to the chosen train-track map above is $\tilde{\psi}_n = L_n^{2k+1} \sigma_1 \sigma_2$.*

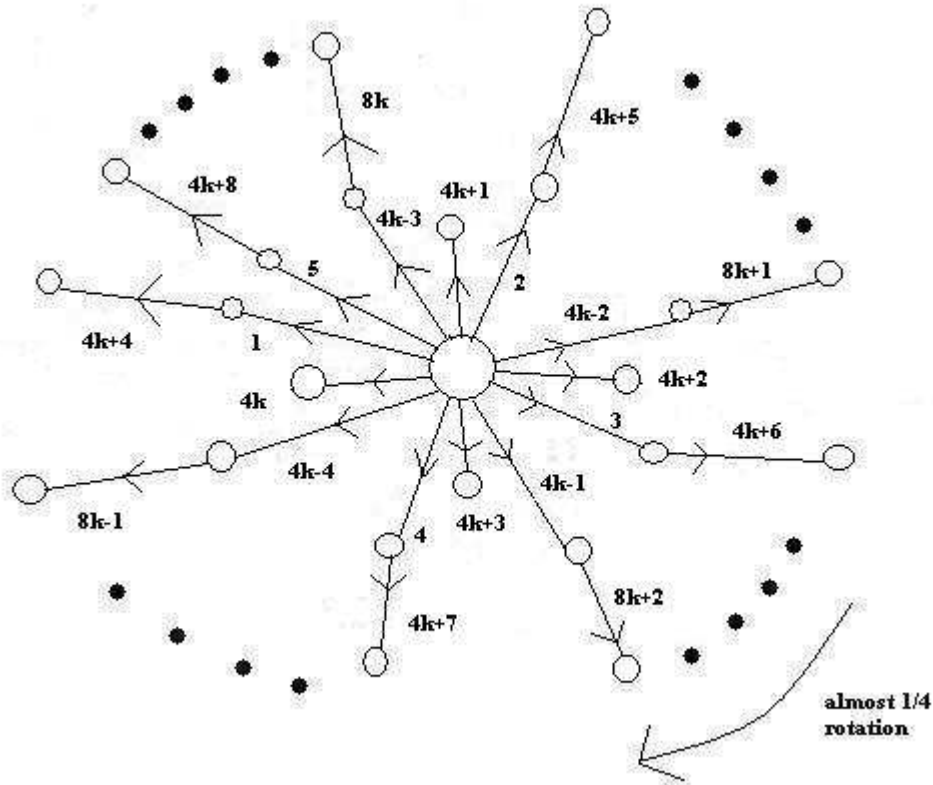
Definition 4.20. *For $n \in \mathbb{N}, n = 4k$ and $k \geq 2$, define the $n \times n$ matrix*

$$\tilde{W}_{i,j}^n = \begin{cases} 1, & (i,j) = (1,2k+1) \\ 1, & (i,j) = (2k, 4k); \\ 2, & (i,j) = (2k+2, 4k); \\ 0, & \text{else .} \end{cases}$$

Fact 4.21. *The Markov matrices for our train-track maps above are $\tilde{M}_n = Z_n + \tilde{W}^n$.*

4.2.3 The Case $n = 8k + 2, k \geq 1$

Consider now the following train-track diagram below



Having constructed these train-tracks, next consider the following train-track maps (omitting peripheral edges) where the (directed) edges are as specified in the train-track diagram:

$$\begin{aligned}
e_1 &\rightarrow e_2 \\
e_2 &\rightarrow e_3 \\
&\dots \\
&\dots \\
e_{4k-2} &\rightarrow e_{4k-1} \\
e_{4k-1} &\rightarrow e_{4k} \\
e_{4k} &\rightarrow e_{4k+1} \\
e_{4k+1} &\rightarrow e_{4k+2} \\
e_{4k+2} &\rightarrow e_{4k+3} \\
e_{4k+3} &\rightarrow e_1 e_{4k+4} \\
e_{4k+4} &\rightarrow e_{4k+5} \\
e_{4k+5} &\rightarrow e_{4k+6} \\
&\dots \\
&\dots \\
e_{8k+1} &\rightarrow e_{8k+2} \\
e_{8k+2} &\rightarrow e_{4k}^{-1} e_1 e_{4k+4} e_{4k+4}^{-1} .
\end{aligned}$$

Specifying some additional information regarding peripheral edges in a natural way gives rise to an essentially unique braid in $B_n/(\partial_n^2)$. Using this particular train-track map, we may compute expressions for the corresponding braid.

Theorem 4.22. *For $n \in \mathbb{N}, n = 8k + 2$ and $k \geq 1$, an expression (in terms of the usual braid generators) for the automorphism $\tilde{\psi}_n$ of D_n corresponding to the chosen train-track map above is $\tilde{\psi}_n = L_n^{2k+1} \sigma_1 \sigma_2$.*

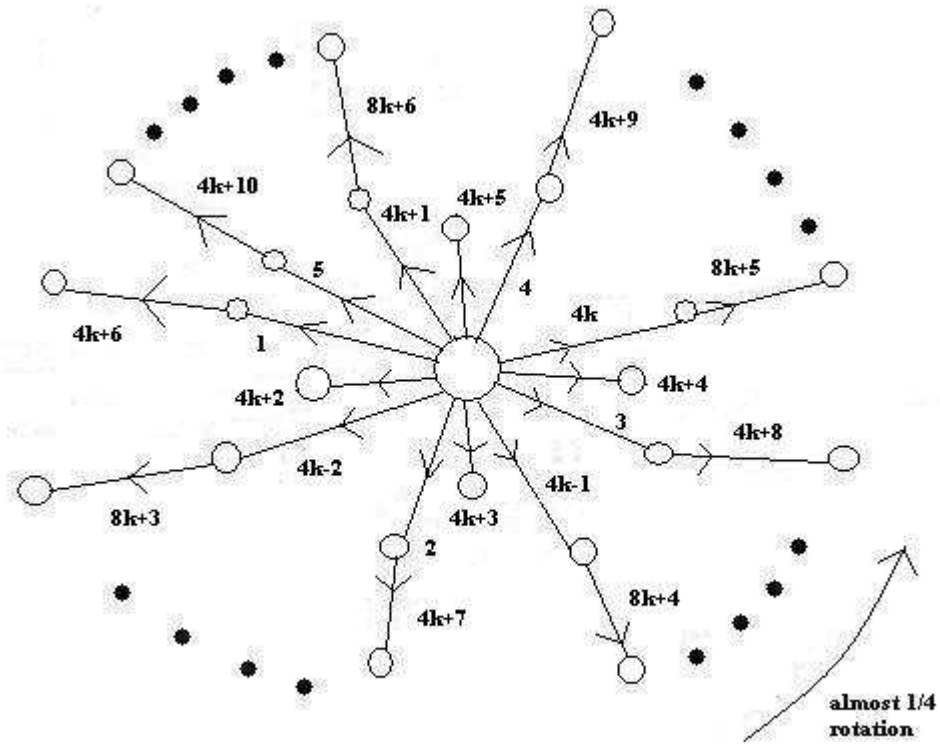
Definition 4.23. *For $n \in \mathbb{N}, n = 8k + 2$ and $k \geq 1$, define the $n \times n$ matrix*

$$W_{i,j}^n = \begin{cases} 1, & (i,j) = (1,4k+3) \\ 1, & (i,j) = (4k, 8k+2); \\ 2, & (i,j) = (4k+4, 8k+2); \\ 0, & \text{else .} \end{cases}$$

Fact 4.24. *The Markov matrices for our train-track maps above are $\tilde{M}_n = Z_n + \tilde{W}^n$.*

4.2.4 The Case $n = 8k + 6, k \geq 1$

We finally consider the following train-track diagram below



Having constructed these train-tracks, next consider the following train-track maps (omitting peripheral edges) where the (directed) edges are as specified in the train-track diagram:

$$e_1 \rightarrow e_2$$

$$e_2 \rightarrow e_3$$

....

....

$$e_{4k} \rightarrow e_{4k+1}$$

$$e_{4k+1} \rightarrow e_{4k+2}$$

$$e_{4k+2} \rightarrow e_{4k+3}$$

$$e_{4k+3} \rightarrow e_{4k+4}$$

$$e_{4k+4} \rightarrow e_{4k+5}$$

$$e_{4k+5} \rightarrow e_1 \quad e_{4k+6}$$

$$e_{4k+6} \rightarrow e_{4k+7}$$

$$e_{4k+7} \rightarrow e_{4k+8}$$

....

....

$$e_{8k+5} \rightarrow e_{8k+6}$$

$$e_{8k+6} \rightarrow e_{4k+2}^{-1} e_1 e_{4k+6} e_{4k+6}^{-1} .$$

Specifying some additional information regarding peripheral edges in a natural way gives rise to an essentially unique braid in $B_n/(\partial_n^2)$. Using this particular train-track map, we may compute expressions for the corresponding braid.

Theorem 4.25. *For $n \in \mathbb{N}, n = 8k + 6$ and $k \geq 1$, an expression (in terms of the usual braid generators) for the automorphism $\tilde{\psi}_n$ of D_n corresponding to the chosen train-track map described above is $\tilde{\psi}_n = L_n^{6k+5} \sigma_1 \sigma_2$.*

Definition 4.26. *For $n \in \mathbb{N}, n = 8k + 6$ odd and $k \geq 1$, define the $n \times n$ matrix*

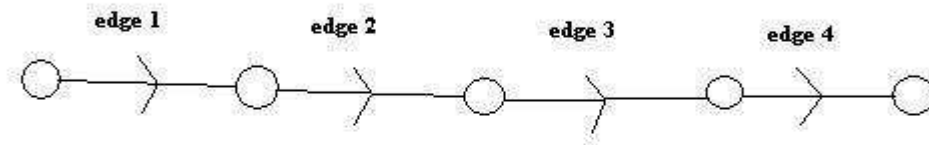
$$\tilde{W}_{i,j}^n = \begin{cases} 1, & (i,j) = (1,4k+5) \\ 1, & (i,j) = (4k+2, 8k+6); \\ 2, & (i,j) = (4k+6, 8k+6); \\ 0, & \text{else .} \end{cases}$$

Fact 4.27. *The Markov matrices for our train-track maps above are $\tilde{M}_n = Z_n + \tilde{W}^n$.*

4.3 Exceptional Cases

4.3.1 The ψ_5 Braid

As it turns out, there is in fact no natural way in which to extend the ψ_n sequence to the cases $n = 3, 4$. This is a subtle point, and more will be said about this later when we study Dehn surgeries. Consequently, the first exceptional case of ψ_n is the case $n = 5$. Consider the following train-track diagram below



Consider then the following train-track map (omitting peripheral edges) where the (directed) edges are as specified in the train-track diagram:

$$e_1 \rightarrow e_2 \ e_3$$

$$e_2 \rightarrow e_4$$

$$e_3 \rightarrow e_4^{-1} \ e_3^{-1}$$

$$e_4 \rightarrow e_2^{-1} \ e_1^{-1} .$$

The corresponding Markov matrix will be

$$M_5 = \begin{pmatrix} 0 & 0 & 0 & 1 \\ 1 & 0 & 0 & 1 \\ 1 & 0 & 1 & 0 \\ 0 & 1 & 1 & 0 \end{pmatrix} .$$

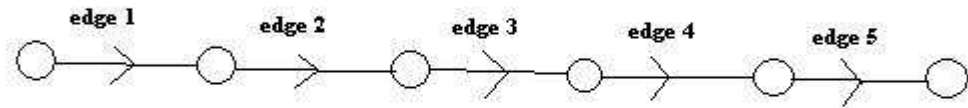
Specifying some additional information regarding peripheral edges in a natural way gives rise to an essentially unique braid in $B_n/(\partial_n^2)$. In spite of the fact that our train-track here is slightly different from those given earlier for other odd n , our braid expression will be the same.

Fact 4.28. *In terms of the usual braid group generators, the braid ψ_5 corresponding to the chosen train-track map above is $\psi_5 = L_5^2 \sigma_1^{-1} \sigma_2^{-1}$.*

Fact 4.29. *The characteristic polynomial of M_5 is $p_5 = x^4 - x^3 - x^2 - x + 1$, so that the growth rate λ_5 of φ_5 satisfies $\lambda_5 \approx 1.722084$.*

4.3.2 The ψ_6 Braid

The next exceptional case to consider is $n = 6$. This case appears to be especially exceptional, even among the other exceptional cases. Consider the following train-track diagram below



Consider then the following train-track map (omitting peripheral edges) where the (directed) edges are as specified in the train-track diagram:

$$e_1 \rightarrow e_2 \ e_3 \ e_4$$

$$e_2 \rightarrow e_5$$

$$e_3 \rightarrow e_5^{-1} \ e_4^{-1}$$

$$e_4 \rightarrow e_3^{-1}$$

$$e_5 \rightarrow e_2^{-1} \ e_1^{-1} .$$

The corresponding Markov matrix will be

$$M_6 = \begin{pmatrix} 0 & 0 & 0 & 0 & 1 \\ 1 & 0 & 0 & 0 & 1 \\ 1 & 0 & 0 & 1 & 0 \\ 1 & 0 & 1 & 0 & 0 \\ 0 & 1 & 1 & 0 & 0 \end{pmatrix}.$$

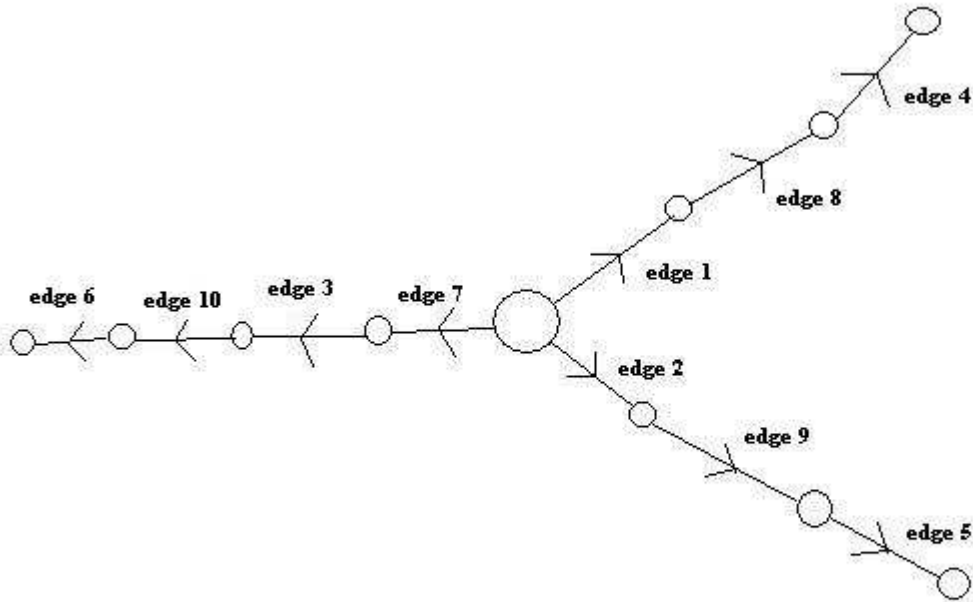
Specifying some additional information regarding peripheral edges in a natural way gives rise to an essentially unique braid in $B_n/(\partial_n^2)$.

Fact 4.30. *In terms of the usual braid group generators, the braid ψ_6 corresponding to the chosen train-track map above is $\psi_6 = \sigma_5\sigma_4\sigma_3\sigma_2\sigma_1\sigma_5\sigma_4\sigma_3\sigma_5\sigma_4$.*

Fact 4.31. *The characteristic polynomial of M_6 is $p_6 = x^5 - 2x^3 - 2x^2 + 1 = (x+1)(x^4 - x^3 - x^2 - x + 1) = (x+1)p_5(x)$, so that the growth rate λ_6 for φ_6 satisfies $\lambda_6 = \lambda_5 \approx 1.722084$.*

4.3.3 The ψ_{10} Braid

Our final exceptional case for the ψ_n sequence is the braid ψ_{10} . Consider the following train-track diagram below



Consider then the following train-track map (omitting peripheral edges) where the (directed) edges are as specified in the train-track diagram:

$$\begin{aligned}
e_1 &\rightarrow e_2 \\
e_2 &\rightarrow e_7 \ e_3 \\
e_3 &\rightarrow e_4 \\
e_4 &\rightarrow e_5 \\
e_5 &\rightarrow e_6 \\
e_6 &\rightarrow e_1^{-1} \ e_7 \\
e_7 &\rightarrow e_1 \ e_8 \\
e_8 &\rightarrow e_9 \\
e_9 &\rightarrow e_{10} \\
e_{10} &\rightarrow e_4^{-1} \ e_8^{-1} .
\end{aligned}$$

The corresponding Markov matrix will be

$$M_{10} = \begin{pmatrix} 0 & 0 & 0 & 0 & 0 & 1 & 1 & 0 & 0 & 0 \\ 1 & 0 & 0 & 0 & 0 & 0 & 0 & 0 & 0 & 0 \\ 0 & 1 & 0 & 0 & 0 & 0 & 0 & 0 & 0 & 0 \\ 0 & 0 & 1 & 0 & 0 & 0 & 0 & 0 & 0 & 1 \\ 0 & 0 & 0 & 1 & 0 & 0 & 0 & 0 & 0 & 0 \\ 0 & 0 & 0 & 0 & 1 & 0 & 0 & 0 & 0 & 0 \\ 0 & 1 & 0 & 0 & 0 & 1 & 0 & 0 & 0 & 0 \\ 0 & 0 & 0 & 0 & 0 & 0 & 1 & 0 & 0 & 1 \\ 0 & 0 & 0 & 0 & 0 & 0 & 0 & 1 & 0 & 0 \\ 0 & 0 & 0 & 0 & 0 & 0 & 0 & 0 & 1 & 0 \end{pmatrix} .$$

Specifying some additional information regarding peripheral edges in a natural way gives rise to an essentially unique braid in $B_n/(\partial_n^2)$. In spite of the fact that our train-track here is slightly different from those given earlier for other $n = 8k + 2$, our braid expression will actually be the same.

Fact 4.32. *In terms of the usual braid group generators, the braid ψ_{10} corresponding to the chosen train-track map above is $\psi_{10} = L_{10}^3 \sigma_1^{-1} \sigma_2^{-1}$.*

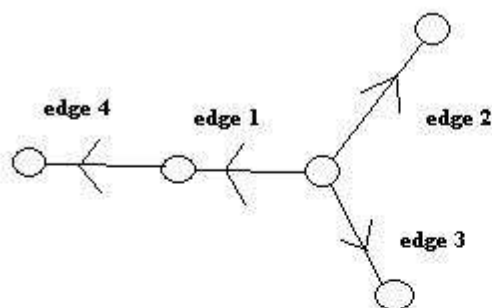
Fact 4.33. *The characteristic polynomial of M_{10} is $p_{10}(x) = x^{10} - 2x^7 - 2x^3 + 1$, so that the growth rate λ_{10} of φ_{10} is $\lambda_{10} \approx 1.352928$.*

4.3.4 The $\tilde{\psi}_3$ Braid

We define the $\tilde{\psi}_3$ simply to be the fundamental braid $\sigma_2\sigma_1^{-1}$ from before. The invariant train-track, train-track map, Markov matrix, etc., were all considered previously.

4.3.5 The $\tilde{\psi}_4$ Braid

Consider the following train-track diagram below



Consider then the following train-track map (omitting peripheral edges) where the (directed) edges are as specified in the train-track diagram:

$$e_1 \rightarrow e_2$$

$$e_2 \rightarrow e_3$$

$$e_3 \rightarrow e_1 e_4$$

$$e_4 \rightarrow e_2^{-1} e_1 e_4 e_4^{-1} .$$

The corresponding Markov matrix will be

$$\tilde{M}_4 = \begin{pmatrix} 0 & 0 & 1 & 1 \\ 1 & 0 & 0 & 1 \\ 0 & 1 & 0 & 0 \\ 0 & 0 & 1 & 2 \end{pmatrix}.$$

Specifying some additional information regarding peripheral edges in a natural way gives rise to an essentially unique braid in $B_n/(\partial_n^2)$.

Fact 4.34. *In terms of the usual braid group generators, the braid $\tilde{\psi}_4$ corresponding to the chosen train-track map above is $\psi_5 = \sigma_3\sigma_2\sigma_1^{-1}$.*

Fact 4.35. *The characteristic polynomial of \tilde{M}_4 is $p_4 = x^4 - 2x^3 - 2x + 1$, so that the growth rate $\tilde{\lambda}_4$ of $\tilde{\psi}_4$ satisfies $\tilde{\lambda}_4 \approx 2.29663$.*

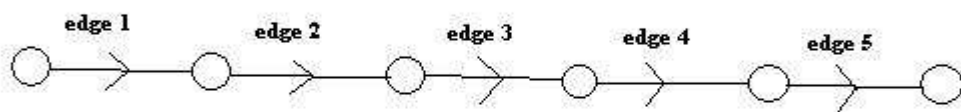
4.3.6 The $\tilde{\psi}_6$ Braid

Our final exceptional case is the $\tilde{\psi}_6$ braids. The most natural definition here seems to be to simply define $\tilde{\psi}_6 = \psi_6 = \sigma_5\sigma_4\sigma_3\sigma_2\sigma_1\sigma_5\sigma_4\sigma_3\sigma_5\sigma_4$. This braid has been considered already above.

4.3.7 The ς_6 Braid

Note that our exceptional braid $\tilde{\psi}_6 = \psi_6$ has a mapping torus consisting of three cusps rather than two, in contrast with the mapping tori of all other $\psi_n, \tilde{\psi}_n$. Taking this into account, one might naturally instead try to define the $\tilde{\psi}_6$ and ψ_6 as a twin pair of low-growth pseudo-Anosov 6-braids having two cusp mapping tori. There is indeed a natural way to do this, although we prefer to call the corresponding braids ς_6 and $\tilde{\varsigma}_6$, reserving the $\psi_6/\tilde{\psi}_6$ notation for the exceptional braid already considered.

Consider the following train-track diagram below



Consider then the following train-track map (omitting peripheral edges) where the (directed) edges are as specified in the train-track diagram:

$$e_1 \rightarrow e_2$$

$$e_2 \rightarrow e_3 \ e_4$$

$$e_3 \rightarrow e_5$$

$$e_4 \rightarrow e_5^{-1} \ e_4^{-1}$$

$$e_5 \rightarrow e_3^{-1} \ e_2^{-1} \ e_1^{-1} .$$

The corresponding Markov matrix will be

$$\begin{pmatrix} 0 & 0 & 0 & 0 & 1 \\ 1 & 0 & 0 & 0 & 1 \\ 0 & 1 & 0 & 0 & 1 \\ 0 & 1 & 0 & 1 & 0 \\ 0 & 0 & 1 & 1 & 0 \end{pmatrix} .$$

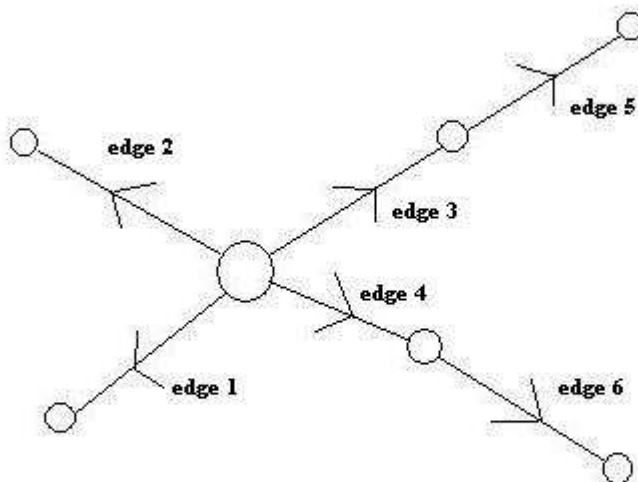
Specifying some additional information regarding peripheral edges in a natural way gives rise to an essentially unique braid in $B_n/(\partial_n^2)$.

Fact 4.36. *In terms of the usual braid group generators, the braid ς_6 corresponding to the chosen train-track map above is $\varsigma_6 = \sigma_5\sigma_4\sigma_3\sigma_2\sigma_1\sigma_5\sigma_4$.*

Fact 4.37. *The characteristic polynomial of the above matrix is $-x^5 + x^4 + x^3 + x^2 + x - 1$, so that the growth rate of ς_6 is approximately 1.8832.*

4.3.8 The $\tilde{\varsigma}_6$ Braid

We include finally for completeness a formulation of the $\tilde{\varsigma}_6$ braid. Consider the following train-track diagram below



Consider then the following train-track map (omitting peripheral edges) where the (directed) edges are as specified in the train-track diagram:

$$e_1 \rightarrow e_2$$

$$e_2 \rightarrow e_3$$

$$e_3 \rightarrow e_4$$

$$e_4 \rightarrow e_1 e_1^{-1} e_2 e_2^{-1} e_3 e_5$$

$$e_5 \rightarrow e_6$$

$$e_6 \rightarrow e_5^{-1} e_3^{-1} e_2 e_2^{-1} e_1 .$$

The corresponding Markov matrix will be

$$\begin{pmatrix} 0 & 0 & 0 & 2 & 0 & 1 \\ 1 & 0 & 0 & 2 & 0 & 2 \\ 0 & 1 & 0 & 1 & 0 & 1 \\ 0 & 0 & 1 & 0 & 0 & 0 \\ 0 & 0 & 0 & 1 & 0 & 1 \\ 0 & 0 & 0 & 0 & 1 & 0 \end{pmatrix}.$$

Specifying some additional information regarding peripheral edges in a natural way gives rise to an essentially unique braid in $B_n/(\partial_n^2)$.

Fact 4.38. *In terms of the usual braid group generators, the braid $\tilde{\zeta}_6$ corresponding to the chosen train-track map above is $\tilde{\zeta}_6 = \sigma_5\sigma_4\sigma_3\sigma_2\sigma_1\sigma_5\sigma_4\sigma_3\sigma_2\sigma_3\sigma_3\sigma_4\sigma_5$.*

Fact 4.39. *The characteristic polynomial of the above matrix is $x^6 - 2x^4 - 2x^3 - 2x^2 + 1$, so that the growth rate of $\tilde{\zeta}_6$ is again approximately 1.8832.*

Chapter 5

Entropy Considerations for the Psi and Psi-Tilde Sequences

5.1 Asymptotic Behavior

Our analysis in Chapter 3 of braids from the ψ_n and $\tilde{\psi}_n$ sequences has thus far been experimental. Having completed the full construction with train-tracks, etc., we would now like to perform a more formal analysis. As is evident from the following results, the (ψ_n) and $(\tilde{\psi}_n)$ sequences appear to have reasonably low growth rate.

Theorem 5.1. *For $n \geq 7$, the growth rate λ_n of ψ_n is equal to the largest real root of the polynomial*

1. $x^{2k+1} - 2x^{k+1} - 2x^k + 1$, when $n = 2k + 1$
2. $x^{4k} - 2x^{2k+1} - 2x^{2k-1} + 1$, when $n = 4k$
3. $x^{8k+2} - 2x^{4k+3} - 2x^{4k-1} + 1$, when $n = 8k + 2$
4. $x^{8k+6} - 2x^{4k+5} - 2x^{4k+1} + 1$, when $n = 8k + 6$.

Moreover the growth rate $\tilde{\lambda}_n$ of $\tilde{\psi}_n$ satisfies $\tilde{\lambda}_n = \lambda_n$.

Corollary 5.2. *We have $\lim_{n \rightarrow \infty} \lambda_n^n = \lim_{n \rightarrow \infty} \tilde{\lambda}_n^n = (2 + \sqrt{3})^2$.*

One may prove the theorem above via a straightforward induction that we omit here. The case of ψ_n , n odd is proved directly in [Hironaka, Kin]. All other cases may be proved similarly. Hironaka and Kin also prove the limiting behavior of the corollary for ψ_n , n odd as well, which generalizes to the other cases.

The constant $(2 + \sqrt{3})^2$ has come up several different places in our investigation, and seems like a useful constant in the braid forcing theory for some reason. We would like to know ultimately whether or not we can improve on this constant somehow among pseudo-Anosov sequences.

Conjecture 5.3. *The (ψ_n) and $(\tilde{\psi}_n)$ sequences attain minimal growth among pseudo-Anosov n -strand braids having mapping tori with 2 cusps.*

A stronger version of this conjecture would be

Conjecture 5.4. *The (ψ_n) and $(\tilde{\psi}_n)$ sequences attain minimal growth among pseudo-Anosov n -strand braids.*

The above conjectures were, after all, a large motivation behind the definition of the ψ_n and $\tilde{\psi}_n$ sequences to begin with, so this shouldn't necessarily surprise us. We believe the first conjecture above is almost certainly true, although it is a bit more difficult to say whether the second one holds. In any case there certainly is a good degree of experimental evidence for both.

Moreover from experimental considerations earlier, we observed many of the lowest growth (beyond absolute minimal growth) braids to have a form similar to the ψ_n and $\tilde{\psi}_n$.

Conjecture 5.5. *Define $K(n)$ to be the largest integer so that the lowest $K(n)$ growth pseudo-Anosov n -strand braids with 2-cusp mapping tori are all achieved by braids with expressions of the form $L_n^z \sigma_1 \sigma_2$ or $L_n^z \sigma_1^{-1} \sigma_2^{-1}$. Then, $K(n) \rightarrow \infty$ as $n \rightarrow \infty$.*

Returning again to Chapter 3 considerations, we recall the braids $\mathcal{U}(\psi_n)$ and $\mathcal{U}(\tilde{\psi}_n)$ with 3-cusp mapping tori. At this point, having gone through the train-track construction of Chapter 4, we proceed to make a critical observation.

Lemma 5.6. *The $\mathcal{U}(\psi_n)$ and $\mathcal{U}(\tilde{\psi}_n)$ can be formed by adding a single puncture to the non-punctured singularity of the invariant train-tracks of Chapter 4 for the ψ_n and $\tilde{\psi}_n$, respectively.*

More generally we expect all of the lowest growth behavior of pseudo-Anosov with mapping tori of any number of cusps to be produced in such a manner. This leads to the more sophisticated conjecture

Conjecture 5.7. *Define $\tilde{K}(n)$ to be the largest integer so that the lowest $\tilde{K}(n)$ growth pseudo-Anosov n -strand braids are all achieved by adding punctures (possibly zero punctures) to invariant train-tracks of braids with expressions of the form $L_n^z \sigma_1 \sigma_2$ or $L_n^z \sigma_1^{-1} \sigma_2^{-1}$. Then, $\tilde{K}(n) \rightarrow \infty$ as $n \rightarrow \infty$.*

One could, of course, study sequences with slightly higher growth than that of the above mentioned ones. All of the train-tracks we have come across thus far in our investigations for pseudo-Anosov n -braids of the form $L_n^z \sigma_1 \sigma_2$ or $L_n^z \sigma_1^{-1} \sigma_2^{-1}$ have either had zero singularities or precisely one central non-punctured singularity, in which case the train-track map is again virtually a rotation as before for the special Chapter 4 braids. Based on this, we note the sequences described in the conjecture above all appear to consist of powers of L_n with a few extra generators tacked on at the

end. Relative to some appropriate notion of “very small dilatation sequence,” this analysis leads to the conjecture of Benson Farb

Conjecture 5.8 (Farb). *All very small dilatation pseudo-Anosov braids should be the product of an element of finite order with something having support contained in a subsurface of universally bounded complexity.*

5.2 Astounding Sequences and the Sequential Value

From the previous section, we now conjecture the minimal growths for a sequence of n -strand pseudo-Anosov braids, n increasing, to be asymptotically $(2 + \sqrt{3})^{\frac{1}{n}}$. As we shall see later, there are numerous other sequences with similar asymptotic behavior, replacing $2 + \sqrt{3}$ with other constants. This leads us to the following quite natural definition.

Definition 5.9. *Consider a sequence (\mathcal{L}_n) of pseudo-Anosov n -braids with corresponding growths $\ell(\mathcal{L}_n)$. Then, define the **sequential value** S of (\mathcal{L}_n) to be $S = \limsup_{n \rightarrow \infty} \ell(\mathcal{L}_n)$.*

Thus our earlier conjecture may be rephrased as

Conjecture 5.10. *The minimal sequential value is $(2 + \sqrt{3})^2$.*

In general one would expect the sequential value to equal ∞ for a given sequence. However, this seems like the appropriate measure of complexity for the lowest possible growth sequences. Sequences exhibiting a finite sequential value appear especially nice to work with.

Definition 5.11. *Call a sequence (\mathcal{L}_n) of pseudo-Anosov n -braids **astounding** if the sequential value S is finite.*

A natural question likely to figure prominently in future research is the following

Question 5.12. *How can one describe explicitly the astounding sequences?*

5.3 Sparsity

Although we have not yet succeeded in proving the minimal sequential value to equal $(2 + \sqrt{3})^2$, what we do know is that the lowest growth pseudo-Anosov braids tend to have sparse Markov matrices as the number of strands gets large. Our above (ψ_n) and $(\tilde{\psi}_n)$ sequences are good examples of this.

Fact 5.13. *The Markov matrices M_n, \tilde{M}_n of Chapter 4 for $\psi_n, \tilde{\psi}_n$, respectively, $n \geq 11$, all have the sum of the entries equal to $n + 4$.*

There are certain upper bounds on the sum of the entries of a Markov matrix for a pseudo-Anosov braid in terms of its growth. For instance,

Theorem 5.14 (Ham, Song [20]). *For a pseudo-Anosov braid having growth λ and $g \times g$ Markov matrix M , the sum $|M|$ of the entries of M satisfies $|M| - g + 1 \leq \lambda^g$.*

Using our low growth sequences (ψ_n) and $(\tilde{\psi}_n)$, we obtain

Corollary 5.15. *Any Markov matrix M for a pseudo-Anosov braid of minimal growth must satisfy $|M| \leq K + 50$, where K is the dimension of M .*

The idea here is that any invariant train-track for a pseudo-Anosov n -braid should have at most $\frac{3}{2}n + P$ edges for some constant P independent of n . Using the limiting value of $(2 + \sqrt{3})^2$ from the ψ_n and $\tilde{\psi}_n$ sequences, one obtains the number 50 above via $50 = \lfloor ((2 + \sqrt{3})^2)^{\frac{3}{2}} - 1 \rfloor$.

We have many ideas on how to potentially improve this bound and suspect the bound to be quite a bit lower. Indeed, we have

Conjecture 5.16. *With possibly the exception of some trivial cases, pseudo-Anosov growth can essentially be minimized by minimizing the sum of the entries for associated Markov matrices.*

Chapter 6

Minimality of the Psi and Psi-Tilde Sequences

6.1 The $\tilde{\psi}_n$ Sequence

6.1.1 The Case of n Odd, $n \geq 5$

Recall that when a pseudo-Anosov n -braid is too complex, it may be computationally intractable to compute directly (even with a good computer algorithm) all of the pseudo-Anosov n -braids forced by this braid. Thus a motivating goal so far has been to understand the simplest possible braids, in hopes of generalizing the braid forcing order among such braids to more complex braids. With this in mind, we arrive at the following quite natural definition

Definition 6.1. *A pseudo-Anosov n -strand braid b is defined to be **minimal** if it does not force any other pseudo-Anosov braid having the same number of strands n .*

Conceivably, for any fixed n , there could be lots of minimal pseudo-Anosov n -braids. However, recall the following fact about surface automorphisms

Fact 6.2. *For any fixed $n \in \mathbb{N}, n \geq 3$, there is a finite set of train-tracks for the n -times punctured disk D_n such that any pseudo-Anosov n -braid has one of these as an invariant train-track.*

Although we shall not pursue the matter rigorously here, there is a natural way in which to factor a pseudo-Anosov n -braid as a sequence in terms of a finite set of “folding operations” applied to an invariant train-track [34, 20]. When the number of folding operations in such a factorization is too large, one generally expects the braid to force some pseudo-Anosov n -braid corresponding to a simpler sequence of folding operations. Taking this into account, we have the following conjecture

Conjecture 6.3. *For any fixed $n \in \mathbb{N}, n \geq 3$, there are finitely many minimal pseudo-Anosov n -braids.*

A natural question then is to ask

Question 6.4. *For a given $n \in \mathbb{N}$, what explicitly are all of the minimal n -braids?*

This seems like a tricky question to tackle. As we shall see later, minimal n -braids are not unique usually, and indeed there can be quite many as n grows (in spite of the finiteness conjecture). For the moment however, let's simply try to find some particular sequence of minimal pseudo-Anosov n -braids. Recall that pseudo-Anosov growth rate is a strictly monotone function. This implies

Lemma 6.5. *Any pseudo-Anosov n -braid achieving minimal growth rate among such braids is necessarily minimal.*

This suggests the $\tilde{\psi}_n$ and ψ_n are natural candidates to test for minimality.

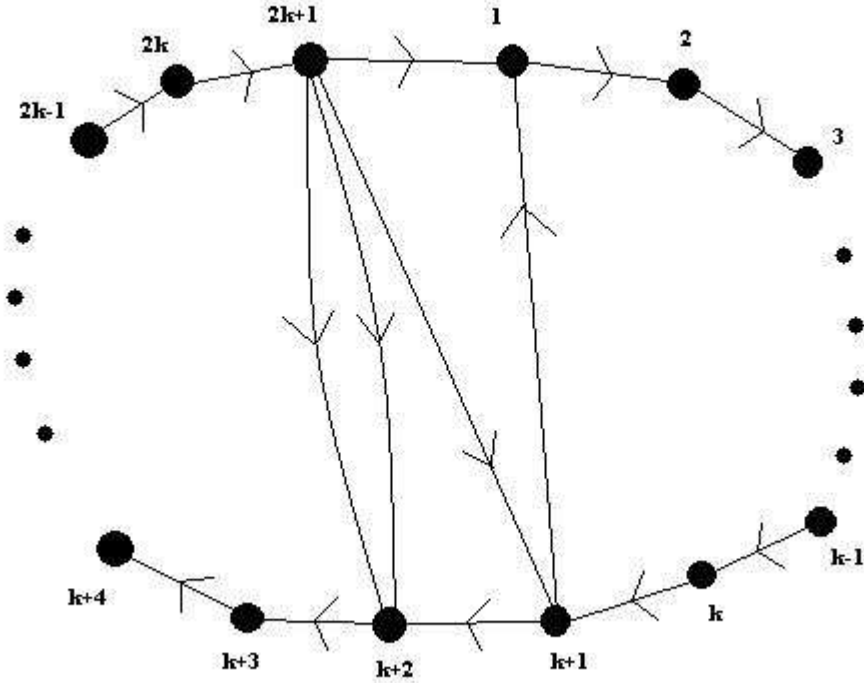
Theorem 6.6. *Whenever defined, the $\tilde{\psi}_n$ and ψ_n are minimal.*

The proof of this fact breaks into cases, according to the way in which the $\tilde{\psi}_n$ and ψ_n are defined. Moreover, the $\tilde{\psi}_n$ case seems easiest to deal with initially.

Theorem 6.7. *For $n \in \mathbb{N}$, n odd and $n \geq 5$, the braid $\tilde{\psi}_n$ is minimal.*

Proof. In order to do this we essentially compute all of the braids forced by these braids, and then check that none are pseudo-Anosov. To this end, we compute all the n -element sets of points invariant under our train-track maps. This involves building the directed adjacency graphs associated to each train-track map. The directed adjacency graph simply consists of one vertex for each main edge, along with one directed edge from v_i to v_j for each time the train-track edge i maps over the train-track edge j . Then, there is a correspondence between the n -element sets of interest and directed cycles of length n in the adjacency graph (considering cycles equivalent if they are the same after a shift of starting vertex). We find that for each of our $\psi_n, \tilde{\psi}_n$ braids that the number of forced braids is extremely small because of the way in which the train-track map is defined nicely.

When $n = 2k + 1$ is odd, the directed adjacency graph for the corresponding Markov map looks like:



In the above diagram, each vertex corresponds to the specified train-track edge in the $\tilde{\psi}_n$ train-track diagram from earlier.

In order to compute the braids forced by $\tilde{\psi}_n$ here, we next compute all of the closed paths in the directed adjacency graph having length $\leq 2k + 1$. By inspection, we find there are exactly 2 closed paths of length k , exactly 2 closed paths of length $k + 1$, exactly 3 closed paths of length $2k$, and exactly 3 closed paths of length $2k + 1$. Here, and throughout the following, we consider two closed paths as being the same even if they have different starting vertices.

For each of the closed paths above, there is some corresponding $\tilde{\psi}_n$ -invariant set. In order to describe these $\tilde{\psi}_n$ -invariant sets, we introduce coordinates on the specified train-tracks from earlier. We parametrize each directed main edge in the natural way with coordinates from the interval $[0, 1]$. Then each point on the train-track is specified as a pair (α, e) , where e is the directed main edge containing the point and α is the coordinate on that directed edge. Having defined such train-track coordinates, we would like to specify our train-track map now in terms of these coordinates. Suppose that the action f_E on a directed main edge E was specified earlier via $f_E : E \rightarrow e_1^{\epsilon_1} e_2^{\epsilon_2} \dots e_j^{\epsilon_j}$, where $\epsilon_i = \pm 1$ indicates the direction in which the edge is traversed. Then we want to use from now on a train-track map for $\tilde{\psi}_n$ defined on each interval $[\frac{i}{j}, \frac{i+1}{j}]$ of E by $(x, E) \rightarrow (jx - i, e_i)$ when $\epsilon_i = 1$,

and by $(x, E) \rightarrow (1 - (jx - i), e_i)$ when $\epsilon_i = -1$. In other words, we want each edge to map linearly over the other edges in the natural way.

The paths of length k in our directed adjacency graph are given by

node $k + 2 \rightarrow$ node $k + 3 \rightarrow$ node $k + 4 \rightarrow \dots \rightarrow$ node $2k + 1 \rightarrow$ node $k + 2$.

We have two such paths as there are two directed edges from vertex (node) $2k + 1$ to vertex $k + 2$.

The corresponding orbits in our train-track are

Orbit 1: $(\frac{2}{3}, k + 2) \rightarrow (\frac{2}{3}, k + 3) \rightarrow (\frac{2}{3}, k + 4) \rightarrow \dots \rightarrow (\frac{2}{3}, 2k + 1) \rightarrow (\frac{2}{3}, k + 2)$

Orbit 2: $(\frac{4}{5}, k + 2) \rightarrow (\frac{4}{5}, k + 3) \rightarrow (\frac{4}{5}, k + 4) \rightarrow \dots \rightarrow (\frac{4}{5}, 2k + 1) \rightarrow (\frac{4}{5}, k + 2)$.

The paths of length $k + 1$ in our directed adjacency graph are given by

1. node 1 \rightarrow node 2 \rightarrow node 3 $\rightarrow \dots \rightarrow$ node $k + 1 \rightarrow$ node 1

2. node $k + 2 \rightarrow$ node $k + 3 \rightarrow$ node $k + 4 \rightarrow \dots \rightarrow$ node $2k + 1 \rightarrow$ node $k + 1 \rightarrow$ node $k + 2$.

The first path above will in fact correspond to some fixed point p lying within the non-punctured central singularity. The second path will have a corresponding orbit

Orbit 3: $(\frac{1}{9}, k + 2) \rightarrow (\frac{1}{9}, k + 3) \rightarrow (\frac{1}{9}, k + 4) \rightarrow \dots \rightarrow (\frac{1}{9}, 2k + 1) \rightarrow (\frac{5}{9}, k + 1) \rightarrow (\frac{1}{9}, k + 2)$.

Two of the paths of length $2k$ are gotten by traversing each path of length k twice. However, these two paths give rise to the same $\tilde{\psi}_n$ -invariant sets as the corresponding paths of length k . Thus, we may disregard these two additional paths. The remaining path of length $2k$ is gotten by simply traversing one path of length k first, and then the other. This path's corresponding orbit in our train-track is

Orbit 4: $(\frac{12}{17}, k + 2) \rightarrow (\frac{12}{17}, k + 3) \rightarrow (\frac{12}{17}, k + 4) \rightarrow \dots \rightarrow (\frac{12}{17}, 2k + 1) \rightarrow (\frac{14}{17}, k + 2) \rightarrow (\frac{14}{17}, k + 3) \rightarrow (\frac{14}{17}, k + 4) \rightarrow \dots \rightarrow (\frac{14}{17}, 2k + 1) \rightarrow (\frac{12}{17}, k + 2)$.

One of the paths of length $2k + 1$ is simply

node 1 \rightarrow node 2 \rightarrow node 3 $\rightarrow \dots \rightarrow$ node $2k + 1 \rightarrow$ node 1.

This path's corresponding orbit is

Orbit 5: $(\frac{5}{7}, 1) \rightarrow (\frac{5}{7}, 2) \rightarrow (\frac{5}{7}, 3) \rightarrow \dots \rightarrow (\frac{5}{7}, k + 1) \rightarrow (\frac{3}{7}, k + 2) \rightarrow (\frac{3}{7}, k + 3) \rightarrow (\frac{3}{7}, k + 4) \rightarrow \dots \rightarrow (\frac{3}{7}, 2k + 1) \rightarrow (\frac{5}{7}, 1)$.

The remaining two paths of length $2k + 1$ are gotten by traversing first the path
 node $k + 2 \rightarrow$ node $k + 3 \rightarrow$ node $k + 4 \rightarrow \dots \rightarrow$ node $2k + 1 \rightarrow$ node $k + 1 \rightarrow$ node $k + 2$
 of length $k + 1$, and then following one of the two paths of length k .

One of these paths will have an orbit corresponding to the punctures of the original $\tilde{\psi}_n$ braid itself, and we shall disregard this orbit. The remaining orbit for this final case will be

Orbit 6: $(\frac{2}{33}, k + 2) \rightarrow (\frac{2}{33}, k + 3) \rightarrow (\frac{2}{33}, k + 4) \rightarrow \dots \rightarrow (\frac{2}{33}, 2k + 1) \rightarrow (\frac{25}{33}, k + 1) \rightarrow (\frac{17}{33}, k + 2) \rightarrow$
 $(\frac{17}{33}, k + 3) \rightarrow (\frac{17}{33}, k + 4) \rightarrow \dots \rightarrow (\frac{17}{33}, 2k + 1) \rightarrow (\frac{2}{33}, k + 2)$.

Now that we have computed the required orbits, we must try to build braids out of these orbits. It turns out we can form exactly 6 $\tilde{\psi}_n$ -invariant sets of order n here. The invariant sets, along with constituent orbits, are

Set 1: Orbit 1, Orbit 2, p

Set 2: Orbit 1, Orbit 3

Set 3: Orbit 2, Orbit 3

Set 4: Orbit 4, p

Set 5: Orbit 5

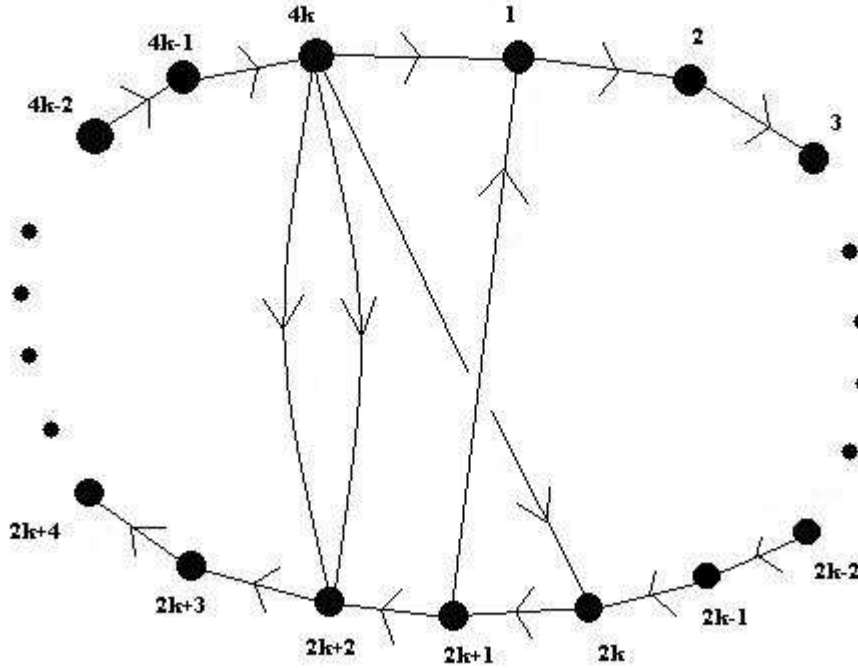
Set 6: Orbit 6.

The braid corresponding to set 1 will be $(\sigma_{n-1}\sigma_{n-2}\dots\sigma_2\sigma_1)^2\sigma_2\sigma_1$, which is reducible. The braid corresponding to set 2 will be $(\sigma_{n-1}\sigma_{n-2}\dots\sigma_2\sigma_1)^2\sigma_1$, which is reducible. The braid corresponding to set 3 will be $(\sigma_{n-1}\sigma_{n-2}\dots\sigma_2\sigma_1)^2\sigma_1$ as well. The braid corresponding to set 4 will be $(\sigma_{n-1}\sigma_{n-2}\dots\sigma_2\sigma_1)^2\sigma_1\sigma_2\sigma_1$, which is reducible. The braid corresponding to set 5 will be $(\sigma_{n-1}\sigma_{n-2}\dots\sigma_2\sigma_1)^2$, which is periodic. The braid corresponding to set 6 will be $(\sigma_{n-1}\sigma_{n-2}\dots\sigma_2\sigma_1)^2$ as well. Thus, $\tilde{\psi}_n$ is indeed minimal in this case. □

6.1.2 The Case $n = 4k, k \geq 2$

Theorem 6.8. *For $n \in \mathbb{N}, n = 4k$ and $k \geq 2$, the braid $\tilde{\psi}_n$ is minimal.*

Proof. When $n = 4k$, the directed adjacency graph for the corresponding Markov map looks like:



In the above diagram, each vertex corresponds to the specified train-track edge in the $\tilde{\psi}_n$ train-track diagram from earlier.

In order to compute the braids forced by $\tilde{\psi}_n$ here, we next compute all of the closed paths in the directed adjacency graph having length $\leq 4k$. By inspection, we find there are exactly 2 closed paths of length $2k - 1$, exactly 2 closed paths of length $2k + 1$, exactly 3 closed paths of length $4k - 2$, and exactly 3 closed paths of length $4k$.

The paths of length $2k - 1$ in our directed adjacency graph are given by
 node $2k + 2 \rightarrow$ node $2k + 3 \rightarrow$ node $2k + 4 \rightarrow \dots \rightarrow$ node $4k \rightarrow$ node $2k + 2$.

We have two such paths as there are two directed edges from vertex (node) $4k$ to vertex $2k + 2$. The corresponding orbits in our train-track are

$$\text{Orbit 1: } \left(\frac{2}{3}, 2k + 2\right) \rightarrow \left(\frac{2}{3}, 2k + 3\right) \rightarrow \left(\frac{2}{3}, 2k + 4\right) \rightarrow \dots \rightarrow \left(\frac{2}{3}, 4k\right) \rightarrow \left(\frac{2}{3}, 2k + 2\right)$$

$$\text{Orbit 2: } \left(\frac{4}{5}, 2k + 2\right) \rightarrow \left(\frac{4}{5}, 2k + 3\right) \rightarrow \left(\frac{4}{5}, 2k + 4\right) \rightarrow \dots \rightarrow \left(\frac{4}{5}, 4k\right) \rightarrow \left(\frac{4}{5}, 2k + 2\right).$$

The paths of length $2k + 1$ in our directed adjacency graph are given by

1. node 1 \rightarrow node 2 \rightarrow node 3 $\rightarrow \dots \rightarrow$ node $2k + 1 \rightarrow$ node 1
2. node $2k + 2 \rightarrow$ node $2k + 3 \rightarrow$ node $2k + 4 \rightarrow \dots \rightarrow$ node $4k \rightarrow$ node $2k \rightarrow$ node $2k + 1 \rightarrow$ node $2k + 2$.

The first path above will in fact correspond to some fixed point p lying within the non-punctured central singularity. The second path will have a corresponding orbit

Orbit 3: $(\frac{1}{9}, 2k+2) \rightarrow (\frac{1}{9}, 2k+3) \rightarrow (\frac{1}{9}, 2k+4) \rightarrow \dots \rightarrow (\frac{1}{9}, 4k) \rightarrow (\frac{5}{9}, 2k) \rightarrow (\frac{5}{9}, 2k+1) \rightarrow (\frac{1}{9}, 2k+2)$.

Two of the paths of length $4k - 2$ are gotten by traversing each path of length $2k - 1$ twice. However, these two paths give rise to the same $\tilde{\psi}_n$ -invariant sets as the corresponding paths of length $2k - 1$. Thus, we may disregard these two additional paths. The remaining path of length $4k - 2$ is gotten by simply traversing one path of length $2k - 1$ first, and then the other. This path's corresponding orbit in our train-track is

Orbit 4: $(\frac{12}{17}, 2k+2) \rightarrow (\frac{12}{17}, 2k+3) \rightarrow (\frac{12}{17}, 2k+4) \rightarrow \dots \rightarrow (\frac{12}{17}, 4k) \rightarrow (\frac{14}{17}, 2k+2) \rightarrow (\frac{14}{17}, 2k+3) \rightarrow (\frac{14}{17}, 2k+4) \rightarrow \dots \rightarrow (\frac{14}{17}, 4k) \rightarrow (\frac{12}{17}, 2k+2)$.

One of the paths of length $4k$ is simply

$$\text{node } 1 \rightarrow \text{node } 2 \rightarrow \text{node } 3 \rightarrow \dots \rightarrow \text{node } 4k \rightarrow \text{node } 1.$$

This path's corresponding orbit is

Orbit 5: $(\frac{5}{7}, 1) \rightarrow (\frac{5}{7}, 2) \rightarrow (\frac{5}{7}, 3) \rightarrow \dots \rightarrow (\frac{5}{7}, 2k+1) \rightarrow (\frac{3}{7}, 2k+2) \rightarrow (\frac{3}{7}, 2k+3) \rightarrow (\frac{3}{7}, 2k+4) \rightarrow \dots \rightarrow (\frac{3}{7}, 4k) \rightarrow (\frac{5}{7}, 1)$.

The remaining two paths of length $4k$ are gotten by traversing first the path

$$\text{node } 2k + 2 \rightarrow \text{node } 2k + 3 \rightarrow \text{node } 2k + 4 \rightarrow \dots \rightarrow \text{node } 4k \rightarrow \text{node } 2k \rightarrow \text{node } 2k + 1 \rightarrow \text{node } 2k + 2$$

of length $2k + 1$, and then following one of the two paths of length $2k - 1$.

One of these paths will have an orbit corresponding to the punctures of the original $\tilde{\psi}_n$ braid itself, and we shall disregard this orbit. The remaining orbit for this final case will be

Orbit 6: $(\frac{2}{33}, 2k+2) \rightarrow (\frac{2}{33}, 2k+3) \rightarrow (\frac{2}{33}, 2k+4) \rightarrow \dots \rightarrow (\frac{2}{33}, 4k) \rightarrow (\frac{25}{33}, 2k) \rightarrow (\frac{25}{33}, 2k+1) \rightarrow (\frac{17}{33}, 2k+2) \rightarrow (\frac{17}{33}, 2k+3) \rightarrow (\frac{17}{33}, 2k+4) \rightarrow \dots \rightarrow (\frac{17}{33}, 4k) \rightarrow (\frac{2}{33}, 2k+2)$.

Now that we have computed the required orbits, we must try to build braids out of these orbits. It turns out we can form exactly 4 $\tilde{\psi}_n$ -invariant sets of order n here. The invariant sets, along with constituent orbits, are

Set 1: Orbit 1, Orbit 3

Set 2: Orbit 2, Orbit 3

Set 3: Orbit 5

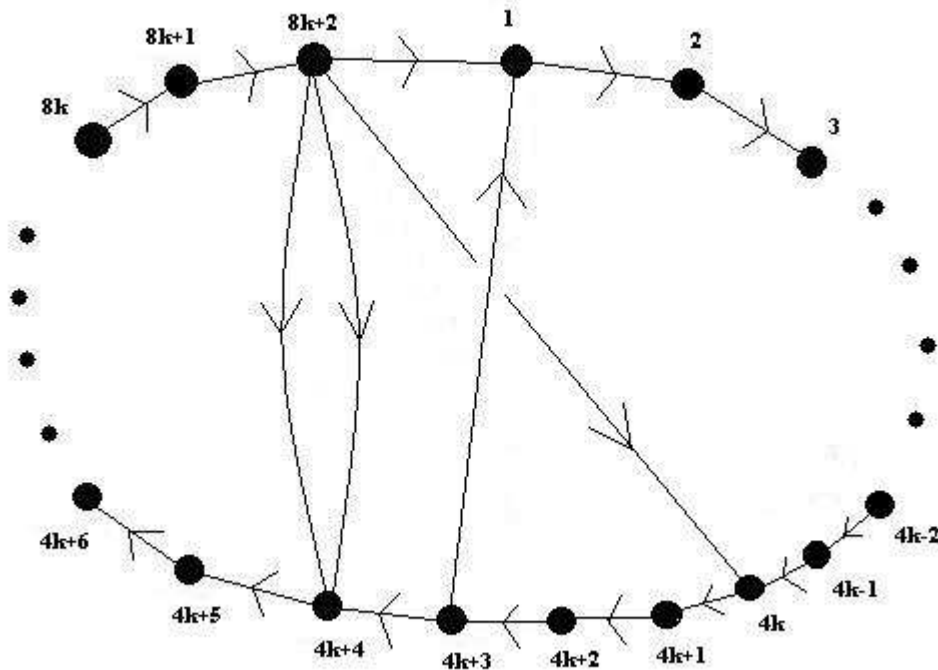
Set 4: Orbit 6.

The braid corresponding to set 1 will be $(\sigma_{n-1}\sigma_{n-2}\dots\sigma_2\sigma_1)^{2k+1}\sigma_1$, which is reducible. The braid corresponding to set 2 will be $(\sigma_{n-1}\sigma_{n-2}\dots\sigma_2\sigma_1)^{2k+1}\sigma_1$ as well. The braid corresponding to set 3 will be $(\sigma_{n-1}\sigma_{n-2}\dots\sigma_2\sigma_1)^{2k+1}$, which is periodic. The braid corresponding to set 4 will be $(\sigma_{n-1}\sigma_{n-2}\dots\sigma_2\sigma_1)^{2k+1}$ as well. Thus, $\tilde{\psi}_n$ is indeed minimal in this case. □

6.1.3 The Case $n = 8k + 2, k \geq 1$

Theorem 6.9. For $n \in \mathbb{N}, n = 8k + 2$ and $k \geq 1$, the braid $\tilde{\psi}_n$ is minimal.

Proof. When $n = 8k + 2$, the directed adjacency graph for the corresponding Markov map looks like:



In the above diagram, each vertex corresponds to the specified train-track edge in the $\tilde{\psi}_n$ train-track diagram from earlier.

In order to compute the braids forced by $\tilde{\psi}_n$ here, we next compute all of the closed paths in the directed adjacency graph having length $\leq 8k + 2$. By inspection, we find there are exactly 2 closed paths of length $4k - 1$, exactly 2 closed paths of length $4k + 3$, exactly 3 closed paths of length $8k - 2$, and exactly 3 closed paths of length $8k + 2$.

The paths of length $4k - 1$ in our directed adjacency graph are given by

node $4k + 4 \rightarrow$ node $4k + 5 \rightarrow$ node $4k + 6 \rightarrow \dots \rightarrow$ node $8k + 2 \rightarrow$ node $4k + 4$.

We have two such paths as there are two directed edges from vertex (node) $8k + 2$ to vertex $4k + 4$. The corresponding orbits in our train-track are

Orbit 1: $(\frac{2}{3}, 4k + 4) \rightarrow (\frac{2}{3}, 4k + 5) \rightarrow (\frac{2}{3}, 4k + 6) \rightarrow \dots \rightarrow (\frac{2}{3}, 8k + 2) \rightarrow (\frac{2}{3}, 4k + 4)$

Orbit 2: $(\frac{4}{5}, 4k + 4) \rightarrow (\frac{4}{5}, 4k + 5) \rightarrow (\frac{4}{5}, 4k + 6) \rightarrow \dots \rightarrow (\frac{4}{5}, 8k + 2) \rightarrow (\frac{4}{5}, 4k + 4)$.

The paths of length $4k + 3$ in our directed adjacency graph are given by

1. node 1 \rightarrow node 2 \rightarrow node 3 $\rightarrow \dots \rightarrow$ node $4k + 3 \rightarrow$ node 1

2. node $4k + 4 \rightarrow$ node $4k + 5 \rightarrow$ node $4k + 6 \rightarrow \dots \rightarrow$ node $8k + 2 \rightarrow$ node $4k \rightarrow$ node $4k + 1 \rightarrow$ node $4k + 2 \rightarrow$ node $4k + 3 \rightarrow$ node $4k + 4$.

The first path above will in fact correspond to some fixed point p lying within the non-punctured central singularity. The second path will have a corresponding orbit

Orbit 3: $(\frac{1}{9}, 4k + 4) \rightarrow (\frac{1}{9}, 4k + 5) \rightarrow (\frac{1}{9}, 4k + 6) \rightarrow \dots \rightarrow (\frac{1}{9}, 8k + 2) \rightarrow (\frac{5}{9}, 4k) \rightarrow (\frac{5}{9}, 4k + 1) \rightarrow (\frac{5}{9}, 4k + 2) \rightarrow (\frac{5}{9}, 4k + 3) \rightarrow (\frac{1}{9}, 4k + 4)$.

Two of the paths of length $8k - 2$ are gotten by traversing each path of length $4k - 1$ twice. However, these two paths give rise to the same $\tilde{\psi}_n$ -invariant sets as the corresponding paths of length $4k - 1$. Thus, we may disregard these two additional paths. The remaining path of length $8k - 2$ is gotten by simply traversing one path of length $4k - 1$ first, and then the other. This path's corresponding orbit in our train-track is

Orbit 4: $(\frac{12}{17}, 4k + 4) \rightarrow (\frac{12}{17}, 4k + 5) \rightarrow (\frac{12}{17}, 4k + 6) \rightarrow \dots \rightarrow (\frac{12}{17}, 8k + 2) \rightarrow (\frac{14}{17}, 4k + 4) \rightarrow (\frac{14}{17}, 4k + 5) \rightarrow (\frac{14}{17}, 4k + 6) \rightarrow \dots \rightarrow (\frac{14}{17}, 8k + 2) \rightarrow (\frac{12}{17}, 4k + 4)$.

One of the paths of length $8k + 2$ is simply

node 1 \rightarrow node 2 \rightarrow node 3 $\rightarrow \dots \rightarrow$ node $8k + 2 \rightarrow$ node 1.

This path's corresponding orbit is

Orbit 5: $(\frac{5}{7}, 1) \rightarrow (\frac{5}{7}, 2) \rightarrow (\frac{5}{7}, 3) \rightarrow \dots \rightarrow (\frac{5}{7}, 4k + 3) \rightarrow (\frac{3}{7}, 4k + 4) \rightarrow (\frac{3}{7}, 4k + 5) \rightarrow (\frac{3}{7}, 4k + 6) \rightarrow \dots \rightarrow (\frac{3}{7}, 8k + 2) \rightarrow (\frac{5}{7}, 1)$.

The remaining two paths of length $8k + 2$ are gotten by traversing first the path

node $4k + 4 \rightarrow$ node $4k + 5 \rightarrow$ node $4k + 6 \rightarrow \dots \rightarrow$ node $8k + 2 \rightarrow$ node $4k \rightarrow$ node $4k + 1 \rightarrow$ node $4k + 2 \rightarrow$ node $4k + 3 \rightarrow$ node $4k + 4$

of length $4k + 3$, and then following one of the two paths of length $4k - 1$.

One of these paths will have an orbit corresponding to the punctures of the original $\tilde{\psi}_n$ braid itself, and we shall disregard this orbit. The remaining orbit for this final case will be

Orbit 6: $(\frac{2}{33}, 4k + 4) \rightarrow (\frac{2}{33}, 4k + 5) \rightarrow (\frac{2}{33}, 4k + 6) \rightarrow \dots \rightarrow (\frac{2}{33}, 8k + 2) \rightarrow (\frac{25}{33}, 4k) \rightarrow (\frac{25}{33}, 4k + 1) \rightarrow (\frac{25}{33}, 4k + 2) \rightarrow (\frac{25}{33}, 4k + 3) \rightarrow (\frac{17}{33}, 4k + 4) \rightarrow (\frac{17}{33}, 4k + 5) \rightarrow (\frac{17}{33}, 4k + 6) \rightarrow \dots \rightarrow (\frac{17}{33}, 8k + 2) \rightarrow (\frac{2}{33}, 4k + 4)$.

Now that we have computed the required orbits, we must try to build braids out of these orbits. It turns out we can form exactly 4 $\tilde{\psi}_n$ -invariant sets of order n here. The invariant sets, along with constituent orbits, are

Set 1: Orbit 1, Orbit 3

Set 2: Orbit 2, Orbit 3

Set 3: Orbit 5

Set 4: Orbit 6.

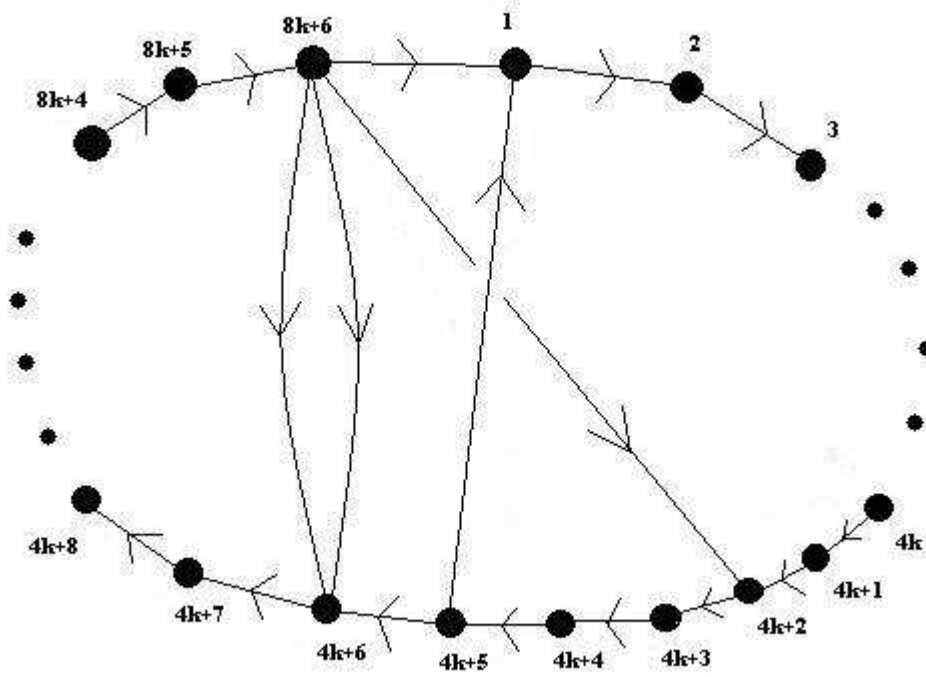
The braid corresponding to set 1 will be $(\sigma_{n-1}\sigma_{n-2}\dots\sigma_2\sigma_1)^{2k+1}\sigma_1$, which is reducible. The braid corresponding to set 2 will be $(\sigma_{n-1}\sigma_{n-2}\dots\sigma_2\sigma_1)^{2k+1}\sigma_1$ as well. The braid corresponding to set 3 will be $(\sigma_{n-1}\sigma_{n-2}\dots\sigma_2\sigma_1)^{2k+1}$, which is periodic. The braid corresponding to set 4 will be $(\sigma_{n-1}\sigma_{n-2}\dots\sigma_2\sigma_1)^{2k+1}$ as well. Thus, $\tilde{\psi}_n$ is indeed minimal in this case.

□

6.1.4 The Case $n = 8k + 6, k \geq 1$

Theorem 6.10. *For $n \in \mathbb{N}, n = 8k + 6$ and $k \geq 1$, the braid $\tilde{\psi}_n$ is minimal.*

Proof. When $n = 8k + 6$, the directed adjacency graph for the corresponding Markov map looks like:



In the above diagram, each vertex corresponds to the specified train-track edge in the $\tilde{\psi}_n$ train-track diagram from earlier.

In order to compute the braids forced by $\tilde{\psi}_n$ here, we next compute all of the closed paths in the directed adjacency graph having length $\leq 8k + 6$. By inspection, we find there are exactly 2 closed paths of length $4k + 1$, exactly 2 closed paths of length $4k + 5$, exactly 3 closed paths of length $8k + 2$, and exactly 3 closed paths of length $8k + 6$.

The paths of length $4k + 1$ in our directed adjacency graph are given by

node $4k + 6 \rightarrow$ node $4k + 7 \rightarrow$ node $4k + 8 \rightarrow \dots \rightarrow$ node $8k + 6 \rightarrow$ node $4k + 6$.

We have two such paths as there are two directed edges from vertex (node) $8k + 6$ to vertex $4k + 6$. The corresponding orbits in our train-track are

Orbit 1: $(\frac{2}{3}, 4k + 6) \rightarrow (\frac{2}{3}, 4k + 7) \rightarrow (\frac{2}{3}, 4k + 8) \rightarrow \dots \rightarrow (\frac{2}{3}, 8k + 6) \rightarrow (\frac{2}{3}, 4k + 6)$

Orbit 2: $(\frac{4}{5}, 4k + 6) \rightarrow (\frac{4}{5}, 4k + 7) \rightarrow (\frac{4}{5}, 4k + 8) \rightarrow \dots \rightarrow (\frac{4}{5}, 8k + 6) \rightarrow (\frac{4}{5}, 4k + 6)$.

The paths of length $4k + 5$ in our directed adjacency graph are given by

1. node 1 \rightarrow node 2 \rightarrow node 3 $\rightarrow \dots \rightarrow$ node $4k + 5 \rightarrow$ node 1
2. node $4k + 6 \rightarrow$ node $4k + 7 \rightarrow$ node $4k + 8 \rightarrow \dots \rightarrow$ node $8k + 6 \rightarrow$ node $4k + 2 \rightarrow$ node $4k + 3 \rightarrow$ node $4k + 4 \rightarrow$ node $4k + 5 \rightarrow$ node $4k + 6$.

The first path above will in fact correspond to some fixed point p lying within the non-punctured central singularity. The second path will have a corresponding orbit

Orbit 3: $(\frac{1}{9}, 4k + 6) \rightarrow (\frac{1}{9}, 4k + 7) \rightarrow (\frac{1}{9}, 4k + 8) \rightarrow \dots \rightarrow (\frac{1}{9}, 8k + 6) \rightarrow (\frac{5}{9}, 4k + 2) \rightarrow (\frac{5}{9}, 4k + 3) \rightarrow (\frac{5}{9}, 4k + 4) \rightarrow (\frac{5}{9}, 4k + 5) \rightarrow (\frac{1}{9}, 4k + 6)$.

Two of the paths of length $8k + 2$ are gotten by traversing each path of length $4k + 1$ twice. However, these two paths give rise to the same $\tilde{\psi}_n$ -invariant sets as the corresponding paths of length $4k + 1$. Thus, we may disregard these two additional paths. The remaining path of length $8k + 2$ is gotten by simply traversing one path of length $4k + 1$ first, and then the other. This path's corresponding orbit in our train-track is

Orbit 4: $(\frac{12}{17}, 4k + 6) \rightarrow (\frac{12}{17}, 4k + 7) \rightarrow (\frac{12}{17}, 4k + 8) \rightarrow \dots \rightarrow (\frac{12}{17}, 8k + 6) \rightarrow (\frac{14}{17}, 4k + 6) \rightarrow (\frac{14}{17}, 4k + 7) \rightarrow (\frac{14}{17}, 4k + 8) \rightarrow \dots \rightarrow (\frac{14}{17}, 8k + 6) \rightarrow (\frac{12}{17}, 4k + 6)$.

One of the paths of length $8k + 6$ is simply

node 1 \rightarrow node 2 \rightarrow node 3 $\rightarrow \dots \rightarrow$ node $8k + 6 \rightarrow$ node 1.

This path's corresponding orbit is

Orbit 5: $(\frac{5}{7}, 1) \rightarrow (\frac{5}{7}, 2) \rightarrow (\frac{5}{7}, 3) \rightarrow \dots \rightarrow (\frac{5}{7}, 4k + 5) \rightarrow (\frac{3}{7}, 4k + 6) \rightarrow (\frac{3}{7}, 4k + 7) \rightarrow (\frac{3}{7}, 4k + 8) \rightarrow \dots \rightarrow (\frac{3}{7}, 8k + 6) \rightarrow (\frac{5}{7}, 1)$.

The remaining two paths of length $8k + 6$ are gotten by traversing first the path

node $4k + 6 \rightarrow$ node $4k + 7 \rightarrow$ node $4k + 8 \rightarrow \dots \rightarrow$ node $8k + 6 \rightarrow$ node $4k + 2 \rightarrow$ node $4k + 3 \rightarrow$ node $4k + 4 \rightarrow$ node $4k + 5 \rightarrow$ node $4k + 6$

of length $4k + 5$, and then following one of the two paths of length $4k + 1$.

One of these paths will have an orbit corresponding to the punctures of the original $\tilde{\psi}_n$ braid itself, and we shall disregard this orbit. The remaining orbit for this final case will be

Orbit 6: $(\frac{2}{33}, 4k + 6) \rightarrow (\frac{2}{33}, 4k + 7) \rightarrow (\frac{2}{33}, 4k + 8) \rightarrow \dots \rightarrow (\frac{2}{33}, 8k + 6) \rightarrow (\frac{25}{33}, 4k + 2) \rightarrow (\frac{25}{33}, 4k + 3) \rightarrow (\frac{25}{33}, 4k + 4) \rightarrow (\frac{25}{33}, 4k + 5) \rightarrow (\frac{17}{33}, 4k + 6) \rightarrow (\frac{17}{33}, 4k + 7) \rightarrow (\frac{17}{33}, 4k + 8) \rightarrow \dots \rightarrow (\frac{17}{33}, 8k + 6) \rightarrow (\frac{2}{33}, 4k + 6)$.

Now that we have computed the required orbits, we must try to build braids out of these orbits. It turns out we can form exactly 4 $\tilde{\psi}_n$ -invariant sets of order n here. The invariant sets, along with constituent orbits, are

Set 1: Orbit 1, Orbit 3

Set 2: Orbit 2, Orbit 3

Set 3: Orbit 5

Set 4: Orbit 6.

The braid corresponding to set 1 will be $(\sigma_{n-1}\sigma_{n-2}\dots\sigma_2\sigma_1)^{6k+5}\sigma_1$, which is reducible. The braid corresponding to set 2 will be $(\sigma_{n-1}\sigma_{n-2}\dots\sigma_2\sigma_1)^{6k+5}\sigma_1$ as well. The braid corresponding to set 3 will be $(\sigma_{n-1}\sigma_{n-2}\dots\sigma_2\sigma_1)^{6k+5}$, which is periodic. The braid corresponding to set 4 will be $(\sigma_{n-1}\sigma_{n-2}\dots\sigma_2\sigma_1)^{6k+5}$ as well. Thus, $\tilde{\psi}_n$ is indeed minimal in this case.

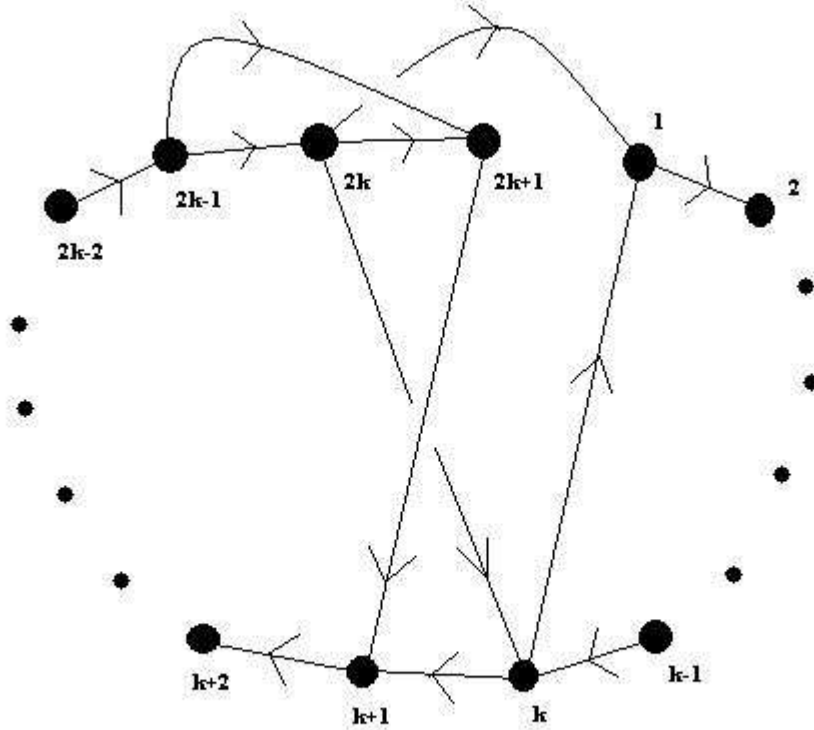
□

6.2 The ψ_n Sequence

6.2.1 The Case of n Odd, $n \geq 7$

Theorem 6.11. *For $n \in \mathbb{N}$, n odd and $n \geq 7$, the braid ψ_n is minimal.*

Proof. When $n = 2k + 1$ is odd, the directed adjacency graph for the corresponding Markov map looks like:



In the above diagram, each vertex corresponds to the specified train-track edge in the ψ_n train-track diagram from earlier.

In order to compute the braids forced by ψ_n here, we next compute all of the closed paths in the directed adjacency graph having length $\leq 2k + 1$. By inspection, we find there are exactly 2 closed paths of length k , exactly 2 closed paths of length $k + 1$, exactly 3 closed paths of length $2k$, and exactly 3 closed paths of length $2k + 1$.

The paths of length k in our directed adjacency graph are given by

1. node 1 \rightarrow node 2 \rightarrow node 3 $\rightarrow \dots \rightarrow$ node $k \rightarrow$ node 1
2. node $k + 1 \rightarrow$ node $k + 2 \rightarrow$ node $k + 3 \rightarrow \dots \rightarrow$ node $2k - 2 \rightarrow$ node $2k - 1 \rightarrow$ node $2k + 1 \rightarrow$ node $k + 1$.

The first path above will in fact correspond to some fixed point p lying within the non-punctured central singularity. The second path will have a corresponding orbit

Orbit 1: $(\frac{1}{3}, k + 1) \rightarrow (\frac{1}{3}, k + 2) \rightarrow (\frac{1}{3}, k + 3) \rightarrow \dots \rightarrow (\frac{1}{3}, 2k - 2) \rightarrow (\frac{1}{3}, 2k - 1) \rightarrow (\frac{2}{3}, 2k + 1) \rightarrow (\frac{1}{3}, k + 1)$.

The paths of length $k + 1$ in our directed adjacency graph are given by

1. node $k + 1 \rightarrow$ node $k + 2 \rightarrow$ node $k + 3 \rightarrow \dots \rightarrow$ node $2k - 1 \rightarrow$ node $2k \rightarrow$ node $k \rightarrow$ node $k + 1$
2. node $k + 1 \rightarrow$ node $k + 2 \rightarrow$ node $k + 3 \rightarrow \dots \rightarrow$ node $2k - 1 \rightarrow$ node $2k \rightarrow$ node $2k + 1 \rightarrow$ node $k + 1$.

These paths, respectively, will have corresponding orbits

Orbit 2: $(\frac{9}{11}, k+1) \rightarrow (\frac{9}{11}, k+2) \rightarrow (\frac{9}{11}, k+3) \rightarrow \dots \rightarrow (\frac{9}{11}, 2k-1) \rightarrow (\frac{7}{11}, 2k) \rightarrow (\frac{10}{11}, k) \rightarrow (\frac{9}{11}, k+1)$

Orbit 3: $(\frac{6}{7}, k+1) \rightarrow (\frac{6}{7}, k+2) \rightarrow (\frac{6}{7}, k+3) \rightarrow \dots \rightarrow (\frac{6}{7}, 2k-1) \rightarrow (\frac{5}{7}, 2k) \rightarrow (\frac{1}{7}, 2k+1) \rightarrow (\frac{6}{7}, k+1)$.

Two of the paths of length $2k$ are gotten by traversing each path of length k twice. However, these two paths give rise to the same ψ_n -invariant sets as the corresponding paths of length k . Thus, we may disregard these two additional paths. The remaining path of length $2k$ is simply

$$\text{node } 1 \rightarrow \text{node } 2 \rightarrow \text{node } 3 \rightarrow \dots \rightarrow \text{node } 2k - 1 \rightarrow \text{node } 2k \rightarrow \text{node } 1.$$

This path's corresponding orbit in our train-track is

Orbit 4: $(\frac{10}{13}, 1) \rightarrow (\frac{10}{13}, 2) \rightarrow (\frac{10}{13}, 3) \rightarrow \dots \rightarrow (\frac{10}{13}, k) \rightarrow (\frac{7}{13}, k+1) \rightarrow (\frac{7}{13}, k+2) \rightarrow (\frac{7}{13}, k+3) \rightarrow \dots \rightarrow (\frac{7}{13}, 2k-1) \rightarrow (\frac{1}{13}, 2k) \rightarrow (\frac{10}{13}, 1)$.

One of the paths of length $2k + 1$ is

$$\text{node } 1 \rightarrow \text{node } 2 \rightarrow \text{node } 3 \rightarrow \dots \rightarrow \text{node } 2k \rightarrow \text{node } k \rightarrow \text{node } 1.$$

This path's corresponding orbit is

Orbit 5: $(\frac{20}{23}, 1) \rightarrow (\frac{20}{23}, 2) \rightarrow (\frac{20}{23}, 3) \rightarrow \dots \rightarrow (\frac{20}{23}, k) \rightarrow (\frac{17}{23}, k+1) \rightarrow (\frac{17}{23}, k+2) \rightarrow (\frac{17}{23}, k+3) \rightarrow \dots \rightarrow (\frac{17}{23}, 2k-1) \rightarrow (\frac{11}{23}, 2k) \rightarrow (\frac{10}{23}, k) \rightarrow (\frac{20}{23}, 1)$.

The remaining two paths of length $2k + 1$ are gotten by traversing first the path

$$\text{node } k + 1 \rightarrow \text{node } k + 2 \rightarrow \text{node } k + 3 \rightarrow \dots \rightarrow \text{node } 2k - 2 \rightarrow \text{node } 2k - 1 \rightarrow \text{node } 2k + 1 \rightarrow \text{node } k + 1$$

of length k , and then following one of the two paths of length $k + 1$.

One of these paths will have an orbit corresponding to the punctures of the original ψ_n braid itself, and we shall disregard this orbit. The remaining orbit for this final case will be

Orbit 6: $(\frac{3}{25}, k+1) \rightarrow (\frac{3}{25}, k+2) \rightarrow (\frac{3}{25}, k+3) \rightarrow \dots \rightarrow (\frac{3}{25}, 2k-1) \rightarrow (\frac{6}{25}, 2k+1) \rightarrow (\frac{19}{25}, k+1) \rightarrow (\frac{19}{25}, k+2) \rightarrow (\frac{19}{25}, k+3) \rightarrow \dots \rightarrow (\frac{19}{25}, 2k-1) \rightarrow (\frac{13}{25}, 2k) \rightarrow (\frac{14}{25}, k) \rightarrow (\frac{3}{25}, k+1)$.

Now that we have computed the required orbits, we must try to build braids out of these orbits. It turns out we can form exactly 5 ψ_n -invariant sets of order n here. The invariant sets, along with constituent orbits, are

Set 1: Orbit 1, Orbit 3

Set 2: Orbit 2, Orbit 3

Set 3: Orbit 4, p

Set 4: Orbit 5

Set 5: Orbit 6.

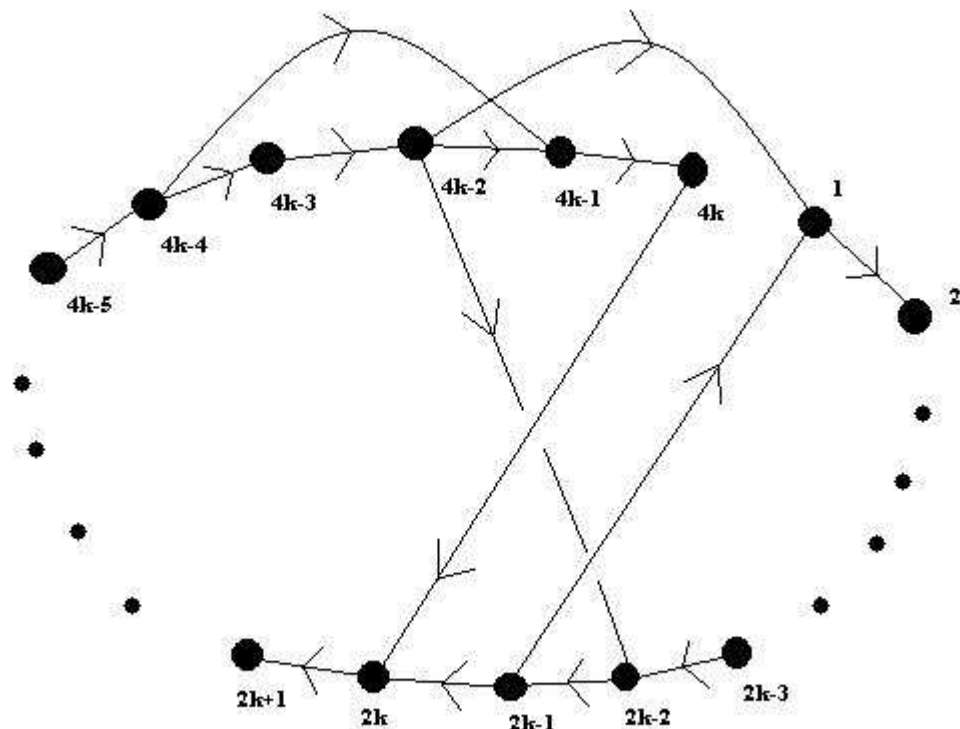
The braid corresponding to set 1 will be $(\sigma_{n-1}\sigma_{n-2}\dots\sigma_2\sigma_1)^2\sigma_1^{-1}$, which is reducible. The braid corresponding to set 2 will be $(\sigma_{n-1}\sigma_{n-2}\dots\sigma_2\sigma_1)^2\sigma_1^{-1}$ as well. The braid corresponding to set 3 will be $(\sigma_{n-1}\sigma_{n-2}\dots\sigma_2\sigma_1)^2\sigma_1^{-1}\sigma_2\sigma_1$, which is reducible. The braid corresponding to set 4 will be $(\sigma_{n-1}\sigma_{n-2}\dots\sigma_2\sigma_1)^2$, which is periodic. The braid corresponding to set 5 will be $(\sigma_{n-1}\sigma_{n-2}\dots\sigma_2\sigma_1)^2$ as well. Thus, ψ_n is indeed minimal in this case.

□

6.2.2 The Case $n = 4k, k \geq 2$

Theorem 6.12. *For $n \in \mathbb{N}, n = 4k$ and $k \geq 2$, the braid ψ_n is minimal.*

Proof. When $n = 4k$, the directed adjacency graph for the corresponding Markov map looks like:



In the above diagram, each vertex corresponds to the specified train-track edge in the ψ_n train-track diagram from earlier.

In order to compute the braids forced by ψ_n here, we next compute all of the closed paths in the directed adjacency graph having length $\leq 4k$. By inspection, we find there are exactly 2 closed paths of length $2k - 1$, exactly 2 closed paths of length $2k + 1$, exactly 3 closed paths of length $4k - 2$, and exactly 3 closed paths of length $4k$.

The paths of length $2k - 1$ in our directed adjacency graph are given by

1. node 1 \rightarrow node 2 \rightarrow node 3 $\rightarrow \dots \rightarrow$ node $2k - 1$ \rightarrow node 1
2. node $2k$ \rightarrow node $2k + 1$ \rightarrow node $2k + 2$ $\rightarrow \dots \rightarrow$ node $4k - 5$ \rightarrow node $4k - 4$ \rightarrow node $4k - 1$ \rightarrow node $4k$ \rightarrow node $2k$.

The first path above will in fact correspond to some fixed point p lying within the non-punctured central singularity. The second path will have a corresponding orbit

Orbit 1: $(\frac{1}{3}, 2k) \rightarrow (\frac{1}{3}, 2k + 1) \rightarrow (\frac{1}{3}, 2k + 2) \rightarrow \dots \rightarrow (\frac{1}{3}, 4k - 5) \rightarrow (\frac{1}{3}, 4k - 4) \rightarrow (\frac{2}{3}, 4k - 1) \rightarrow (\frac{2}{3}, 4k) \rightarrow (\frac{1}{3}, 2k)$.

The paths of length $2k + 1$ in our directed adjacency graph are given by

1. node $2k \rightarrow$ node $2k + 1 \rightarrow$ node $2k + 2 \rightarrow \dots \rightarrow$ node $4k - 3 \rightarrow$ node $4k - 2 \rightarrow$ node $2k - 2 \rightarrow$
node $2k - 1 \rightarrow$ node $2k$
2. node $2k \rightarrow$ node $2k + 1 \rightarrow$ node $2k + 2 \rightarrow \dots \rightarrow$ node $4k - 2 \rightarrow$ node $4k - 1 \rightarrow$ node $4k \rightarrow$
node $2k$.

These paths, respectively, will have corresponding orbits

Orbit 2: $(\frac{9}{11}, 2k) \rightarrow (\frac{9}{11}, 2k + 1) \rightarrow (\frac{9}{11}, 2k + 2) \rightarrow \dots \rightarrow (\frac{9}{11}, 4k - 4) \rightarrow (\frac{7}{11}, 4k - 3) \rightarrow (\frac{7}{11}, 4k - 2) \rightarrow$
 $(\frac{10}{11}, 2k - 2) \rightarrow (\frac{10}{11}, 2k - 1) \rightarrow (\frac{9}{11}, 2k)$

Orbit 3: $(\frac{6}{7}, 2k) \rightarrow (\frac{6}{7}, 2k + 1) \rightarrow (\frac{6}{7}, 2k + 2) \rightarrow \dots \rightarrow (\frac{6}{7}, 4k - 4) \rightarrow (\frac{5}{7}, 4k - 3) \rightarrow (\frac{5}{7}, 4k - 2) \rightarrow$
 $(\frac{1}{7}, 4k - 1) \rightarrow (\frac{1}{7}, 4k) \rightarrow (\frac{6}{7}, 2k)$.

Two of the paths of length $4k - 2$ are gotten by traversing each path of length $2k - 1$ twice. However, these two paths give rise to the same ψ_n -invariant sets as the corresponding paths of length $2k - 1$. Thus, we may disregard these two additional paths. The remaining path of length $4k - 2$ is simply

$$\text{node } 1 \rightarrow \text{node } 2 \rightarrow \text{node } 3 \rightarrow \dots \rightarrow \text{node } 4k - 3 \rightarrow \text{node } 4k - 2 \rightarrow \text{node } 1.$$

This path's corresponding orbit in our train-track is

Orbit 4: $(\frac{10}{13}, 1) \rightarrow (\frac{10}{13}, 2) \rightarrow (\frac{10}{13}, 3) \rightarrow \dots \rightarrow (\frac{10}{13}, 2k - 1) \rightarrow (\frac{7}{13}, 2k) \rightarrow (\frac{7}{13}, 2k + 1) \rightarrow (\frac{7}{13}, 2k + 2) \rightarrow$
 $\dots \rightarrow (\frac{7}{13}, 4k - 4) \rightarrow (\frac{1}{13}, 4k - 3) \rightarrow (\frac{1}{13}, 4k - 2) \rightarrow (\frac{10}{13}, 1)$.

One of the paths of length $4k$ is

$$\text{node } 1 \rightarrow \text{node } 2 \rightarrow \text{node } 3 \rightarrow \dots \rightarrow \text{node } 4k - 2 \rightarrow \text{node } 2k - 2 \rightarrow \text{node } 2k - 1 \rightarrow \text{node } 1.$$

This path's corresponding orbit is

Orbit 5: $(\frac{20}{23}, 1) \rightarrow (\frac{20}{23}, 2) \rightarrow (\frac{20}{23}, 3) \rightarrow \dots \rightarrow (\frac{20}{23}, 2k - 1) \rightarrow (\frac{17}{23}, 2k) \rightarrow (\frac{17}{23}, 2k + 1) \rightarrow (\frac{17}{23}, 2k + 2) \rightarrow$
 $\dots \rightarrow (\frac{17}{23}, 4k - 4) \rightarrow (\frac{11}{23}, 4k - 3) \rightarrow (\frac{11}{23}, 4k - 2) \rightarrow (\frac{10}{23}, 2k - 2) \rightarrow (\frac{10}{23}, 2k - 1) \rightarrow (\frac{20}{23}, 1)$.

The remaining two paths of length $4k$ are gotten by traversing first the path

$$\text{node } 2k \rightarrow \text{node } 2k + 1 \rightarrow \text{node } 2k + 2 \rightarrow \dots \rightarrow \text{node } 4k - 5 \rightarrow \text{node } 4k - 4 \rightarrow \text{node } 4k - 1 \rightarrow \text{node } 4k \rightarrow \text{node } 2k$$

of length $2k - 1$, and then following one of the two paths of length $2k + 1$.

One of these paths will have an orbit corresponding to the punctures of the original ψ_n braid itself, and we shall disregard this orbit. The remaining orbit for this final case will be

$$\begin{aligned} \text{Orbit 6: } & \left(\frac{3}{25}, 2k\right) \rightarrow \left(\frac{3}{25}, 2k+1\right) \rightarrow \left(\frac{3}{25}, 2k+2\right) \rightarrow \dots \rightarrow \left(\frac{3}{25}, 4k-4\right) \rightarrow \left(\frac{6}{25}, 4k-1\right) \rightarrow \left(\frac{6}{25}, 4k\right) \rightarrow \\ & \left(\frac{19}{25}, 2k\right) \rightarrow \left(\frac{19}{25}, 2k+1\right) \rightarrow \left(\frac{19}{25}, 2k+2\right) \rightarrow \dots \rightarrow \left(\frac{19}{25}, 4k-4\right) \rightarrow \left(\frac{13}{25}, 4k-3\right) \rightarrow \left(\frac{13}{25}, 4k-2\right) \rightarrow \\ & \left(\frac{14}{25}, 2k-2\right) \rightarrow \left(\frac{14}{25}, 2k-1\right) \rightarrow \left(\frac{3}{25}, 2k\right). \end{aligned}$$

Now that we have computed the required orbits, we must try to build braids out of these orbits. It turns out we can form exactly 4 ψ_n -invariant sets of order n here. The invariant sets, along with constituent orbits, are

Set 1: Orbit 1, Orbit 3

Set 2: Orbit 2, Orbit 3

Set 3: Orbit 5

Set 4: Orbit 6.

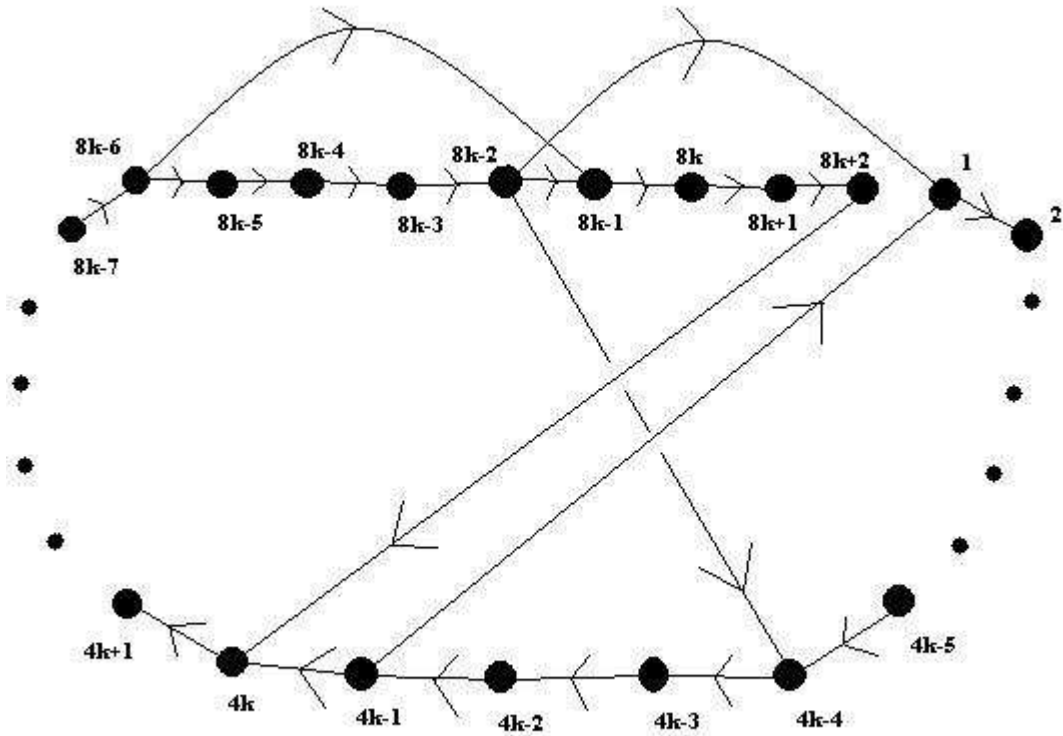
The braid corresponding to set 1 will be $(\sigma_{n-1}\sigma_{n-2}\dots\sigma_2\sigma_1)^{2k+1}\sigma_1^{-1}$, which is reducible. The braid corresponding to set 2 will be $(\sigma_{n-1}\sigma_{n-2}\dots\sigma_2\sigma_1)^{2k+1}\sigma_1^{-1}$ as well. The braid corresponding to set 3 will be $(\sigma_{n-1}\sigma_{n-2}\dots\sigma_2\sigma_1)^{2k+1}$, which is periodic. The braid corresponding to set 4 will be $(\sigma_{n-1}\sigma_{n-2}\dots\sigma_2\sigma_1)^{2k+1}$ as well. Thus, ψ_n is indeed minimal in this case.

□

6.2.3 The Case $n = 8k + 2, k \geq 2$

Theorem 6.13. *For $n \in \mathbb{N}, n = 8k + 2$ and $k \geq 2$, the braid ψ_n is minimal.*

Proof. When $n = 8k + 2$, the directed adjacency graph for the corresponding Markov map looks like:



In the above diagram, each vertex corresponds to the specified train-track edge in the ψ_n train-track diagram from earlier.

In order to compute the braids forced by ψ_n here, we next compute all of the closed paths in the directed adjacency graph having length $\leq 8k + 2$. By inspection, we find there are exactly 2 closed paths of length $4k - 1$, exactly 2 closed paths of length $4k + 3$, exactly 3 closed paths of length $8k - 2$, and exactly 3 closed paths of length $8k + 2$.

The paths of length $4k - 1$ in our directed adjacency graph are given by

1. node 1 \rightarrow node 2 \rightarrow node 3 $\rightarrow \dots \rightarrow$ node $4k - 1$ \rightarrow node 1
2. node $4k$ \rightarrow node $4k + 1$ \rightarrow node $4k + 2$ $\rightarrow \dots \rightarrow$ node $8k - 7$ \rightarrow node $8k - 6$ \rightarrow node $8k - 1$ \rightarrow node $8k$ \rightarrow node $8k + 1$ \rightarrow node $8k + 2$ \rightarrow node $4k$.

The first path above will in fact correspond to some fixed point p lying within the non-punctured central singularity. The second path will have a corresponding orbit

Orbit 1: $(\frac{1}{3}, 4k) \rightarrow (\frac{1}{3}, 4k + 1) \rightarrow (\frac{1}{3}, 4k + 2) \rightarrow \dots \rightarrow (\frac{1}{3}, 8k - 7) \rightarrow (\frac{1}{3}, 8k - 6) \rightarrow (\frac{2}{3}, 8k - 1) \rightarrow (\frac{2}{3}, 8k) \rightarrow (\frac{2}{3}, 8k + 1) \rightarrow (\frac{2}{3}, 8k + 2) \rightarrow (\frac{1}{3}, 4k)$.

The paths of length $4k + 3$ in our directed adjacency graph are given by

1. node $4k \rightarrow$ node $4k + 1 \rightarrow$ node $4k + 2 \rightarrow \dots \rightarrow$ node $8k - 3 \rightarrow$ node $8k - 2 \rightarrow$ node $4k - 4 \rightarrow$
node $4k - 3 \rightarrow$ node $4k - 2 \rightarrow$ node $4k - 1 \rightarrow$ node $4k$
2. node $4k \rightarrow$ node $4k + 1 \rightarrow$ node $4k + 2 \rightarrow \dots \rightarrow$ node $8k \rightarrow$ node $8k + 1 \rightarrow$ node $8k + 2 \rightarrow$
node $4k$.

These paths, respectively, will have corresponding orbits

$$\text{Orbit 2: } \left(\frac{9}{11}, 4k\right) \rightarrow \left(\frac{9}{11}, 4k+1\right) \rightarrow \left(\frac{9}{11}, 4k+2\right) \rightarrow \dots \rightarrow \left(\frac{9}{11}, 8k-6\right) \rightarrow \left(\frac{7}{11}, 8k-5\right) \rightarrow \left(\frac{7}{11}, 8k-4\right) \rightarrow$$

$$\left(\frac{7}{11}, 8k-3\right) \rightarrow \left(\frac{7}{11}, 8k-2\right) \rightarrow \left(\frac{10}{11}, 4k-4\right) \rightarrow \left(\frac{10}{11}, 4k-3\right) \rightarrow \left(\frac{10}{11}, 4k-2\right) \rightarrow \left(\frac{10}{11}, 4k-1\right) \rightarrow \left(\frac{9}{11}, 4k\right)$$

$$\text{Orbit 3: } \left(\frac{6}{7}, 4k\right) \rightarrow \left(\frac{6}{7}, 4k+1\right) \rightarrow \left(\frac{6}{7}, 4k+2\right) \rightarrow \dots \rightarrow \left(\frac{6}{7}, 8k-6\right) \rightarrow \left(\frac{5}{7}, 8k-5\right) \rightarrow \left(\frac{5}{7}, 8k-4\right) \rightarrow$$

$$\left(\frac{5}{7}, 8k-3\right) \rightarrow \left(\frac{5}{7}, 8k-2\right) \rightarrow \left(\frac{1}{7}, 8k-1\right) \rightarrow \left(\frac{1}{7}, 8k\right) \rightarrow \left(\frac{1}{7}, 8k+1\right) \rightarrow \left(\frac{1}{7}, 8k+2\right) \rightarrow \left(\frac{6}{7}, 4k\right).$$

Two of the paths of length $8k - 2$ are gotten by traversing each path of length $4k - 1$ twice. However, these two paths give rise to the same ψ_n -invariant sets as the corresponding paths of length $4k - 1$. Thus, we may disregard these two additional paths. The remaining path of length $8k - 2$ is simply

$$\text{node } 1 \rightarrow \text{node } 2 \rightarrow \text{node } 3 \rightarrow \dots \rightarrow \text{node } 8k - 3 \rightarrow \text{node } 8k - 2 \rightarrow \text{node } 1.$$

This path's corresponding orbit in our train-track is

$$\text{Orbit 4: } \left(\frac{10}{13}, 1\right) \rightarrow \left(\frac{10}{13}, 2\right) \rightarrow \left(\frac{10}{13}, 3\right) \rightarrow \dots \rightarrow \left(\frac{10}{13}, 4k-1\right) \rightarrow \left(\frac{7}{13}, 4k\right) \rightarrow \left(\frac{7}{13}, 4k+1\right) \rightarrow \left(\frac{7}{13}, 4k+2\right) \rightarrow$$

$$\dots \rightarrow \left(\frac{7}{13}, 8k-6\right) \rightarrow \left(\frac{1}{13}, 8k-5\right) \rightarrow \left(\frac{1}{13}, 8k-4\right) \rightarrow \left(\frac{1}{13}, 8k-3\right) \rightarrow \left(\frac{1}{13}, 8k-2\right) \rightarrow \left(\frac{10}{13}, 1\right).$$

One of the paths of length $8k + 2$ is

$$\text{node } 1 \rightarrow \text{node } 2 \rightarrow \text{node } 3 \rightarrow \dots \rightarrow \text{node } 8k - 2 \rightarrow \text{node } 4k - 4 \rightarrow \text{node } 4k - 3 \rightarrow \text{node } 4k - 2 \rightarrow$$

$$\text{node } 4k - 1 \rightarrow \text{node } 1.$$

This path's corresponding orbit is

$$\text{Orbit 5: } \left(\frac{20}{23}, 1\right) \rightarrow \left(\frac{20}{23}, 2\right) \rightarrow \left(\frac{20}{23}, 3\right) \rightarrow \dots \rightarrow \left(\frac{20}{23}, 4k-1\right) \rightarrow \left(\frac{17}{23}, 4k\right) \rightarrow \left(\frac{17}{23}, 4k+1\right) \rightarrow \left(\frac{17}{23}, 4k+2\right) \rightarrow$$

$$\dots \rightarrow \left(\frac{17}{23}, 8k-6\right) \rightarrow \left(\frac{11}{23}, 8k-5\right) \rightarrow \left(\frac{11}{23}, 8k-4\right) \rightarrow \left(\frac{11}{23}, 8k-3\right) \rightarrow \left(\frac{11}{23}, 8k-2\right) \rightarrow \left(\frac{10}{23}, 4k-4\right) \rightarrow$$

$$\left(\frac{10}{23}, 4k-3\right) \rightarrow \left(\frac{10}{23}, 4k-2\right) \rightarrow \left(\frac{10}{23}, 4k-1\right) \rightarrow \left(\frac{20}{23}, 1\right).$$

The remaining two paths of length $8k + 2$ are gotten by traversing first the path

$$\text{node } 4k \rightarrow \text{node } 4k + 1 \rightarrow \text{node } 4k + 2 \rightarrow \dots \rightarrow \text{node } 8k - 7 \rightarrow \text{node } 8k - 6 \rightarrow \text{node } 8k - 1 \rightarrow \text{node } 8k$$

$$\rightarrow \text{node } 8k + 1 \rightarrow \text{node } 8k + 2 \rightarrow \text{node } 4k$$

of length $4k - 1$, and then following one of the two paths of length $4k + 3$.

One of these paths will have an orbit corresponding to the punctures of the original ψ_n braid itself, and we shall disregard this orbit. The remaining orbit for this final case will be

$$\begin{aligned} \text{Orbit 6: } & \left(\frac{3}{25}, 4k\right) \rightarrow \left(\frac{3}{25}, 4k+1\right) \rightarrow \left(\frac{3}{25}, 4k+2\right) \rightarrow \dots \rightarrow \left(\frac{3}{25}, 8k-6\right) \rightarrow \left(\frac{6}{25}, 8k-1\right) \rightarrow \left(\frac{6}{25}, 8k\right) \rightarrow \\ & \left(\frac{6}{25}, 8k+1\right) \rightarrow \left(\frac{6}{25}, 8k+2\right) \rightarrow \left(\frac{19}{25}, 4k\right) \rightarrow \left(\frac{19}{25}, 4k+1\right) \rightarrow \left(\frac{19}{25}, 4k+2\right) \rightarrow \dots \rightarrow \left(\frac{19}{25}, 8k-6\right) \rightarrow \\ & \left(\frac{13}{25}, 8k-5\right) \rightarrow \left(\frac{13}{25}, 8k-4\right) \rightarrow \left(\frac{13}{25}, 8k-3\right) \rightarrow \left(\frac{13}{25}, 8k-2\right) \rightarrow \left(\frac{14}{25}, 4k-4\right) \rightarrow \left(\frac{14}{25}, 4k-3\right) \rightarrow \\ & \left(\frac{14}{25}, 4k-2\right) \rightarrow \left(\frac{14}{25}, 4k-1\right) \rightarrow \left(\frac{3}{25}, 4k\right). \end{aligned}$$

Now that we have computed the required orbits, we must try to build braids out of these orbits. It turns out we can form exactly 4 ψ_n -invariant sets of order n here. The invariant sets, along with constituent orbits, are

Set 1: Orbit 1, Orbit 3

Set 2: Orbit 2, Orbit 3

Set 3: Orbit 5

Set 4: Orbit 6.

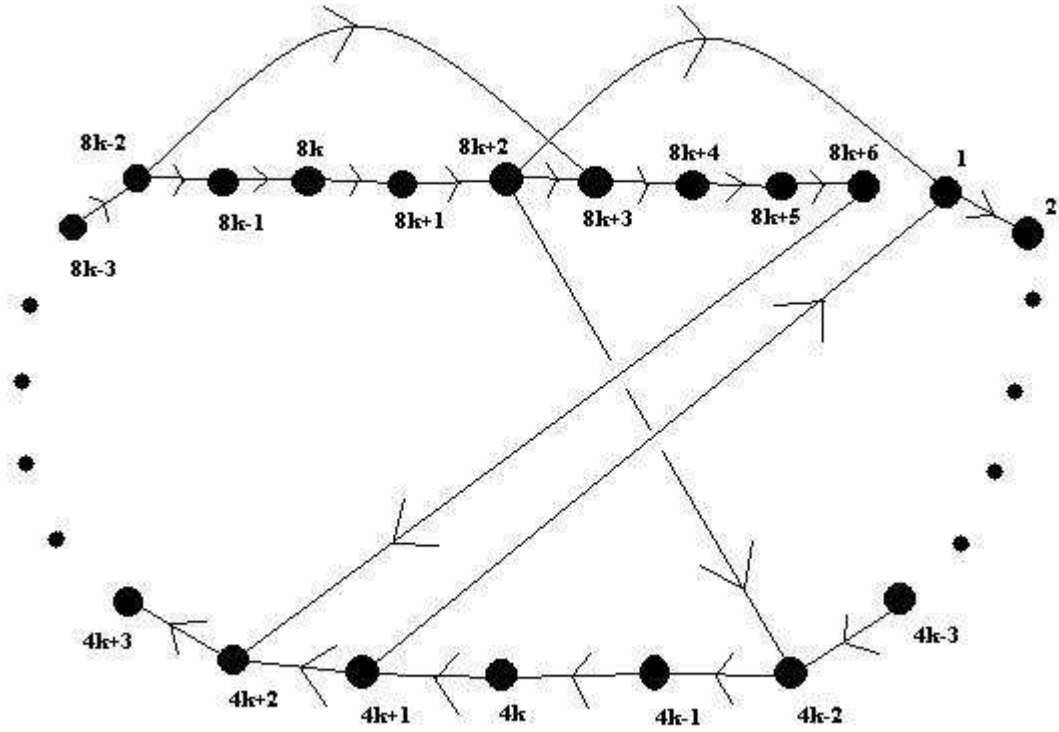
The braid corresponding to set 1 will be $(\sigma_{n-1}\sigma_{n-2}\dots\sigma_2\sigma_1)^{2k+1}\sigma_1^{-1}$, which is reducible. The braid corresponding to set 2 will be $(\sigma_{n-1}\sigma_{n-2}\dots\sigma_2\sigma_1)^{2k+1}\sigma_1^{-1}$ as well. The braid corresponding to set 3 will be $(\sigma_{n-1}\sigma_{n-2}\dots\sigma_2\sigma_1)^{2k+1}$, which is periodic. The braid corresponding to set 4 will be $(\sigma_{n-1}\sigma_{n-2}\dots\sigma_2\sigma_1)^{2k+1}$ as well. Thus, ψ_n is indeed minimal in this case.

□

6.2.4 The Case $n = 8k + 6, k \geq 1$

Theorem 6.14. *For $n \in \mathbb{N}, n = 8k + 6$ and $k \geq 1$, the braid ψ_n is minimal.*

Proof. When $n = 8k + 6$, the directed adjacency graph for the corresponding Markov map looks like:



In the above diagram, each vertex corresponds to the specified train-track edge in the ψ_n train-track diagram from earlier.

In order to compute the braids forced by $\tilde{\psi}_n$ here, we next compute all of the closed paths in the directed adjacency graph having length $\leq 8k + 6$. By inspection, we find there are exactly 2 closed paths of length $4k + 1$, exactly 2 closed paths of length $4k + 5$, exactly 3 closed paths of length $8k + 2$, and exactly 3 closed paths of length $8k + 6$.

The paths of length $4k + 1$ in our directed adjacency graph are given by

1. node 1 \rightarrow node 2 \rightarrow node 3 $\rightarrow \dots \rightarrow$ node $4k + 1$ \rightarrow node 1
2. node $4k + 2$ \rightarrow node $4k + 3$ \rightarrow node $4k + 4$ $\rightarrow \dots \rightarrow$ node $8k - 3$ \rightarrow node $8k - 2$ \rightarrow node $8k + 3$ \rightarrow node $8k + 4$ \rightarrow node $8k + 5$ \rightarrow node $8k + 6$ \rightarrow node $4k + 2$.

The first path above will in fact correspond to some fixed point p lying within the non-punctured central singularity. The second path will have a corresponding orbit

Orbit 1: $(\frac{1}{3}, 4k + 2) \rightarrow (\frac{1}{3}, 4k + 3) \rightarrow (\frac{1}{3}, 4k + 4) \rightarrow \dots \rightarrow (\frac{1}{3}, 8k - 3) \rightarrow (\frac{1}{3}, 8k - 2) \rightarrow (\frac{2}{3}, 8k + 3) \rightarrow (\frac{2}{3}, 8k + 4) \rightarrow (\frac{2}{3}, 8k + 5) \rightarrow (\frac{2}{3}, 8k + 6) \rightarrow (\frac{1}{3}, 4k + 2)$.

The paths of length $4k + 5$ in our directed adjacency graph are given by

1. node $4k + 2 \rightarrow$ node $4k + 3 \rightarrow$ node $4k + 4 \rightarrow \dots \rightarrow$ node $8k + 1 \rightarrow$ node $8k + 2 \rightarrow$ node $4k - 2 \rightarrow$ node $4k - 1 \rightarrow$ node $4k \rightarrow$ node $4k + 1 \rightarrow$ node $4k + 2$
2. node $4k + 2 \rightarrow$ node $4k + 3 \rightarrow$ node $4k + 4 \rightarrow \dots \rightarrow$ node $8k + 4 \rightarrow$ node $8k + 5 \rightarrow$ node $8k + 6 \rightarrow$ node $4k + 2$.

These paths, respectively, will have corresponding orbits

$$\text{Orbit 2: } \left(\frac{9}{11}, 4k+2\right) \rightarrow \left(\frac{9}{11}, 4k+3\right) \rightarrow \left(\frac{9}{11}, 4k+4\right) \rightarrow \dots \rightarrow \left(\frac{9}{11}, 8k-2\right) \rightarrow \left(\frac{7}{11}, 8k-1\right) \rightarrow \left(\frac{7}{11}, 8k\right) \rightarrow \left(\frac{7}{11}, 8k+1\right) \rightarrow \left(\frac{7}{11}, 8k+2\right) \rightarrow \left(\frac{10}{11}, 4k-2\right) \rightarrow \left(\frac{10}{11}, 4k-1\right) \rightarrow \left(\frac{10}{11}, 4k\right) \rightarrow \left(\frac{10}{11}, 4k+1\right) \rightarrow \left(\frac{9}{11}, 4k+2\right)$$

$$\text{Orbit 3: } \left(\frac{6}{7}, 4k+2\right) \rightarrow \left(\frac{6}{7}, 4k+3\right) \rightarrow \left(\frac{6}{7}, 4k+4\right) \rightarrow \dots \rightarrow \left(\frac{6}{7}, 8k-2\right) \rightarrow \left(\frac{5}{7}, 8k-1\right) \rightarrow \left(\frac{5}{7}, 8k\right) \rightarrow \left(\frac{5}{7}, 8k+1\right) \rightarrow \left(\frac{5}{7}, 8k+2\right) \rightarrow \left(\frac{1}{7}, 8k+3\right) \rightarrow \left(\frac{1}{7}, 8k+4\right) \rightarrow \left(\frac{1}{7}, 8k+5\right) \rightarrow \left(\frac{1}{7}, 8k+6\right) \rightarrow \left(\frac{6}{7}, 4k+2\right).$$

Two of the paths of length $8k + 2$ are gotten by traversing each path of length $4k + 1$ twice. However, these two paths give rise to the same ψ_n -invariant sets as the corresponding paths of length $4k + 1$. Thus, we may disregard these two additional paths. The remaining path of length $8k + 2$ is simply

$$\text{node } 1 \rightarrow \text{node } 2 \rightarrow \text{node } 3 \rightarrow \dots \rightarrow \text{node } 8k + 1 \rightarrow \text{node } 8k + 2 \rightarrow \text{node } 1.$$

This path's corresponding orbit in our train-track is

$$\text{Orbit 4: } \left(\frac{10}{13}, 1\right) \rightarrow \left(\frac{10}{13}, 2\right) \rightarrow \left(\frac{10}{13}, 3\right) \rightarrow \dots \rightarrow \left(\frac{10}{13}, 4k+1\right) \rightarrow \left(\frac{7}{13}, 4k+2\right) \rightarrow \left(\frac{7}{13}, 4k+3\right) \rightarrow \left(\frac{7}{13}, 4k+4\right) \rightarrow \dots \rightarrow \left(\frac{7}{13}, 8k-2\right) \rightarrow \left(\frac{1}{13}, 8k-1\right) \rightarrow \left(\frac{1}{13}, 8k\right) \rightarrow \left(\frac{1}{13}, 8k+1\right) \rightarrow \left(\frac{1}{13}, 8k+2\right) \rightarrow \left(\frac{10}{13}, 1\right).$$

One of the paths of length $8k + 6$ is

$$\text{node } 1 \rightarrow \text{node } 2 \rightarrow \text{node } 3 \rightarrow \dots \rightarrow \text{node } 8k + 2 \rightarrow \text{node } 4k - 2 \rightarrow \text{node } 4k - 1 \rightarrow \text{node } 4k \rightarrow \text{node } 4k + 1 \rightarrow \text{node } 1.$$

This path's corresponding orbit is

$$\text{Orbit 5: } \left(\frac{20}{23}, 1\right) \rightarrow \left(\frac{20}{23}, 2\right) \rightarrow \left(\frac{20}{23}, 3\right) \rightarrow \dots \rightarrow \left(\frac{20}{23}, 4k+1\right) \rightarrow \left(\frac{17}{23}, 4k+2\right) \rightarrow \left(\frac{17}{23}, 4k+3\right) \rightarrow \left(\frac{17}{23}, 4k+4\right) \rightarrow \dots \rightarrow \left(\frac{17}{23}, 8k-2\right) \rightarrow \left(\frac{11}{23}, 8k-1\right) \rightarrow \left(\frac{11}{23}, 8k\right) \rightarrow \left(\frac{11}{23}, 8k+1\right) \rightarrow \left(\frac{11}{23}, 8k+2\right) \rightarrow \left(\frac{10}{23}, 4k-2\right) \rightarrow \left(\frac{10}{23}, 4k-1\right) \rightarrow \left(\frac{10}{23}, 4k\right) \rightarrow \left(\frac{10}{23}, 4k+1\right) \rightarrow \left(\frac{20}{23}, 1\right).$$

The remaining two paths of length $8k + 6$ are gotten by traversing first the path

$$\text{node } 4k + 2 \rightarrow \text{node } 4k + 3 \rightarrow \text{node } 4k + 4 \rightarrow \dots \rightarrow \text{node } 8k - 3 \rightarrow \text{node } 8k - 2 \rightarrow \text{node } 8k + 3 \rightarrow \text{node } 8k + 4 \rightarrow \text{node } 8k + 5 \rightarrow \text{node } 8k + 6 \rightarrow \text{node } 4k + 2$$

of length $4k + 1$, and then following one of the two paths of length $4k + 5$.

One of these paths will have an orbit corresponding to the punctures of the original ψ_n braid itself, and we shall disregard this orbit. The remaining orbit for this final case will be

$$\begin{aligned} \textbf{Orbit 6: } & \left(\frac{3}{25}, 4k + 2\right) \rightarrow \left(\frac{3}{25}, 4k + 3\right) \rightarrow \left(\frac{3}{25}, 4k + 4\right) \rightarrow \dots \rightarrow \left(\frac{3}{25}, 8k - 2\right) \rightarrow \left(\frac{6}{25}, 8k + 3\right) \rightarrow \\ & \left(\frac{6}{25}, 8k + 4\right) \rightarrow \left(\frac{6}{25}, 8k + 5\right) \rightarrow \left(\frac{6}{25}, 8k + 6\right) \rightarrow \left(\frac{19}{25}, 4k + 2\right) \rightarrow \left(\frac{19}{25}, 4k + 3\right) \rightarrow \left(\frac{19}{25}, 4k + 4\right) \rightarrow \dots \rightarrow \\ & \left(\frac{19}{25}, 8k - 2\right) \rightarrow \left(\frac{13}{25}, 8k - 1\right) \rightarrow \left(\frac{13}{25}, 8k\right) \rightarrow \left(\frac{13}{25}, 8k + 1\right) \rightarrow \left(\frac{13}{25}, 8k + 2\right) \rightarrow \left(\frac{14}{25}, 4k - 2\right) \rightarrow \left(\frac{14}{25}, 4k - 1\right) \rightarrow \\ & \left(\frac{14}{25}, 4k\right) \rightarrow \left(\frac{14}{25}, 4k + 1\right) \rightarrow \left(\frac{3}{25}, 4k + 2\right). \end{aligned}$$

Now that we have computed the required orbits, we must try to build braids out of these orbits. It turns out we can form exactly 4 ψ_n -invariant sets of order n here. The invariant sets, along with constituent orbits, are

Set 1: Orbit 1, Orbit 3

Set 2: Orbit 2, Orbit 3

Set 3: Orbit 5

Set 4: Orbit 6.

The braid corresponding to set 1 will be $(\sigma_{n-1}\sigma_{n-2}\dots\sigma_2\sigma_1)^{6k+5}\sigma_1^{-1}$, which is reducible. The braid corresponding to set 2 will be $(\sigma_{n-1}\sigma_{n-2}\dots\sigma_2\sigma_1)^{6k+5}\sigma_1^{-1}$ as well. The braid corresponding to set 3 will be $(\sigma_{n-1}\sigma_{n-2}\dots\sigma_2\sigma_1)^{6k+5}$, which is periodic. The braid corresponding to set 4 will be $(\sigma_{n-1}\sigma_{n-2}\dots\sigma_2\sigma_1)^{6k+5}$ as well. Thus, ψ_n is indeed minimal in this case.

□

6.3 Exceptional Cases

The only remaining cases to consider now are the $\tilde{\psi}_6 = \psi_6$ and ψ_{10} braids. We guarantee the proof of minimality is almost exactly the same as previous cases, and omit this proof here. We would like to note that, based on personal communication, Cho and Ham [9] appear to be currently in the process of writing a proof that minimal growth among pseudo-Anosov 6-braids is attained by the $\tilde{\psi}_6 = \psi_6$ braid. This of course implies that this particular braid is minimal necessarily.

Chapter 7

Initial Analysis of Mapping Tori

7.1 Kirby Calculus

In order to proceed, we will find it quite useful at this stage to introduce the notion of Dehn surgery. The background presented in this section may be found in Gompf and Stipsicz [18].

Definition 7.1. *Let K be a knot in an oriented 3–manifold, with a closed tubular neighborhood νK diffeomorphic to the solid torus $S^1 \times D^2$. A **Dehn surgery** on K is the operation of removing the interior of νK and gluing in a copy of $S^1 \times D^2$ by any diffeomorphism φ of the boundary tori.*

Similarly one could consider Dehn surgery on a link, which simply consists of Dehn surgeries on some subset of components of the link. The Dehn surgery construction is central to the study of 3–manifolds, as is evidenced by the following result

Theorem 7.2 (Lickorish-Wallace). *Any closed, oriented, connected 3–manifold M is realized by (integral) Dehn surgery on a link L in the 3–sphere S^3 .*

We note that it is possible for different toral diffeomorphisms to potentially give rise to the same manifold following Dehn surgery

Theorem 7.3. *Let m and n be a meridian and a longitude respectively on the boundary torus of a tubular neighborhood of the knot K in S^3 . Let φ_1 and φ_2 be two toral diffeomorphisms, and suppose the homology classes $[\varphi_1(m)], [\varphi_2(m)]$ satisfy $[\varphi_1(m)] = [p_1m + q_1n]$ and $[\varphi_2(m)] = [p_2m + q_2n]$ with $\frac{p_1}{q_1} = \frac{p_2}{q_2}$. Then, the manifolds resulting from Dehn surgery corresponding to φ_1 and φ_2 , respectively, are homeomorphic.*

It follows from this result that one may specify a Dehn surgery on a knot via the fraction described above, referred to as a **surgery coefficient**.

Given two links in S^3 and a set of surgery coefficients on some components of each link, we would ideally like some method for determining whether the resulting manifolds are homeomorphic. For this purpose, let's introduce the following operation.

Definition 7.4. Let L be a link in S^3 with surgery coefficients associated to some subset of components of L . Let K be some unknotted component of L with surgery coefficient $r = \frac{p}{q}$. Assume without loss of generality that any component linked with K always passes through K in the same direction. A **Rolfsen twist** operation of order n on L with respect to K replaces L with the link identical to L except that the trivial braid consisting of z arcs passing through K is changed to a full n twist ∂_z^{2n} , replaces the coefficient r of K by $\frac{p}{q+np}$, and replaces the coefficient r_i of any component K_i linked with K by $r_i + n(\text{linking number}(K_i, K))^2$.

Some additional background here may be found in [32].

Theorem 7.5. Let L and L' be links with rational coefficients in S^3 . Then the resulting 3-manifolds obtained by Dehn surgery are (orientation-preserving) diffeomorphic iff L can be transformed into L' by a sequence of Rolfsen twists (together with isotopies and inserting and deleting components with coefficient ∞ , i.e., coefficient $\frac{1}{0}$).

We shall proceed next to apply this theorem in understanding the ψ_n and $\tilde{\psi}_n$ better.

7.2 Dehn Surgery Realization of Mapping Tori

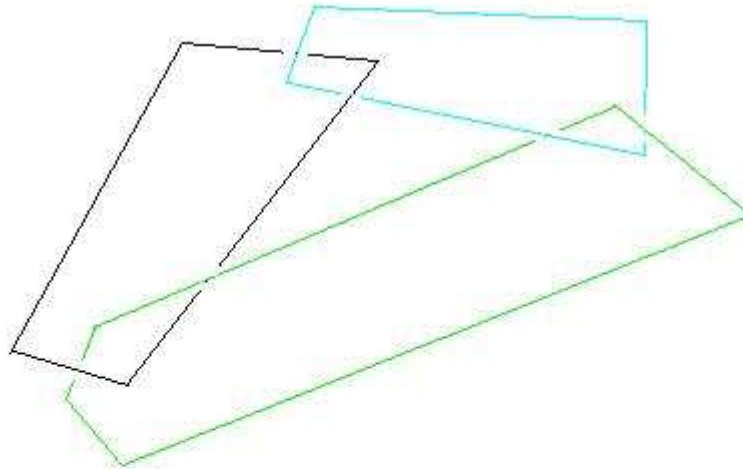
7.2.1 The Case of ψ_n, n Odd

Recall our sequences $(\mathcal{U}(\psi_n))$ and $(\mathcal{U}(\tilde{\psi}_n))$ from earlier in Chapter 3. These braids on an even number of strands were observed to have quite low growth rate among pseudo-Anosov braids with 3-cusp mapping tori. It was observed in Chapter 5 that these braids are indeed related to the ψ_n and $\tilde{\psi}_n$ in a nice way.

Fact 7.6. The $\mathcal{U}(\psi_n)$ and $\mathcal{U}(\tilde{\psi}_n)$ may be constructed by simply adding a single puncture to the central non-punctured singularity of the ψ_n and $\tilde{\psi}_n$, respectively.

The mapping tori of the $\mathcal{U}(\psi_n)$ and $\mathcal{U}(\tilde{\psi}_n)$ have an especially nice property.

Definition 7.7. Consider the 3-component link pictured below



We call this link the **alternating 3-chain link**. We define the **magic 3-manifold**, denoted M_{magic} , to be the complement of this link in the 3-sphere S^3 .

Theorem 7.8. *The mapping tori of the $\mathcal{U}(\psi_n)$ and $\mathcal{U}(\tilde{\psi}_n)$ are all isomorphic to M_{magic} .*

This may be proved via a straightforward induction argument for each case (n odd, $n=4k$, etc.) in the definition of the sequences. The base cases may be checked directly with the SnapPea program (or Snap if exact arithmetic is preferred).

Consequently, gluing a solid torus into the cusp corresponding to the new central puncture yields the mapping tori of the ψ_n and $\tilde{\psi}_n$. This gives us the following corollary.

Corollary 7.9. *The mapping tori of the ψ_n and $\tilde{\psi}_n$ are isometric to Dehn surgeries on M_{magic} .*

Our argument above worked for non-exceptional values of n . However, again the validity of this statement may be checked directly with Snap for the small number of exceptional cases.

Actually, it turns out a bit more can be said here.

Theorem 7.10. *The mapping tori of the (ψ_n) and $(\tilde{\psi}_n)$ sequence braids are all isometric to manifolds obtained by Dehn surgery on a single cusp of M_{magic} , with the exception of $n = 6$. The mapping tori for the exceptional $\psi_6, \tilde{\psi}_6$ are actually isometric to M_{magic} . Otherwise, the surgery coefficients for the ψ_n sequence are*

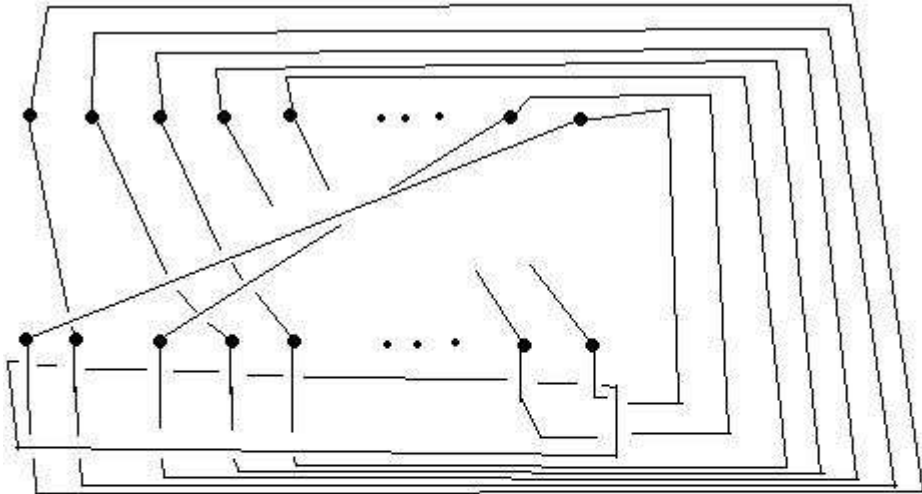
1. $\frac{k+1}{k}, n = 2k + 1$ odd
2. $\frac{2k+1}{2k-1}, n = 4k$
3. $\frac{4k+3}{4k-1}, n = 8k + 2$
4. $\frac{4k+5}{4k+1}, n = 8k + 6$.

The numerators/denominators of these surgery coefficients correspond to the exponents of nonzero terms in the characteristic polynomials of Theorem 2.1. Further, the surgery coefficients corresponding to $\tilde{\psi}_n$ and ψ_n are reciprocals when $n \geq 5$ and $n \neq 6$.

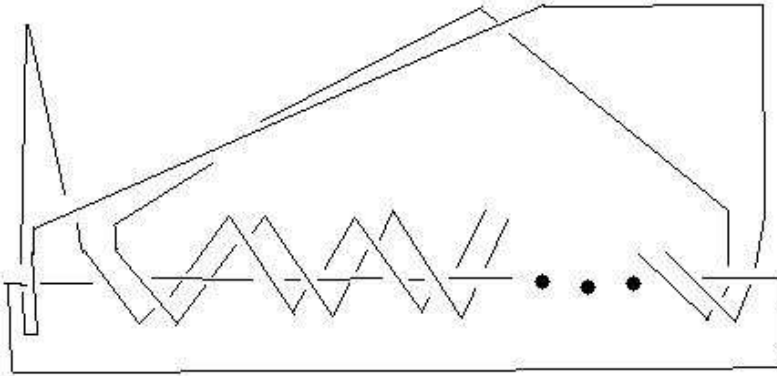
Let's take an explicit look now at the proof for ψ_n in the event that n is odd.

Theorem 7.11. *When $n \in \mathbb{N}, n = 2k + 1$ odd and $n \geq 7$, the mapping torus of ψ_n is isometric to the hyperbolic manifold obtained by $\frac{k+1}{k}$ surgery on a component of M_{magic} .*

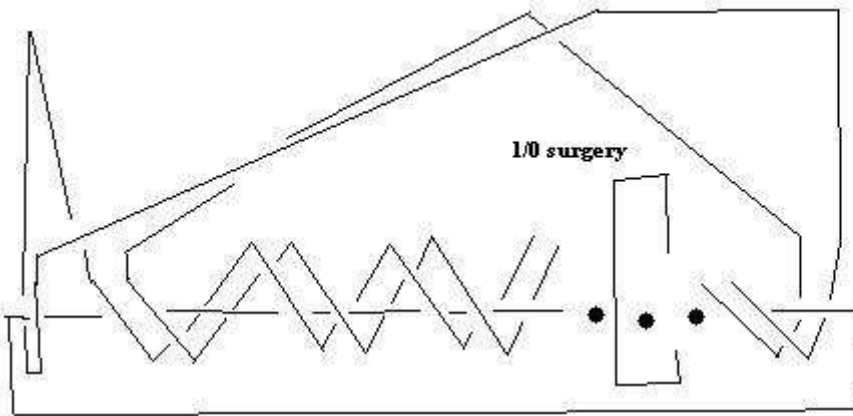
Proof. The proof is basically a series of pictures, assuming the ideas about Kirby calculus outlined earlier. The mapping torus of ψ_n will be isometric to the complement in S^3 of the link pictured below, obtained by forming the usual braid closure of ψ_n and adding an additional component around all of the braid strands.



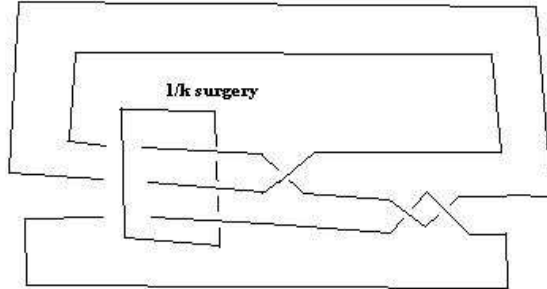
Observe that we may isotope this link to the following link



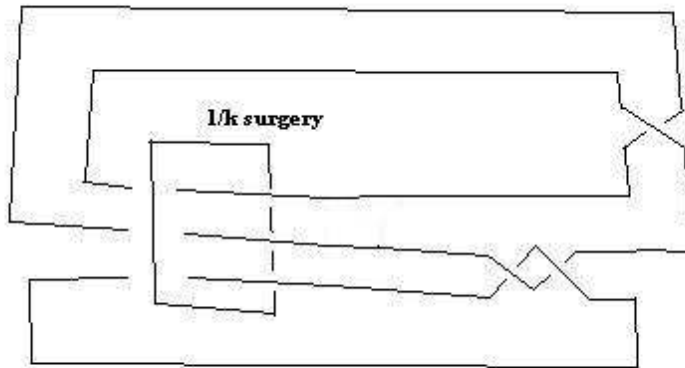
Then, we add a new central link component with surgery coefficient ∞



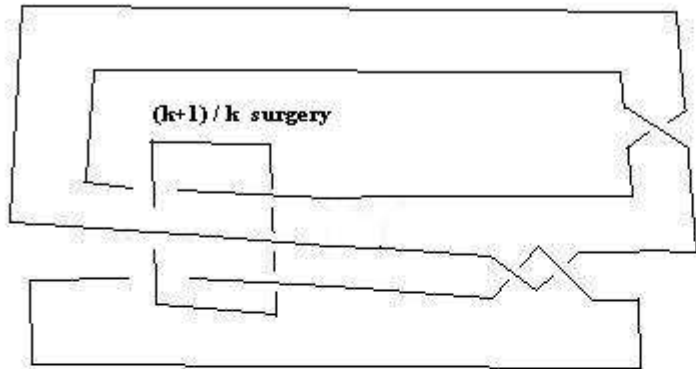
Now, we can perform a Rolfsen twist of order k along the new component. The resulting link will simply be the closure of the 3-braid $\sigma_2^2\sigma_1^{-1}$, but with an extra component around the braid strands. Note also that our surgery coefficient transforms from ∞ to $\frac{1}{k}$.



Maneuvering the σ_1^{-1} strand through the transverse component yields



Performing now a Rolfsen twist of order 1 on the bottom component of the diagram changes the surgery coefficient on the transverse component from $\frac{1}{k}$ to $\frac{1}{k} + 1 = \frac{k+1}{k}$. This gives our last diagram



We observe finally that this last link component is isotopic to the alternating 3–chain link, thus completing our proof.

□

7.2.2 Other Cases

Having proved the above Dehn surgery result in the case of ψ_n , n odd and $n \geq 7$, we note briefly on the nature of the proof in remaining cases. First, the proof for $\tilde{\psi}_n$ is virtually identical to the above argument in the case where n is odd. For other values of n , our arguments are in fact quite similar, although one must perform an additional Rolfsen twist in order to arrive at the desired coefficient. The reason for this additional Rolfsen twist is that there are several asymmetrical spokes in these cases, rather than just one as before.

7.3 Volume Concept

Dehn surgeries on M_{magic} have been studied by Martelli and Petronio [27].

Theorem 7.12. *Dehn surgery on a component of M_{magic} yields a hyperbolic manifold precisely when the surgery coefficient is not equal to 0, 1, 2, 3, or ∞ .*

Note above that we have used a slightly different convention than Martelli and Petronio so that surgery coefficients of interest would be positive. Recall next the following result of Thurston

Theorem 7.13 (Thurston). *The mapping torus of a braid is hyperbolic iff the braid is pseudo-Anosov.*

These two results in conjunction with our description of the mapping tori of the ψ_n and $\tilde{\psi}_n$ yield the following nice corollary.

Corollary 7.14. *The ψ_n and $\tilde{\psi}_n$ are all pseudo-Anosov.*

Notice that if one tried to extend the Dehn surgery coefficient pattern of the ψ_n to possible braids ψ_3 and ψ_4 , one would have coefficients of 2 and 3, respectively. By the above analysis of Martelli and Petronio, such coefficients would give non-hyperbolic manifolds. This explains finally why there is no natural pseudo-Anosov extension of the ψ_n to the cases $n = 3, 4$.

We introduce now the “volume concept” relative to the braid forcing problem. Observe that M_{magic} has relatively low volume ≈ 5.33 .

Conjecture 7.15. *M_{magic} attains minimal volume among orientable 3–cusp hyperbolic 3–manifolds.*

There is a well-known result of Thurston regarding surgeries on hyperbolic 3–manifolds

Theorem 7.16 (Thurston). *Any finite volume hyperbolic 3–manifold obtained by non-trivial hyperbolic Dehn surgery on another finite volume hyperbolic 3–manifold necessarily has lower volume.*

Recall from earlier our conjecture that, as n gets large, all the lowest growth pseudo-Anosov braids should have mapping tori isometric to manifolds either isometric to M_{magic} or resulting from Dehn surgery on M_{magic} . Further understanding of the volume spectrum implies the mapping tori of extremely low growth pseudo-Anosov n –braids for a given n should all have really low volume. We note this may not necessarily be the case however if growth is low, but not low enough.

Theorem 7.17 (Kin, Takasawa [24]). *There exist sequences (α_n) of n –strand pseudo-Anosov braids with growth tending to 1 whose mapping tori have precisely 2 cusps and have volume tending to ∞ .*

In spite of this, we make the following conjecture

Conjecture 7.18 (Kin, Takasawa). *All of the lowest possible growth pseudo-Anosov sequences have extremely low volume mapping tori.*

Related ideas regarding the connection between growth and volume may be found in [25].

We note that in the case of $n = 6$, one may find pseudo-Anosov 6–braids with mapping tori of lower volume than the mapping torus of ψ_6 . We suspect this behavior in the $n = 6$ case may be a very unusual exception however owing to the exceptional definition of ψ_6 .

The ψ_n braids, n odd, have been used by Hironaka and Kin [22] to produce some relatively low-growth surface automorphisms of closed orientable genus g surfaces. In connection with the Lehmer problem however, Leininger [26] has found a lower-growth automorphism than the corresponding automorphism of Hironaka and Kin on the genus five surface. The question of finding lowest growth automorphisms of higher genus surfaces seems tricky, but the above volume concept suggests a possible method for producing low dilatation automorphisms of orientable genus g surfaces.

Conjecture 7.19 (Kin, Takasawa). *In order to find very low dilatation automorphisms of orientable genus g surfaces Σ_g , one can simply study low-volume hyperbolic 3–manifolds fibered over Σ_g and use the monodromy automorphism. Conversely, one should be able to produce lots of low-volume fibered hyperbolic 3–manifolds by taking the mapping tori of very low dilatation automorphisms of Σ_g .*

Fortunately, the KnotTwister program referenced earlier allows one to compute growth of automorphisms corresponding to various fiberings of hyperbolic 3–manifolds. We hope to use KnotTwister in the future to produce some low-growth automorphisms of higher genus surfaces by inputting different low-volume orientable hyperbolic 3–manifolds, although we have not had the opportunity yet to do so.

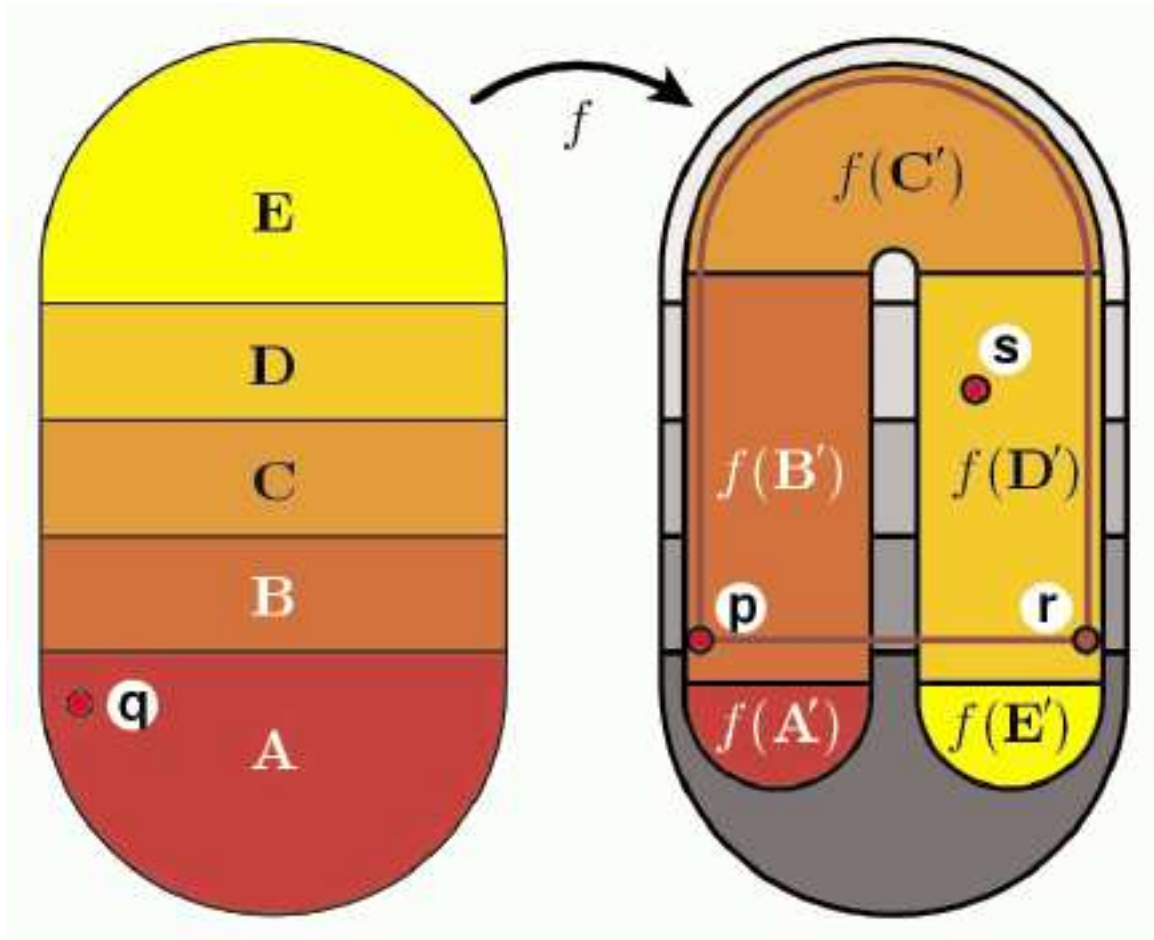
Chapter 8

Horseshoe Braids

8.1 The Horseshoe Map

We begin this chapter with a preliminary informal look at a well-known example in dynamical systems. Consider the diagram below [33]

http://www.scholarpedia.org/wiki/images/6/68/Smale_Horseshoe_Shub1.gif



On the left-hand side, we initially have a capped-off rectangle. Let's denote this region by \tilde{R} and consider it as a subset of the closed unit disk in \mathbb{R}^2 . The central rectangle is further subdivided into equal subrectangles B, C, D , and is capped off on the sides by closed half-disk regions A, E . We would like to consider now a particular map of \tilde{R} to itself. Basically we stretch the region \tilde{R} , fold it sideways, and place it back into the region \tilde{R} as depicted in the diagram. Moreover, we do so in such a way that the rectangles B and D are stretched a factor of 2 vertically and contracted by a factor of 2 horizontally. The idea is to model Anosov behavior to some extent. The regions A and E are mapped into A , while C is mapped into E . Finally, we extend this map $f : \tilde{R} \rightarrow \tilde{R}$ to a diffeomorphism of the entire closed disk to itself. Any such map constructed in this manner is referred to as a **Smale horseshoe map**.

Horseshoe maps are similar in the sense that dynamics of finite orbits within the rectangular part of \tilde{R} may be described in a standard fashion symbolically. Let $x, H(x), H^2(x), \dots, H^{n-1}(x)$ be some orbit of size n in $B \cup D$ for some horseshoe map H . We may associate a length n sequence $y_1 y_2 \dots y_n$ of 0s and 1s to our orbit by defining $y_i = 0$ if $H^{i-1}(x) \in B$ and $y_i = 1$ if $H^{i-1}(x) \in D$. Indeed finite orbits of a horseshoe map may be described uniquely via (the set of cyclic permutations of) such a sequence. Given such dynamic similarity, we will now often refer to **the** horseshoe map as any member of this class of horseshoe maps. This is okay in our context since the induced braids relative to corresponding orbits for different horseshoe maps should be the same.

8.2 “The Forcing Relation for Horseshoe Braid Types”

Our title for this section has been placed in quotations as it refers not only to the title of a paper by de Carvalho and Hall [11], but also to the conjectured global structure of the braid forcing order for braids relative to orbits of the horseshoe map. Before stating this conjecture, we need some preliminary definitions.

Definition 8.1. *Let P be a (non-fixed point) horseshoe orbit with some corresponding symbolic horseshoe code c_P . Denote by \bar{c}_P the semi-infinite sequence formed by simply repeating c_P ad infinitum. We assume implicitly throughout without loss of generality from now on unless otherwise specified that \bar{c}_P is strictly greater than $\sigma_i(\bar{c}_P)$ in the unimodal order for $1 \leq i < n$ when defining c_P (otherwise, just shift). If the semi-infinite sequence \bar{c}_P does not contain the sub-word 010, we change temporarily the final symbol of c_P to a 1 (this does not affect braid type). If c_P does not begin with the sequence 10, we define the **height** $q(c_P)$ of c_P to be $\frac{1}{2}$. Otherwise, we may write $\bar{c}_P = 10^{\kappa_1} 1^{\mu_1} 0^{\kappa_2} 1^{\mu_2} \dots$, where each $\kappa_i \geq 0$, each μ_i is either 1 or 2, and $\mu_i = 1$ only if $\kappa_{i+1} > 0$. For each $r \geq 1$, define $I_r(c_P) = (\frac{r}{2r + \sum_{i=1}^r \kappa_i}, \frac{r}{(2r-1) + \sum_{i=1}^r \kappa_i}]$, and let $s \geq 1$ be the least integer such that either $\mu_s = 1$ or $\cap_{i=1}^{s+1} I_i(c_P) = \emptyset$. Find x, y so that $\cap_{i=1}^s I_i(c_P) = (x, y]$. Then, in this case, define the **height** $q(c_P)$ of c_P to be $q(c_P) = x$ when $\mu_s = 2$ and $w < z$ for all $w \in I_{s+1}(c_P)$ and $z \in \cap_{i=1}^s I_i(c_P)$,*

and define instead $q(c_P) = y$ when either $\mu_s = 1$, or $\mu_s = 2$ and $w > z$ for all $w \in I_{s+1}(c_P)$ and $z \in \cap_{i=1}^s I_i(c_P)$.

The above definition is somewhat convoluted, but appears to contain some rather essential information regarding Dehn surgery coefficients associated to mapping tori.

Definition 8.2. Let P be a period N orbit of the horseshoe which is not of finite order braid type, with height $q = q(P) = \frac{m}{n} \in (0, \frac{1}{2}]$ in lowest terms. Then, we define the **prefix** of P to be the word $c_q = 10^{\kappa_1} 1^2 0^{\kappa_2} 1^2 \dots 1^2 0^{\kappa_m} 1$, where $\kappa_1 = \lfloor \frac{n}{m} \rfloor - 1$ and $\kappa_i = \lfloor \frac{in}{m} \rfloor - \lfloor \frac{(i-1)n}{m} \rfloor - 2$ if $2 \leq i \leq m$.

Definition 8.3. Let P be a period N orbit of the horseshoe which is not of finite order braid type, with height $q = q(P) = \frac{m}{n} \in (0, \frac{1}{2}]$ in lowest terms and denote the prefix of P as before by c_q . The **decoration** of P is defined to \star if $N = n + 2$, and to be the element w of $\{0, 1\}^{N-n-3}$ such that $c_P = (c_q)_1^0 w_1^0$ if $N \geq n + 3$ (in the preceding expression, the singled-out separating digits could potentially be 0 or 1). We write from now on $P = P_q^w$ for a periodic orbit of height q and decoration w .

Definition 8.4. Denote by $\tilde{\mathcal{D}}_w$ the set of all periodic orbits of the horseshoe with given decoration w .

Definition 8.5. Let w be a decoration, and define $q_w \in (0, \frac{1}{2}] \cap \mathbb{Q}$ by $q_\star = \frac{1}{2}$ and

$$q_w = \min_{0 \leq i \leq k+2} q(\sigma^i(\overline{10w0}))$$

if $w \in \{0, 1\}^k$.

Finally we are in a position to give the formal statement of the braid forcing conjecture for horseshoe type braids. We consider here only the statement for periodic orbits, although the more general statement from de Carvalho and Hall [11] applies to homoclinic orbits as well. Below, $bt(P_q^w)$ represents the braid type of P_q^w and it is assumed in general that $q \leq q_w, q' \leq q_{w'}$.

Conjecture 8.6 (de Carvalho, Hall). Let w and w' be decorations. Then

1. $bt(P_q^w) = bt(P_{q'}^{w'})$ if and only if $q = q'$ and $bt(P_0^w) = bt(P_0^{w'})$.
2. If $0 < q < q_w$, then P_q^w has pseudo-Anosov braid type.
3. All of the periodic orbits in $\{P_q^w : 0 < q < q_w\}$ have the same topological train track type.
4. The family $\tilde{\mathcal{D}}_w$ is totally ordered by \preceq , with $P_q^w \preceq P_r^w$ if and only if $q \geq r$.
5. If $q < q'$ and $bt(P_0^w) \succeq bt(P_0^{w'})$, then $P_q^w \succeq P_{q'}^{w'}$.

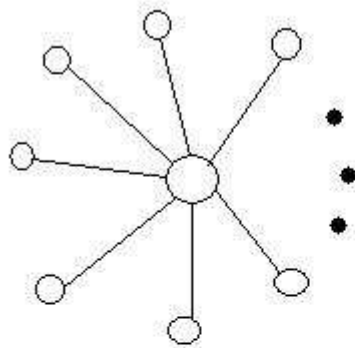
Some additional references for the material of this section (and indeed, chapter) are [10], [12], [13], [15], [19].

8.3 Star-Shaped Train-Tracks

This section briefly examines some especially nice sets of invariant train-tracks for studying braids. The simplest is the n -star

Definition 8.7 (de Carvalho, Hall [14]). *Define an n -star train-track to be one having one central singularity and n main edges meeting that singularity, joined cyclically by peripheral edges and each having a peripheral edge loop attached at the opposite vertex.*

Below is a diagram of the typical n -star train-track



Using the especially nice structure of these train-tracks, we have

Theorem 8.8 (de Carvalho, Hall [14]). *The conjecture of the preceding section holds for horseshoe braids having invariant n -star train-tracks.*

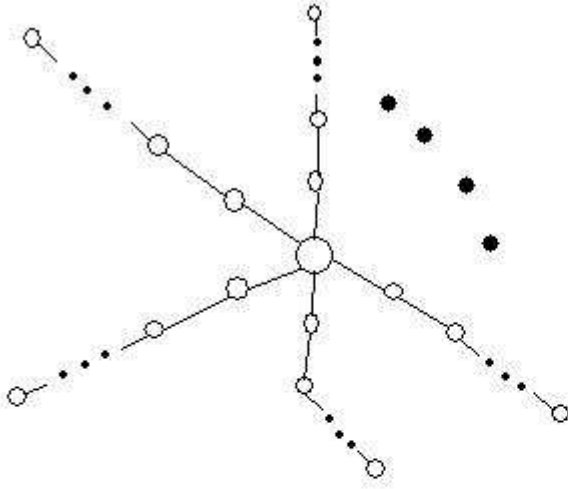
More generally, we define

Definition 8.9. *Define a **generalized (n,m) -star train-track** to be one having one central singularity and n main edges meeting that singularity, joined cyclically by peripheral edges, with each main edge being the first edge of a linear “spoke” of m main edges such that*

1. *each main edge beyond the first one is connected to at most two other main edges*

2. any two adjacent main edges on this “spoke” are attached by a single peripheral edge loop
3. the “last” main edge on the “line” (i.e., the one only connected to one other main edge) has a peripheral edge loop attached to its vertex not adjacent on any other main edge .

Below is a diagram for the typical generalized (n, m) -star train-track



While generalized (n, m) -star train-tracks can be especially nice to work with, it appears experimentally that valuable information about the set of pseudo-Anosov braids is lost by only looking at such train-tracks. For instance, it seems that really low growth behavior simply cannot be generated by such train-tracks (i.e., there are many low-growth pseudo-Anosov braids that do not have invariant generalized star-shaped train-tracks). The problem is that generalized star-shaped train-tracks are simply too symmetrical. In searching for the lowest entropy pseudo-Anosov braids, one is essentially attempting to break symmetry in the least possible way. Too much symmetry results in a braid being periodic or reducible.

Observe that the braids ψ_n and $\tilde{\psi}_n$, n odd and $n \geq 7$, have train-tracks that are quite similar to generalized $(2, m)$ -star train-tracks. Indeed the train-tracks for these braids described earlier are formed by simply adding a main edge and corresponding peripheral edge loop to a single spoke (ψ_n case) or deleting a main edge and corresponding peripheral edge loop from a single spoke ($\tilde{\psi}_n$ case) of a generalized $(2, m)$ -star train-track. For this reason, the train-tracks were referred to by

Hironaka and Kin as “star-like” [22]. We generalize this notion

Definition 8.10. Define a train-track to be **star-like** if it is obtained from a generalized (n, m) –star train-track by adding or deleting a single main edge (and its corresponding end peripheral edge loop). In the case of adding a main edge, we refer to the resulting train-track by $\tau_{m,n}^+$. If instead an edge is deleted, we use the notation $\tau_{m,n}^-$.

These star-like train-tracks will be the focus of our next section.

8.4 The $\Omega_{p,q}$ and $\tilde{\Omega}_{p,q}$ Braids

Recall the braids $\Omega_{p,q}$ and $\tilde{\Omega}_{p,q}$ defined in the introductory chapter

Definition 8.11. We define the n –strand $\Omega_{p,q}$ braids, where $n = pq + 1$ and q is a fixed natural number, via

1. $\Omega_{p,q} = L_n^p \sigma_1^{-1} \sigma_2^{-1}$, when $p > 1$ and $p \in \mathbb{N}$
2. $\Omega_{p,q} = L_n^{n-1} \sigma_1 \sigma_2$, when $p = 1$.

Definition 8.12. We define the n –strand $\tilde{\Omega}_{p,q}$ braids, where $n = pq + 2$ and q is a fixed natural number, via

1. $\tilde{\Omega}_{p,q} = L_n^p (\sigma_1^{-1} \sigma_2^{-1}) (\sigma_{n-1} \sigma_{n-2} \dots \sigma_{n-p})$, when $p > 1$ and $p \in \mathbb{N}$
2. $\tilde{\Omega}_{p,q} = L_n^{n-1} (\sigma_1 \sigma_2) L_n \sigma_1^{-1}$, when $p = 1$.

Lemma 8.13. The braids $\Omega_{p,q}$ have $\tau_{p,q}^+$ as invariant train-tracks.

The expressions for the $\Omega_{p,q}$ and $\tilde{\Omega}_{p,q}$ are quite similar, but slightly different. Consider the following definition, generalizing the idea behind the $\mathcal{U}(\psi_n)$ and $\mathcal{U}(\tilde{\psi}_n)$.

Definition 8.14. Let b be a pseudo-Anosov braid with invariant train-track τ . Define the **symmetrizing braid** $\mathcal{U}(b, \tau)$ to be the braid formed by simply adding a single puncture to each non-punctured singularity of τ and then using the same automorphism otherwise as for b .

Fact 8.15. We have $\tilde{\Omega}_{p,q} = \mathcal{U}(\Omega_{p,q}, \tau_{p,q}^+)$.

A key idea later on is that the mapping tori of symmetrizing braids tend to possess certain nice symmetries not necessarily exhibited by mapping tori of the initial braids themselves.

Why are we interested now in the $\Omega_{p,q}$ and $\tilde{\Omega}_{p,q}$ families here? Observe that in the case $p = 2$, for instance, $\Omega_{2,q} = \psi_{2q+1}$. Are they related to previous braids more generally in any way?

Theorem 8.16 (de Carvalho, Hall). *The $\Omega_{p,q}$ and $\tilde{\Omega}_{p,q}$ are braids of horseshoe type. More specifically, in terms of height and decoration, $\Omega_{p,q} = P_{\frac{p-1}{(p-1)q+1}}^{0^{q-3}}$ when $q \geq 3$, where 0^{q-3} denotes simply a string of $q-3$ zeros. (There are similar expressions in the cases $q = 1, 2$.)*

Theorem 8.17. *The $\Omega_{p,q}$ braids have mapping tori resulting from $\frac{(p-1)q+1}{q}$ Dehn surgery on a cusp of M_{magic} .*

What other sorts of horseshoe braids have this sort of property? Using similar considerations as those presented in Chapter 7, we find

Corollary 8.18. *The $\tilde{\Omega}_{p,q}$ have mapping tori isometric to M_{magic} .*

Experimentally, the braids corresponding to positive surgeries on M_{magic} tend to have star-shaped train-tracks, with some number of “spokes” of length j and other “spokes” of length $j+1$. However, the ones having having more than one spoke of each kind seem to twist too many times and avoid being of horseshoe type. We know from the description $\psi_{2q+1} = \Omega_{2,q}$ that the ψ_n, n odd are of horseshoe type. In spite of this, the $\tilde{\psi}_n, n$ odd fail to be of horseshoe type. More generally, we observe the braids corresponding to positive surgeries on M_{magic} with $\tau_{m,n}^-$ train-tracks to not quite work out when looking for a horseshoe description. However, the ones with $\tau_{m,n}^+$ train-tracks work out just right and these seem to be almost exactly the $\Omega_{p,q}$.

Conjecture 8.19. *With possibly some trivial exceptions, and up to natural symmetries, the set $\{\Omega_{p,q} : p, q \in \mathbb{N}\}$ is precisely the set of horseshoe braids corresponding to positive surgeries on M_{magic} .*

We conjectured earlier that the lowest growth braids came from surgeries on M_{magic} . It seems quite reasonable to extend this line of reasoning to horseshoe braids and consequently

Conjecture 8.20. *When $n \neq r+1, r$ prime, pseudo-Anosov growth is often minimized by braids in the set $\{\Omega_{p,q} : p, q \in \mathbb{N}\}$.*

The case $n = r+1, r$ prime, requires a bit of additional care. Recall our conjecture earlier that the lowest growth pseudo-Anosov braids with 3-cusp mapping tori were often formed by adding a puncture to the non-punctured singularities of lowest growth pseudo-Anosov braids with 2-cusp mapping tori. In the case where r is an odd prime, the conjectured lowest growth pseudo-Anosov r -braids are the ψ_r and $\tilde{\psi}_r$ braids. Since the ψ_r braids are horseshoe, we consequently conjecture the minimal growth pseudo-Anosov $(r+1)$ -strand braids of horseshoe type with 3-cusp mapping tori to be the ones formed by adding punctures to the ψ_r braids. This sequence will have the same sequential value as the ψ_r sequence, which is equal to $(2 + \sqrt{3})^2$. Among pseudo-Anosov braids with 2-cusp mapping tori not isometric to positive surgeries on M_{magic} , we conjectured earlier that the minimal sequential value is that obtained by the $\tilde{\theta}_n$ sequence, which was experimentally

approximated to be in the interval $[30, 40]$. Moreover, based on the volume minimization/entropy minimization concept, it seems unlikely that sequences of pseudo-Anosov $(r+1)$ -braids of horseshoe type with mapping tori of more than 3 cusps will achieve lower growth either than these braids with 3-cusp mapping tori. Synthesizing all of this, we arrive at

Conjecture 8.21. *When $n = r + 1, r$ an (odd) prime, pseudo-Anosov growth is generally minimized by the $\mathcal{U}(\psi_r, \tau_{2, \frac{r-1}{2}}^+)$ braids.*

Moreover, one would expect the following

Conjecture 8.22. *Define $J(n)$ to be the largest integer so that the lowest $J(n)$ growths among pseudo-Anosov horseshoe n -braids may be attained by braids of the form $\Omega_{p,q}$ and $\tilde{\Omega}_{p,q}$. Then, $J(n) \rightarrow \infty$ and $n \rightarrow \infty$.*

Observe next that, when $n - 1$ is composite, there are potentially many ways to factor $n - 1$ as $p \times q$. This raises the question

Question 8.23. *In the case where $n - 1$ is composite, for what choices of $p, q > 1$ with $n = pq + 1$ does $\Omega_{p,q}$ have lowest growth?*

In the case where n is odd, we recall that it is conjectured the $\psi_n = \Omega_{2,q}$ perform best. More generally, it appears from experiment that one essentially gets the best results by choosing p as small as possible.

Definition 8.24. *We define the (H_n) sequence, $n \in \mathbb{N}, n \geq 7$, via*

1. *if $n - 1 = p$, with $p = 2k + 1$ a prime, then $H_n = \mathcal{U}(\psi_r, \tau_{2,k}^+) = \tilde{\Omega}_{2,k} = L_n^2(\sigma_1^{-1}\sigma_2^{-1})(\sigma_{n-1}\sigma_{n-2})$*
2. *if $n - 1$ is composite, with smallest prime factor α and corresponding quotient $\beta = \frac{n-1}{\alpha}$, then $H_n = \Omega_{\alpha,\beta} = L_n^\alpha \sigma_1^{-1} \sigma_2^{-1}$.*

Having defined this critical sequence, we arrive at the final conjecture concerning horseshoe growth

Conjecture 8.25 (Horseshoe Growth Minimization). *For most naturals n where H_n is defined, growth among horseshoe braids is minimized by the H_n .*

8.5 Forcing for M_{magic}

Recall that the definition of braid forcing order is intended to generalize the idea of the period forcing order of interval maps in the classical Sharkovskii Theorem. Consequently, we would like to find analogues of the Sharkovskii Theorem in the pseudo-Anosov braid forcing setting.

Theorem 8.26 (Carvalho, Hall). $\Omega_{p,q} \succeq \Omega_{p',q'}$ iff $\frac{(p-1)q+1}{p-1} \geq \frac{(p'-1)q'+1}{p'-1}$ and $q \leq q'$.

Note that our expression $\frac{(p-1)q+1}{q}$ for the surgery coefficient corresponding to $\Omega_{p,q}$ is quite similar to the expression $\frac{(p-1)q+1}{p-1}$ of the theorem. This suggests an approach for computing the more general order with respect to M_{magic} .

Conjecture 8.27. *After some simple coordinate change on M_{magic} , the braid forcing order on the set of braids corresponding to positive surgeries on M_{magic} is essentially given by the usual order on surgery coefficients (along with perhaps some auxiliary condition, i.e., $q \leq q'$).*

We observed earlier that the ψ_n and $\tilde{\psi}_n$ braids were all minimal. These were braids where the surgery coefficients were very close to 1. Considering now surgeries of fixed denominator, the horseshoe theory applies in fact to show that the $\Omega_{p,2}$ are all minimal. More generally,

Conjecture 8.28. *Pseudo-Anosov braids with mapping tori resulting from non-trivial surgery on M_{magic} are all minimal.*

We suspect however that not all minimal pseudo-Anosov braids arise from surgeries on M_{magic} . For instance, we suspect the $\tilde{\theta}_n$ braids defined earlier are potentially minimal as well, although we have not computed this yet.

Last, observe that if we fix q , the sequences $\Omega_{p,q}$ will be linearly ordered (i.e., $\Omega_{p,q} \succeq \Omega_{p',q}$ iff $p \leq p'$). The above concepts thus imply the existence of many linearly ordered sequences of minimal braids in the forcing partial order. Some related ideas may be found in [28], [29].

Chapter 9

Mapping Tori with More Cusps

9.1 Construction of the θ_n Sequence

Having observed that many low-growth pseudo-Anosov braids have mapping tori isometric to surgeries on M_{magic} , and moreover having analyzed such braids to some extent, we would now like to ask

Question 9.1. *What are the lowest growth pseudo-Anosov n -braids whose mapping tori are not isometric to surgeries on M_{magic} ?*

Using the strategy from Chapter 3, i.e., looking at braids forced by powers of the fundamental braid $\tilde{\psi}_3$, we stumbled across the sequence $\tilde{\theta}_n$.

Definition 9.2. *Define the n -strand braid sequence $\tilde{\theta}_n$ via $\theta_n = L_n^3 \sigma_1^{-1} \sigma_2^{-1} \sigma_{n-4}^{-1} \sigma_{n-5}^{-1}$ for $n = 4 + 3k, k \in \mathbb{N}$.*

Conjecture 9.3. *The sequence $(\tilde{\theta}_n)$, defined for $n = 4 + 3k, k \in \mathbb{N}$, attains minimal growth among pseudo-Anosov n -braids with mapping tori not isometric to M_{magic} .*

Defining a_n to be the growth of θ_n , we observe that $a = \lim_{n \rightarrow \infty} a_n^n$ exists and appears experimentally to satisfy $30 \leq a \leq 40$.

Fact 9.4. *The sequence $\tilde{\theta}_n$ is astounding when defined.*

We have not found any other pseudo-Anosov n -braids in the quotient of the braid group by its center attaining the exact same growth as ψ_n or $\tilde{\psi}_n$ in the non-exceptional cases. In other words, these two braids appear to usually be the unique minimizers in the quotient $B_n/(\partial_n^2)$ for pseudo-Anosov growth. However, we do not observe a similar sort of phenomenon with the $\tilde{\theta}_n$ braids. In fact, as n grows, there appear to be many pseudo-Anosov n -braids attaining the same growth as $\tilde{\theta}_n$, with the number of such braids growing at least linearly. For instance, we note that often the related braids $L_n^3 \sigma_1^{-1} \sigma_2^{-1} \sigma_{i+1}^{-1} \sigma_i^{-1}$ are pseudo-Anosov n -braids of the same growth as $\tilde{\theta}_n$ for varying i .

Recall now that when n was odd the braids $\tilde{\psi}_n$ were of horseshoe type [22], although this was not true in the case of n even. Moreover, in spite of this, the ψ_n were not in fact horseshoe in the case of n odd either. This leads us to

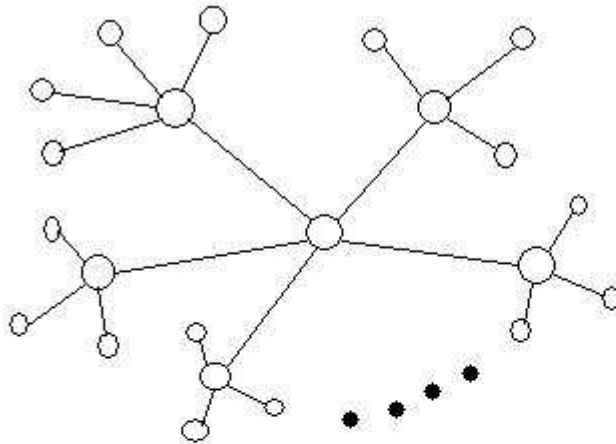
Question 9.5. *Are there pseudo-Anosov n -braids of horseshoe type attaining the same growth rates as the $\tilde{\theta}_n$ for some subsequence of \mathbb{N} ?*

We are not sure whether the $\tilde{\theta}_n$ are horseshoe themselves, but nonetheless the resolution to this question brings us to the natural θ_n sequence.

Definition 9.6. *We define the braid θ_n , for $n = 4 + 3k$ and $k \in \mathbb{N}$, to be the horseshoe braid with horseshoe code $10^{k+1}10^k10^k$.*

Lemma 9.7. *The braid θ_n is pseudo-Anosov with growth rate equal to that of $\tilde{\theta}_n$.*

We conclude this section by taking a look at invariant train-tracks for the θ_n . Consider the train-tracks of the diagram below.



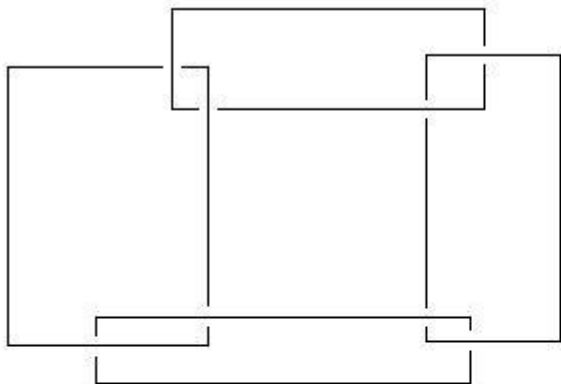
By putting a single puncture in each valence 1 vertex of the above train-track diagram, one in fact gets an invariant train-track for the corresponding braid θ_n . We denote the invariant train-track above corresponding to the θ_n , respectively, by \clubsuit_n^1 .

9.2 Surgeries on M_{hip} and M_{cool}

Recall from earlier the nice property of the $\mathcal{U}(\psi_n)$ and $\mathcal{U}(\tilde{\psi}_n)$.

Theorem 9.8. *The mapping tori of the $\mathcal{U}(\psi_n)$ and $\mathcal{U}(\tilde{\psi}_n)$ are all isomorphic to M_{magic} .*

We observe now a similar nice property for the $\mathcal{U}(\theta_n, \clubsuit_n^1)$. First consider the link pictured below.



Definition 9.9. *Define the manifold \tilde{M}_{hip} to be the complement in S^3 of the link pictured above.*

We conjectured earlier the magic manifold M_{magic} should attain minimal volume among orientable hyperbolic 3-manifolds of 3 cusps [27].

Conjecture 9.10. *The manifold \tilde{M}_{hip} attains minimal volume among orientable hyperbolic 3-manifolds of 4 cusps.*

Theorem 9.11. *The mapping tori of the $\mathcal{U}(\theta_n, \clubsuit_n^1)$ are all isometric to a hyperbolic 4-cusp 3-manifold of the same volume as \tilde{M}_{hip} .*

From this result, we make the following definition

Definition 9.12. *Define the **hip manifold**, denoted M_{hip} , to be the manifold formed as the mapping torus of any $\mathcal{U}(\theta_n, \clubsuit_n^1)$.*

These considerations above lead to the following corollary

Corollary 9.13. *The mapping tori of the θ_n are all isometric to Dehn surgeries on the hyperbolic 4-cusp 3-manifold M_{hip} having the same volume as \tilde{M}_{hip} , possibly \tilde{M}_{hip} itself.*

Analogous to the way in which we proceeded from M_{magic} to M_{hip} , we would now like to ask

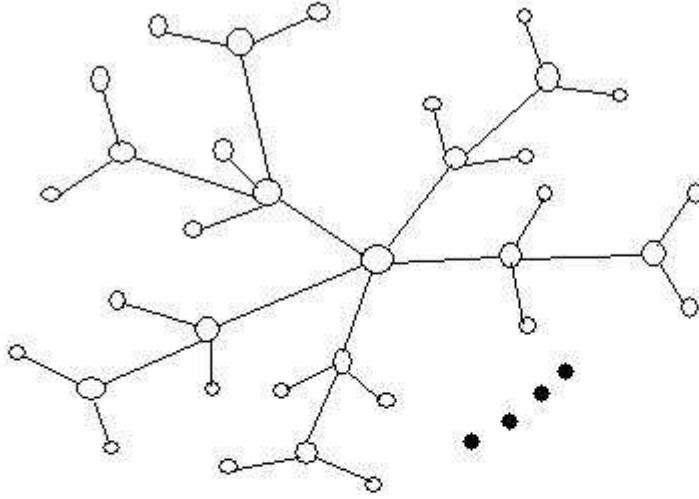
Question 9.14. *What are the lowest growth pseudo-Anosov n -braids not corresponding to surgery on an orientable hyperbolic 4-cusp 3-manifold of the same volume as M_{hip} ?*

This seems like a challenging question in general to answer. Recall that among the ψ_n braids there was an infinite subsequence of horseshoe braids. Moreover, the θ_n sequence above, having the same growth as the $\tilde{\theta}_n$ sequence, consisted entirely of horseshoe braids. This suggests trying to answer the above question in the setting of horseshoe braids for some infinite subset of \mathbb{N} at first. The number of horseshoe n -braids is a finite, relatively small number for relatively low n , in stark contrast with the case of all pseudo-Anosov n -braids, so we would expect this to be quite a bit more tractable computationally.

Recall that, in the case of $n = 2k + 3$, our braids ψ_n had horseshoe codes of the form $10^{k+1}10^k$. Next, by definition, our θ_n braids were defined by horseshoe codes for $n = 3k + 4$ via $\theta_n = 10^{k+1}10^k10^k$. This critical observation suggests attempting to generalize these horseshoe codes in some way. Two reasonable possibilities for the next stage of generality are horseshoe codes of the form $10^{k+1}10^k10^k10^k$ and $10^{k+1}10^{k+1}10^k10^k$. It is the latter expression we prefer to focus on for now.

Definition 9.15. *Define the braid \dagger_n , for $n = 4k + 6$ and $k \in \mathbb{N}$, to be the horseshoe braid with horseshoe code $10^{k+1}10^{k+1}10^k10^k$.*

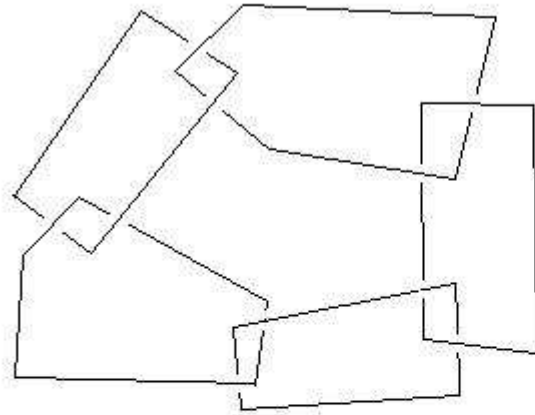
We observe a corresponding set of invariant train-tracks \clubsuit_n^2 in the diagram below



In the diagrams above, one gets the \dagger_n braids by placing a single puncture in each singularity of valence 1 in the train-track graph and performing a suitable train-track map. We point out at this stage that the train-track maps for the invariant train-tracks given in the cases of θ_n and \dagger_n are again essentially rotations of the train-track, just like for the ψ_n and $\tilde{\psi}_n$, except with an additional bit of twist. If one generalizes the construction further, i.e., a sequence beyond the θ_n and \dagger_n , it is possible that the additional bit of twist could get larger and larger. We're not quite sure at this stage exactly how large the extra twist could conceivably get for the more complex sequences.

We observe experimentally that the braids $\mathcal{U}(\dagger_n, \clubsuit_n^2)$ have very low growth (possibly minimal) among pseudo-Anosov n -braids with 5-cusp mapping tori. Such braids are necessarily not derived from Dehn surgery on a 4-cusp hyperbolic 3-manifold. We expect the braids $\mathcal{U}(\dagger_n, \clubsuit_n^2)$ to have relatively low growth among braids not coming from Dehn surgery on a minimal volume orientable 4-cusp hyperbolic 3-manifold. Of course the braids \dagger_n , as well as ones formed by puncturing an appropriate subset of the non-punctured singularities, would have the same growth on fewer number of strands. We are not sure yet, however, whether any such braids correspond to surgeries on M_{hip} or other conjectured minimal volume orientable 4-cusp hyperbolic 3-manifolds.

In analogy with \tilde{M}_{hip} , we would like to produce a corresponding manifold for the \dagger_n sequence. Consider the following link diagram below



Definition 9.16. Define the manifold \tilde{M}_{cool} to be the complement in S^3 of the link pictured above.

Conjecture 9.17. The manifold \tilde{M}_{cool} attains minimal volume among orientable hyperbolic 5-manifolds of 4 cusps.

Theorem 9.18. The mapping tori of the $\mathcal{U}(\dagger_n, \clubsuit_n^2)$ are all isometric to a hyperbolic 5-cusp 3-manifold of the same volume as \tilde{M}_{cool} .

From this result, we make the following definition

Definition 9.19. Define the **cool manifold**, denoted M_{cool} , to be the manifold formed as the mapping torus of any $\mathcal{U}(\dagger_n, \clubsuit_n^2)$.

The considerations above lead to the following corollary

Corollary 9.20. The mapping tori of the \dagger_n are all isometric to Dehn surgeries on the hyperbolic 5-cusp 3-manifold M_{cool} having the same volume as \tilde{M}_{cool} , possibly \tilde{M}_{cool} itself.

9.3 Minimally Twisted Chain Links and the Finite Cyclic Whitehead Link Covers

The motivations for the considerations of the preceding two sections may not be entirely clear at the moment. We hope to clarify some of these ideas in this final section of the thesis. This section hopes to outline a strategy for computing the braid forcing order on a quite large set of pseudo-Anosov braids, perhaps, ultimately, all. Indeed this proposed method appears somewhat complex, building on the much more straightforward ideas of preceding chapters, and has not become apparent until recently. Nonetheless, it seems like the method that is most likely to be fruitful. Following out the strategy presented here is our ongoing research at the moment.

Recall that in Chapter 8 we arrived at the conclusion that the braid forcing order for braids having mapping tori isometric to surgeries on M_{magic} should be determined explicitly by simply comparing surgery coefficients in some nice coordinates for M_{magic} . Our goal now is to arrive at a similar result for surgeries on some larger manifolds. This brings up the question

Question 9.21. *What larger manifolds should we use in describing the mapping tori via surgeries?*

Conceivably there are zillions of sorts of manifolds one could use to try to do the job. However, there are several requirements we look for at this stage to make our job as easy as possible, while still retaining a reasonable degree of generality. We observe first that a single finite volume hyperbolic 3-manifold will fail to describe lots of behavior corresponding to mapping tori. Moreover the work of Kin and Takasawa [24] described earlier shows there are pseudo-Anosov n -braids with entropy tending to zero and mapping tori of 2 cusps with volume tending to infinity. Thus, a single finite volume hyperbolic 3-manifold should not even necessarily be expected to model low growth well. This suggests we should be looking actually for a sequence $(Q_n)_{n \in \mathbb{N}}$ of increasingly more complex manifolds upon which to do surgeries perhaps, rather than a single finite volume manifold. We would like to incorporate braids with mapping tori of potentially many cusps, so the manifolds in our sequence should ideally have an increasing number of cusps as n gets large. In order to make generalization of the surgery/braid forcing relation from Q_n to Q_{n+1} as painless as possible, each manifold of the sequence should be related to preceding manifolds in a convenient manner (i.e., we would hope it is possible to obtain each manifold from Dehn surgery on the next). We would also like Q_{n+1} to have some mapping tori of relatively simple (the simplest if possible, perhaps) pseudo-Anosov braids not described via surgery on Q_n . Otherwise we might not stand a ghost of a chance of being able to do additional computations explicitly in Q_{n+1} .

Based on all of these considerations, as well as the analysis of the preceding two sections, we are left with natural choices for Q_1, Q_2 , and Q_3 . The most natural choices seem to be simply $Q_1 = M_{magic}$, $Q_2 = M_{hip}$, and $Q_3 = M_{cool}$. In connection with this, building on the horseshoe code

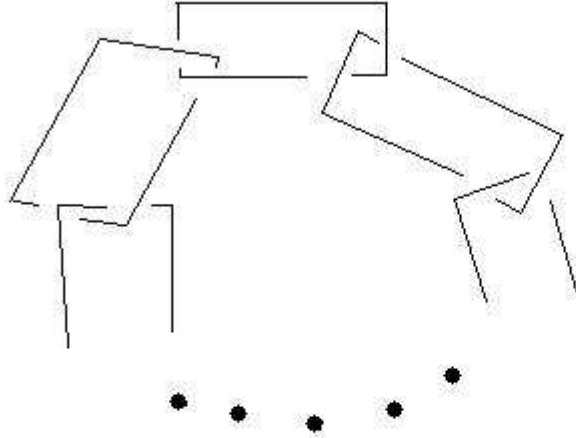
pattern of the $\psi_n, \theta_n, \dagger_n$ for appropriate n suggests the following definition

Definition 9.22. *Define the horseshoe braid \diamond_k^j on $n = (2k + 3)h$ strands to be the braid with horseshoe code $(10^{k+1})^h(10^k)^h$ when $j = 2h$ is even. In the event that $j = 2h + 1$ is odd, we define the horseshoe braid \diamond_k^j on $n = (2k + 3)h + (k + 1)$ strands to be the braid with horseshoe code $(10^{k+1})^h(10^k)^{h+1}$.*

Observe that $\diamond_k^2 = \psi_{2k+3}$, $\diamond_k^3 = \theta_{3k+4}$, and $\diamond_k^4 = \dagger_{4k+6}$. It might not necessarily be unreasonable to choose Q_n to be something like $\mathcal{U}(\diamond_1^{n+1}, \tau)$ for an appropriate invariant train-track τ of \diamond_1^{n+1} , generalizing the construction from the last section. We have not yet had the opportunity to compute the properties of these braids for larger n . We expect nonetheless that the manifolds should be quite simple orientable $(n + 2)$ -cusped hyperbolic 3-manifolds, possibly minimal volume, for relatively low n . This suggests another potential choice for the Q_n . It is generally believed that volume is an extremely good measure of complexity for hyperbolic 3-manifolds [35]. Since our Q_1, Q_2 , and Q_3 should be lowest volume orientable hyperbolic 3-manifolds on 3, 4, and 5 cusps, respectively, why not simply choose Q_n to be some appropriate minimal volume orientable hyperbolic $(n + 2)$ -cusp hyperbolic 3-manifold. This leads us to

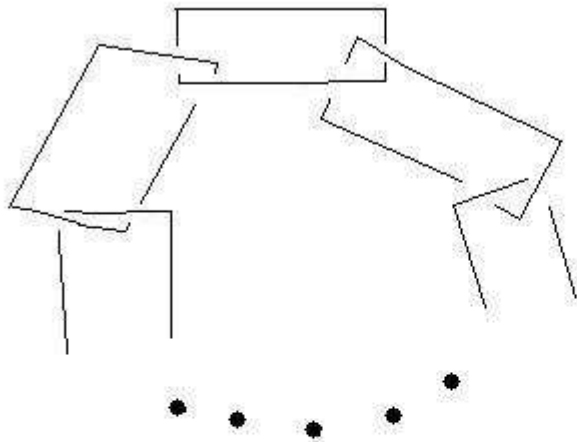
Question 9.23. *What is the minimal volume attained amongst orientable hyperbolic n -cusp 3-manifolds for any given n ? Moreover, for each such n , what exactly is the set of corresponding manifolds realizing this volume?*

In an attempt to understand this question, we have begun looking at some low-volume sequences of manifolds. Consider first the n -chain link diagram below



Definition 9.24. We define the **alternating n -chain link** to be the n -component link depicted above, where, for each pair of adjacent unknotted components, the left component (moving clockwise round) passes first over and then under the right component.

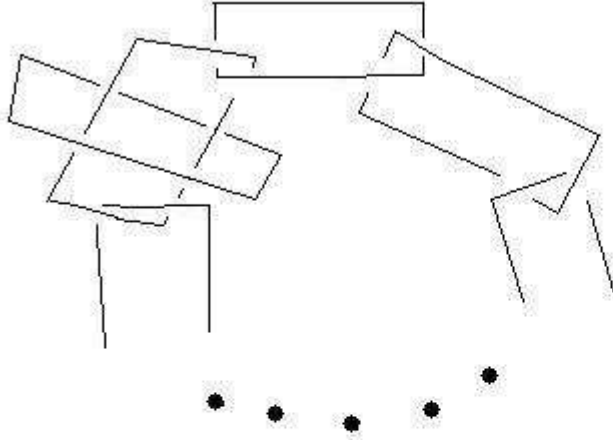
We are not so much interested in the alternating n -chain links, but more in a related set of links. Consider the diagram below



Definition 9.25. We define the *minimally twisted n -chain link* to be the n -component link depicted above, in which the crossing pairs between adjacent unknotted components alternate between over/under and under/over the whole way round (in contrast to the constant over/under behavior of the alternating link), when n is even. In the event that n is odd, we assume there are two successive pairs where the under/over behavior is repeated, while otherwise the behavior alternates between over/under and under/over crossings.

The above chain links have been considered in [2] and [35].

Observe that the complement of the minimally twisted 5-chain link in S^3 is precisely the manifold \tilde{M}_{cool} . We note that the complements of the minimally twisted n -chain links in S^3 seem to give very low volume orientable hyperbolic 3-manifolds when $5 \leq n \leq 10$. This is not, however, necessarily the case when n becomes sufficiently large. In connection with this, another family of links of interest here may be formed by simply adding an additional unknotted link component around the minimally twisted n -chain links (see diagram below).



The complements of the links above in S^3 are hyperbolic and have volumes equal to successive finite cyclic covers of the usual Whitehead link (perhaps they are isometric?). Indeed, when we consider orientable hyperbolic n -cusped 3-manifolds for a fixed $n > 10$, the finite cyclic covers of the Whitehead link complement have lower volume than minimally twisted n -chain links. Experimentally we have not found lower-volume asymptotic behavior on many cusps.

Conjecture 9.26. *Let V_8 denote be the volume of the Whitehead link complement in S^3 and let H_n be a volume minimizing sequence of orientable hyperbolic n -cusped 3-manifolds. Then, $\lim_{n \rightarrow \infty} \frac{\text{vol}(H_n)}{n} = V_8$.*

The same conjecture has been made recently by Agol [1] as well. We note that the volumes of the finite cyclic covers of the Whitehead link complement are simply successive multiples of the volume V_8 . Based on discussions with several experts in the field — Adams, Agol, Calegari, Dunfield, Kin, Takasawa — no manifolds of lower volume are known than those of the families described above for $n \geq 5$, despite plenty of computer experiments. It is perhaps not necessarily unreasonable at this stage to conjecture that volume among orientable n -cusped hyperbolic 3-manifolds can be minimized by: the Weeks manifold when $n = 0$, the figure-eight-knot complement in S^3 when $n = 1$, the Whitehead link complement in S^3 when $n = 2$, M_{magic} when $n = 3$, M_{hip} when $n = 4$, complements of the minimally twisted n -chain links in S^3 when $5 \leq n \leq 10$, and finite cyclic covers

of the Whitehead link complement when $n \geq 11$. This seems like a somewhat bold conjecture at the moment however and more experimentation/research will need to be done first before one can say for sure. In connection with this, it seems potentially fruitful to build a catalogue of the different non-isometric orientable n -cusped hyperbolic 3-manifolds attaining such volumes.

Question 9.27. *For fixed n , what orientable hyperbolic n -cusped 3-manifolds attain the same volumes as the minimally twisted n -chain link complements and n -cusped finite cyclic Whitehead link covers?*

Based on the links considered previously in relation to the Whitehead link complements (additional link component around the minimally twisted link), the two families described above should be related to one another via Dehn surgery. It has been observed by Agol that there should be some orientable hyperbolic 3-manifold not resulting from Dehn surgery on a finite cyclic cover of the Whitehead link complement. Nonetheless, one might expect a wealth of hyperbolic 3-manifolds to be produced in such a manner. This leads us to the following questions.

Question 9.28. *What (orientable) hyperbolic 3-manifolds may be constructed via surgery on a finite cyclic cover of the Whitehead link complement?*

Question 9.29. *What (orientable) hyperbolic 3-manifolds may be constructed via surgery on some orientable n -cusped hyperbolic 3-manifold having the same volume as either a finite cyclic cover of the Whitehead link complement or a minimally twisted n -chain link complement on the same number of cusps?*

Question 9.30. *What mapping tori of pseudo-Anosov braids may be constructed via surgery on some orientable n -cusped hyperbolic 3-manifold having the same volume as either a finite cyclic cover of the Whitehead link complement or a minimally twisted n -chain link complement on the same number of cusps?*

It is the last question that is of particular interest to us in regards to the problem of this thesis. We would eventually like to be able to understand the forcing order on such braids in terms of a Dehn surgery condition on the corresponding sequences of manifolds above.

Bibliography

- [1] I. Agol, *The minimal volume orientable hyperbolic 2-cusped 3-manifolds*, arXiv:0804.0043v1.
- [2] K. Baker, *Surgery descriptions and volumes of berge knots i: Large volume berge knots*, arXiv:math/0509054v1.
- [3] M. Bestvina and M. Handel, *Train-tracks for surface homeomorphisms*, *Topology* **34** (1995), 109–140.
- [4] S. Bigelow, *The burau representation is not faithful for $n = 5$* , *Geometry and Topology* **3** (1999), 397–404.
- [5] J. Birman, *Braids, links, and mapping class groups*, Princeton Univ. Press, Princeton, NJ.
- [6] P. Boyland, *Topological methods in surface dynamics*, *Topology and its Applications* **58** (1994), 223–298.
- [7] R. Brown, *Generating quadratic pseudo-anosov homeomorphisms of closed surfaces*, *Geometriae Dedicata* **97** (2003), 129–150.
- [8] D. Calegari, *Foliations and the geometry of 3-manifolds*, Oxford Mathematical Monographs, Oxford, UK.
- [9] J. Cho and J. Ham, *The minimal dilatation of a genus two surface*, (in progress).
- [10] A. de Carvalho and T. Hall, *Pruning theory and thurston's classification of surface homeomorphisms*, *J. Eur. Math. Soc.* **3** (2001), 287–333.
- [11] ———, *The forcing relation for horseshoe braid types*, *Experimental Math.* **11** (2002), 271–288.
- [12] ———, *How to prune a horseshoe*, *Nonlinearity* **15** (2002), R19–R68.
- [13] ———, *Conjugacies between horseshoe braids*, *Nonlinearity* **16** (2003), 1329–1338.
- [14] ———, *Braid forcing and star-shaped train tracks*, *Topology* **43** (2004), 247–287.
- [15] ———, *Unimodal generalized pseudo-anosov maps*, *Geometry and Topology* **8** (2004), 1127–1188.

- [16] J. Franks and E. Rykken, *Pseudo-anosov homeomorphisms with quadratic expansion*, Proceedings of the AMS **127** (1999), 2183–2192.
- [17] R. Ghrist, P. Holmes, and M. Sullivan, *Knots and links in three-dimensional flows*, Springer-Verlag.
- [18] R. Gompf and A. Stipsicz, *4-manifolds and kirby calculus*, American Mathematical Society, Providence, RI.
- [19] T. Hall, *The creation of horseshoes*, Nonlinearity **7** (1994), 861–924.
- [20] J. Ham and W. T. Song, *The minimum dilatation of pseudo-anosov 5-braids*, arXiv:math/0506295v3.
- [21] M. Handel, *The forcing partial order on the three times punctured disk*, Ergodic Theory and Dynamical Systems **17** (1997), 593–610.
- [22] E. Hironaka and E. Kin, *A family of pseudo-anosov braids with small dilatation*, arXiv:math/0507012v1.
- [23] E. Kin, *The forcing partial order on a family of braids forced by pseudo-anosov 3-braids*, arXiv:0711.4398v1.
- [24] E. Kin and M. Takasawa, *An asymptotic behavior of the dilatation for a family of pseudo-anosov braids*, arXiv:0711.3009v1.
- [25] ———, *Two invariants of pseudo-anosov mapping classes: Dilatation vs. hyperbolic volume*, (in progress).
- [26] C. Leininger, *On groups generated by two positive multi-twists: Teichmüller curves and lehmer’s number*, Geometry and Topology **8** (2004), 1301–1359.
- [27] B. Martelli and C. Petronio, *Dehn filling of the magic 3-manifold*, arXiv:math/0204228v3.
- [28] T. Matsuoka, *Braids of periodic points and a 2-dimensional analogue of sharkovskii’s ordering*, Dynamical Systems and Nonlinear Oscillations (G. Ikegami, ed.), World Scientific Press, 1968.
- [29] Z. Nitecki, *Topological dynamics on the interval*, Ergodic Theory and Dynamical Systems II: Proceedings Special Year, Maryland 1979 – 80 (A. Katok, ed.), Birkhauser, Boston, 1982.
- [30] R. Penner, *Bounds on least dilatations*, Proceedings of the A. M. S. **113** (1991), 443–450.
- [31] R. Penner and J. Harer, *Combinatorics of train tracks*, Princeton Univ. Press, Princeton, NJ.
- [32] D. Rolfsen, *Knots and links*, Publish or Perish, Houston, TX.

- [33] S. Smale and M. Shub, *Smale horseshoe*, http://www.scholarpedia.org/article/Smale_horseshoe.
- [34] W. T. Song, K. Ko, and J. Los, *Entropies of braids*, *J. Knot Theory and its Ramifications* **11** (2002), 647–666.
- [35] W. Thurston, *The geometry and topology of three-manifolds*, <http://www.msri.org/publications/books/gt3m/>.